
Editorial Office of *Earth's Cryosphere (Kriosfera Zemli)*
Institute of Geography, Russian Academy of Sciences
37 Vavilov str., office 22, Moscow, 117312, Russia
Editorial staff: *N.V. Arutyunyan, N.G. Belova, O.V. Levochkina, O.M. Lisitsyna, G.E. Oblogov*
Phone: 8(985) 957-10-01, e-mail: kriozem@gmail.com

Journal promoted by
Russian Academy of Sciences, Siberian Branch, Novosibirsk
Earth's Cryosphere Institute, Tyumen Scientific Centre SB RAS, Tyumen
Melnikov Permafrost Institute, SB RAS, Yakutsk

Editorial Manager *M.A. Trashkeeva*
Designed by *N.F. Suranova*
Typeset by *N.M. Raizvikh*

English text by *M.A. Korkka, V.A. Krutikova, V.V. Kuzovkin, N.N. Mzhelskaya*

RUSSIAN ACADEMY OF SCIENCES
SIBERIAN BRANCH
EARTH'S CRYOSPHERE INSTITUTE, TYUMEN SCIENTIFIC CENTRE

EARTH'S CRYOSPHERE
SCIENTIFIC JOURNAL

Founded in January 1997	6 issues per year	Vol. XXV, No. 4	July–August 2021

CONTENTS

EARTH'S CRYOSPHERE
SCIENTIFIC JOURNAL

Kriosfera Zemli, 2021, vol. XXV, No. 4, pp. 3–13

FUNDAMENTAL ISSUES OF EARTH'S CRYOSPHERE

CRYOLITHOSTRATIGRAPHY AND CRYOFACIES ANALYSIS

V.E. Tumskoy

Melnikov Permafrost Institute, SB RAS,
Merzlotnaya str. 36, Yakutsk, 677010, Russia; vtumskoy@gmail.com

The present article discusses the current theoretical problem of the dissection of thicknesses of frozen Quaternary formations for the purpose of reconstructing the history of their development, stratigraphy and mapping. This justifies the utilization of the cryofacies and cryoformation methods. Cryolithostratigraphy is discussed as a new branch of science at the junction of cryolithology and climatostratigraphy. The concepts of "cryofacies", "cryogenic contact", "cryogenic formation" are defined; distinctive types of cryofacies cryostratigraphy and cryogenic contacts are highlighted. A range of cryolithological studies from the primary dissection of frozen thicknesses to the solution of cryolithostratigraphic problems is proposed. The relationship between cryolithostratigraphy and paleocryolithostratigraphy is revealed.

Key words: *cryolithostratigraphy, climatostratigraphy, cryofacies, cryostratigraphy, cryogenic contact, cryogenic formation.*

INTRODUCTION

The main objective of Quaternary geology is the "subdivision of the Quaternary deposits by age, genesis and the subsequent reconstruction of paleoenvironmental conditions, geological processes and minerogeny" [*Astakhov, 2008, p. 10*]. The stratigraphic subdivision of Quaternary deposits is based on the climatostratigraphic approach [*Stratigraphic code..., 2019*]: specific paragenetic combinations of fine-grained sediments are formed during geological epochs with relatively stable climatic conditions. The set of genetic deposition types and the properties of their composition, structure and deposition conditions do change depending on climate: conditions are warmer or colder. Simultaneously occurring changes in flora and fauna, isotopic composition of atmospheric precipitation etc. can be reflected in the composition of Quaternary deposits and can serve as additional source of paleoenvironmental information. The existing stratigraphic chart of Quaternary deposits, which was originally created for formerly glaciated regions, is based on the alternation of climate epochs leading to the i) advance and retreat of ice sheets and ii) formation of corresponding glacial/non-glacial sediments [*Zubakov, 1986; French, 2007*]. The stratigraphy of the Quaternary for coastal regions of the Arctic [*Saks, 1948*] and, for example, the Caspian Sea [*Zubakov, 1986*] is predominantly based on the alternation of submarine and subaerial conditions. These differences in stratigraphic principles lead to peculiarities in local and regional Quaternary stratigraphic charts despite this local/regional stratigraphy reflects the general dynamics of global climatic conditions.

In this paper we analyze the problem of subdividing Quaternary horizons in permafrost. Many peculiarities of the stratification and interrelation of frozen deposits can only be correctly interpreted using the principles of cryolithology. Significant changes in the structure of deposits occur while freezing of these deposits, segregation of ice and the formation of massive ground ice. Thawing of frozen deposits is usually accompanied by a i) disturbance of the initial depositional banding, ii) changes in the composition of deposits etc. Misunderstanding of resulting stratigraphy inherited from the cryogenesis of sediments as a whole, as well as from the cryolithogenesis, had often led and leads to misconception of the genesis and subsequent transformation of frozen deposits under a certain environmental conditions. Such misconceptions can further be reflected in existing geological maps, stratigraphic charts, paleoenvironmental reconstructions, etc. Presently, the application of the cryolithological approach for subdividing of frozen Quaternary formations has led to the emergence of a cryostratigraphic analysis – a scientific direction at the junction of Quaternary geology, geocryology and paleoclimatology.

SUBDIVISION OF FROZEN DEPOSITS AND IDENTIFICATION OF CRYOFACIES

Cryofacies analysis is considered as the main geological approach in permafrost studies [*Katasonov, 1972, 1973; Ershov, 1982; Popov et al., 1985; Badu, 2010*]. Its fundamentals were first formulated in 1954 in E.M. Katasonov's PhD thesis, where he named it "the method of geocryological facies", but this work has not been fully published until 2009 [*Katasonov,*

2009]. Later this method has been named as "cryofacies analysis" [*Kaplina, 1988*]. "The cryofacies analysis is the main, most general cryolithological approach. Its essence is the subdivision of permafrost. Within the geological section one subdivides and comprehensively studies the genetic varieties and facies of deposits of different composition, ice content and structure which i) had formed under different permafrost and landscape conditions or ii) had been freezing during different stages of early diagenesis" [*Katasonov, 1972, p. 29*]. E.M. Katasonov named such facies as *geocryological facies* implying deposits characterized by two groups of genetic features: sediment features on the one hand and cryogenic (ice content, cryogenic structure and the structure of the ice inclusions themselves) features on the other [*Katasonov, 2009*]. These were later named as *cryofacies* [*Zhestkova, 1982; Kaplina, 1988*]. T.N. Kaplina didn't give a clear definition of the concept of "cryofacies", but she implied a geological body with a specific cryogenic structure. "Cryolithogenic facies" is a conceptually very similar term (although used more often in engineering-geology) which we interpret as "a homogeneous geological body whose cryogenic structure (including physical properties) is justified by a joint sedimentation and the process of cryodiagenesis" [*Usov, 2015, p. 19*].

Thus, the utilization of the cryofacies analysis for the subdivision of permafrost is based on the peculiarities of their cryostratigraphy. It is a complex of textural and structural properties of deposits which are justified by their cryogenic transformation and ice segregation before, during and after the process of their freezing [*Zhestkova, 1982*]. Cryostratigraphy is determined by all types of ground ice: pore ice, segregated ice and massive ice. Application of cryofacies analysis results in the identification of cryofacies in the permafrost section.

Many studies have been dedicated to research questions related to the facies analysis of the geological environment [*Shantser, 1966; Krasheninnikov, 1971; Shvanov, 1982; Tseisler, 2002; Vyltsan, 2002*]. Currently the term "facies" is dualistic: on one hand, it is a set of local environmental conditions (facies conditions) in which deposition occurs; on the other hand, it is a specific geological body which has been formed in these conditions and has characteristic formation indicators (facies indicators) [*Petrov, 2012*]. The facies can be identified according to different criteria, but not in accordance with geography or sedimentology only (seismic facies, for example). The identification of cryofacies corresponds to principles of the identification of facies in geology. The cryostructure of deposits is the criterion for this identification.

In the author's opinion, cryofacies can be identified based on different considerations. On one hand, cryofacies can be identified based on geological and sedimentological indicators followed by the description of their cryostructure given that freezing is a secondary process ("cryogenic diagenesis") in relation to deposition, even for syncryogenic deposits (for example, this approach is used in [*Melnikov et al., 2015*]). In this case, the boundaries between cryofacies are determined primarily by changes in the composition of deposits, conditions of occurrence, layering structure etc. On the other hand, cryofacies can be identified according to cryostructure itself. In this case, one can attribute deposits with f.e. different composition or water content to a certain facies.

To give this concept a more cryolithological meaning, author considers ***the cryofacies*** *as* ***a part of a permafrost section characterized by specific cryostratigraphy (both structure-forming and massive ice) which had been formed under relatively stable freezing conditions and is characterized by homogeneity or a regular change in space***. Thus, cryofacies are distinguished from one another based on the complex of permafrost structure given the structure-forming and massive ground ice. Freezing conditions as complex of the freezing direction of deposits, their thermal regime, composition, properties and the set of cryogenic geological processes represent the cryofacies conditions.

Massive ice bodies can be considered as individual cryofacies. In the literature, structure-forming segregated ice is considered as a mineral while massive ice is attributed to a type of frozen rock [*Ershov, 1982*]. The latter can be considered as part of a permafrost consisted of ice with a relatively homogenous structure (cryolith). In this regard, terms "cryostructure" and "cryotexture" would have different meaning, being transformed into the concepts of structure and texture of ice. Depending on the goals of studies, any massive ground ice can be considered as individual cryofacies, although this is most efficient for individual bodies of buried, cave and intrusive types of ice. Wedge ice which forms a polygonal structure within the structure-forming ground ice, must be taken into consideration as an element of its cryostratigraphy when solving most cryolithological or cryostratigraphic problems.

Cryofacies can most clearly be subdivided within fine-grained deposits containing lenses of ice that form cryostructures since these lenses highlight and exhibit freezing directions and features. The description of cryofacies suggested above allows us to identify them within all types of frozen deposits, rather than within cryolithogenic deposits only (accumulating in conditions of existing permafrost) [*Katasonov, 1973, 2009*]. The proposed description expands the possibilities of using the cryofacies analysis, although it can differently be applicable to frozen deposits of various cryogenic genesis.

TYPES OF CRYOFACIES AND CRYOGENIC CONTACTS

Identification of cryofacies is resulted from the study of permafrost cryostratigraphy. At the same time, the identifying attribute of each cryofacies is the type of cryostructure of frozen deposits within each one. The type of boundaries between cryofacies is key for distinguishing them from each other and for establishing the stages of their formation.

Two types of frozen deposits can be defined: with primary and secondary cryostructure (PC and SC, respectively) given the time of cryostructure formation. PC is considered in case if the cryostructure of deposits has been forming syngenetically or in case these deposits undergone a prolonged regional deep thawing during the previous thermochron. Appealing to the types of cryolithogenesis discussed in the work of N.N. Romanovskii [*1993*], i) deposits of the subaerial and subglacial groups of the syncryogenic types, ii) deposits of shallow waters of the subaqueous group and initially unfrozen specifically subaqueous deposits, iii) epicryogenic fine-grained deposits which had been frozen synchronously and asynchronously are attributed to PC deposits. Deposits, i) cryostructure of which is related to the freezing of taliks, ii) the boundaries of which affect the configuration of the freezing front, the temperature field and the type of ice segregation, etc. belong to SC deposits. These can be frozen deposits which i) formed uring epicryogenic freezing of thawed sediments of taliks, ii) are parasyncryogenic and quasi-syncryogenic permafrost as well as part of synchronously epicryogenic permafrost.

PC within cryofacies can be either relatively homogenous or naturally change in space. The latter is usually related to changes in composition, water content and geothermal gradient with depth given relatively stable freezing conditions at the surface. At the current stage of the study, author highlights four types of PC permafrost forming during the single stage of freezing: **homogenous, directional, cyclical and chaotic** (Fig. 1). ***Homogenous cryostructure*** is characterized by the homogenous characteristics of cryogenic structures and massive ice (approximately equal thickness of ice lenses, distance between them or cell sizes of the cryostructure, grid parameters of ice wedges, etc.). ***Directional cryostructure*** is characterized by a regular change in the permafrost cryostructure in one or several directions, for example, a gradual increase in the distance between ice lenses or their thickness (for example, classic cryostructure of an epigenetically frozen fine-grained deposits), a regular decrease in the width of ice wedges, etc. ***Cyclical cryostructure*** is characterized by a periodic repetition in the section of the main features of the cryostructure pattern. A classic example is horizons of syncryogenic deposits with belt cryostructures. The types of permafrost cryostructures described above are distinguished based on the geometry of cryostructures or massive ice and can be supplemented if necessary. ***Chaotic cryostructure*** is characterized by irregular changes in permafrost within the cryofacies, which is a distinguishing trait of the deposition itself. The nature of such cryostructure can be a complex spatial distribution of the composition and properties of the deposits (water content, organic matter content, etc.) and ground ice. Each of the aforementioned cryostructure types can be characterized by an additional definition reflecting the nature of the cryostructure more accurately (see description of Fig. 1).

The SC permafrost types are the same as PC permafrost types excluding cyclical cryostructure. The difference lies in various cryostructure geometry and ice content distribution owing to a more complex configuration of the freezing front (or fronts).

Of course, it is necessary to keep in mind the scale effect when describing cryostructure: it's description can vary depending on the size of the documented part of the permafrost section. The characteristic size of cryofacies varies usually from several tens of centimeters to hundreds of meters horizontally and down the section.

Initial cryostructure can change horizontally during the syncryogenic sedimentation as well as during the epicryogenic freezing of an unfrozen deposits or deposits that have been thawed for a long time. The character of these horizonal changes depends on landscape conditions at the surface, the composition and water content of the deposits, developing exogenous geological (including cryogenic) processes etc. As a result, the cryostructure can be different even in simultaneously freezing deposits. At the same time, the cryostructure of developing cryofacies can gradually or abruptly change in a horizontal space. As a result of such freezing the cryostruc-

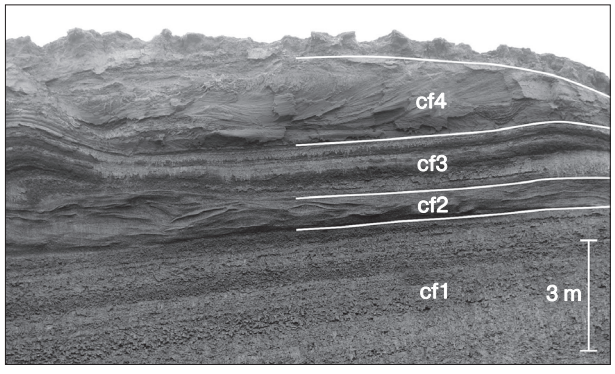

Fig. 1. Example of some types of cryostructure (CS) of cryofacies in the section:

cf1 – homogenous (homogenous reticulate CS), cf2 – chaotic (chaotic diagonal-lens CS), cf3 – cyclical (parallel-cyclical CS), cf4 – chaotic (chaotic diagonal-layered CS).

ture down the section will also differ. Herewith, the strongest variability will be characteristic of the syncryogenic deposits or the near-surface horizons of epicryogenic deposits.

PC permafrost can further change in several ways. It can be preserved in the section, can undergo full or partial destruction as the result of erosion, can fully or partially thaw. In case it is fully eroded, it's cryostructure disappears and the organo-mineral component is re-deposited becoming the part of new deposition unit. In case it is eroded partially (for example, during the formation of thermo-erosion gullies or as the result of the activity of a complex of slope processes), the new sediments infilling the formed depressions will be characterized by another cryostructure since these sediments undergo freezing at a different conditions. It's sedimentation structure and cryostructure adjacent to surrounding deposits would depend on the morphometry of the formed depression and the properties of non-eroded deposits (composition, temperature, etc). Once the newly formed portion of sediments is frozen, it is considered as PC permafrost (Fig. 2).

Taberated and/or taberal formations form if permafrost thaws [*Demidyuk et al., 1963; Romanovskii, 1993*]. Taberated formations are resulted from the thaw of low ice content deposits: deposits mainly preserve their initial sedimentary structure insignificantly subsiding with predominantly geochemical changes. Taberal formations are resulted from the thaw of high ice content deposits accompanied by the i) *in situ* re-deposition or ii) partial removal of the organo-mineral component with a total or almost total change of its initial sedimentary structure. The ice content threshold between these types of formations is arbitrary since the preservation/loss of initial sedimentary structure depends on the composition and ice content of the deposits. Taberal and taberated deposits are considered as SC permafrost in case if repeated freezing occurs. This SC is determined not by new freezing conditions (temperature, water content, etc.) only, but also by the geometry of the preserved underlying or enclosing frozen PC permafrost.

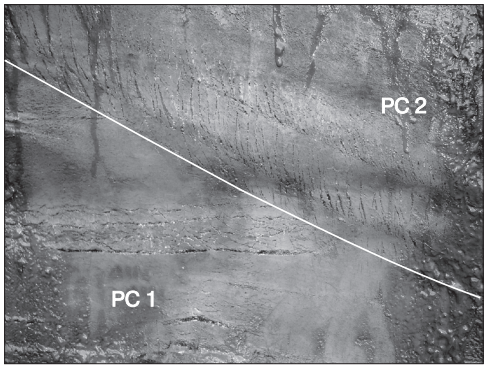

Fig. 2. Example of erosional cryogenic contact (shown by the white line) of two frozen layers.

The layer with primary cryostructure (PC 2) which fills the thermo-erosional gully is contained within the frozen deposits with PC 1.

We are unable to determine whether the observed cryostructure of the deposits is primary or secondary in many cases if a PC permafrost thaws completely and then re-freeze again. In some cases, paleocryogenic deposits such as postcryogenic structures or pseudomorphs can help in interpreting the sections (for example, in case of marine and lacustrine deposits). Such problems of interpreting the section can appear very often given the cyclicality of different periods in the permafrost evolution. Its solution requires additional geological data.

Based on the above mentioned, it is clear that the nature of boundaries between cryofacies with different cryostructure is important for determining the interlinkages between them. Therefore, they require special attention similarly as in a traditional geological facies analysis. It is necessary to note, that before analyzing boundaries between cryofacies, one needs to take into account two terms – cryogenic boundary and cryogenic contact.

The author defines the interface between deposits of different cryogenic states (for example, between frozen and thawed, frozen and cooled, cooled and thawed, etc.) as ***cryogenic boundary***.

The interface between deposits of varying cryostructure, i.e. between cryofacies, is defined as ***cryogenic contact***. Author presently highlights three types of cryogenic contacts: ***sedimentary cryogenic, erosional cryogenic and thaw contacts***.

Sedimentary cryogenic contacts (SCC) form as a result of changes in i) facies conditions during the sediment deposition (when the composition and/or properties of sediments change), ii) cryofacies conditions of freezing during the process of syncryolithogenesis as well as during epigenetic freezing of deposits of different composition. SCC separate cryofacies that represent PC permafrost. SCC can exist in syncryogenic deposits, separate the epi- and syncryogenic permafrost, can be present in epicryogenic, parasyncryogenic and diacryogenic permafrost. In terms of the nature of manifestation, one can define *gradual* and *abrupt* SCC depending on the extent to which the transformation from one type of cryostructure to another is "stretched out" spatially.

Erosional cryogenic contacts (ECC) are associated with a partial permafrost erosion when the appeared erosional depression is infilled with new sediments freezing under different conditions (Fig. 2). At the same time, sedimentational changes in deposit structure are usually clearly distinguished at contacts of this type (the composition of the material and especially the conditions of its occurrence, layering type, etc. change). Two cases can be considered: i) ECC divides two PC cryofacies and ii) ECC di-

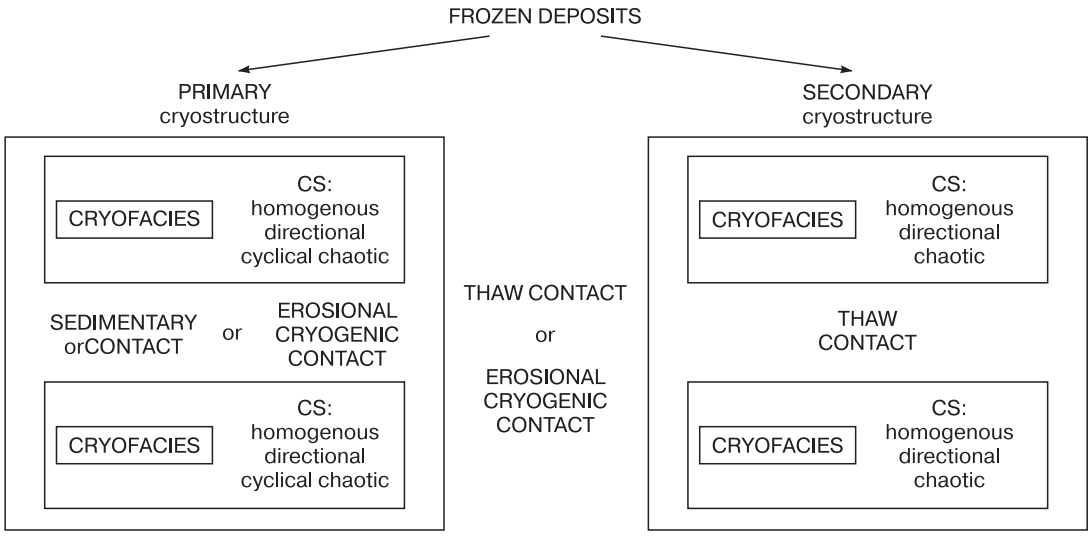

Fig. 3. Possible relationships of cryofacies with various types of cryostructure (CS) and cryogenic contacts.

vides SC and PC cryofacies. Contacts between Late Pleistocene Ice complex deposits of different ages are an example in the first case [*Tumskoy, 2004, 2012*]; contacts between taberal formations of alas depressions and deposits infilling the Late Holocene thermo-erosional gullies dissecting these alas depressions are the second case.

Thaw contacts (TC) are associated with the i) partial permafrost thaw, ii) formation of taberal and/or taberated formations and their subsequent freezing. TC divide underlying (enclosing) frozen PC deposits from the taberated or taberal formations characterized by SC. TC are also known as "thaw unconformity" [*Mackay, 1966; French, 2007*].

Figure 3 shows possible options of interlinkages between cryofacies with different types of cryostructure and cryogenic contacts.

RESULTS OF CRYOFACIES ANALYSIS

Subdivision of permafrost according to cryostructure and ice content, i.e. identification of cryofacies, is one of the main results of permafrost cryolithological studies. Most often it is carried out for cryolithogenic deposits. According to E.M. Katasonov [*2009*], cryostructure of the cryolithogenic deposits is largely determined by their geological genesis. He assumed that the main advantage of applying cryofacies analysis is the possibility to consider cryostructure of cryolithogenic deposits as an additional source of information about the geological genesis of deposits [*Katasonov, 1965, 1972, 2009*]. That is in an agreement with other geocryologists' work [*Vtyurin et al., 1957; Romanovskii, 1961*]. However, it has fast become evident, that permafrost cryostructure is determined by the thermal regime at the time of its freezing, grain-size composition, water content and other parameters [*Vtyurin, Gasanov, 1962*]. Despite the dependency of all these parameters on the conditions of facies formation and deposit freezing, they are not "direct functions" of their geological genesis. Therefore, permafrost cryostructure does not allow us to definitely determine the geological genesis of deposits, but it helps to judge more precisely about the peculiarities of ground freezing.

In the author's opinion it is critically important to clearly understand the difference between the result of facies and cryofacies research. The facies analysis of Quaternary deposits allows us to reconstruct peculiarities of deposition and landscape conditions within the same geological timeframe on the neighboring territories by determining the affiliation of deposits with specific facies conditions of deposition, genetic series and/or the type of Quaternary deposits. The cryofacies analysis allows us to determine ground freezing conditions and the freezing mechanism. For cryolithogenic deposits, we imply freezing conditions as: i) thermal conditions at the surface of the deposits and the temperature distribution throughout the section on its top, ii) water content of the deposits, iii) the configuration of cryogenic boundaries, iv) in many cases, the set and the nature of cryogenic geological processes. By the freezing mechanism (or type of cryolithogenesis) we imply the interlinkages between deposition processes and the transformation of deposits into permafrost in time. These mechanisms can be distinguished based on various criteria: either i) by the presence or absence of a deposition process during perennial freezing or ii) by the ratio of the geological age of the deposits and their cryogenic age. In the author's opinion, these are different things but given the specificity of this paper it is important to note that such approach leads to highlighting two main types of permafrost: sync-

ryogenic and epicryogenic [*Popov, 1953; Dostovalov, Kudryavtsev, 1967*]. These two types of permafrost formation are currently being considered as their cryogenic (permafrost) genesis. Herewith, geological genesis significantly differs in meaning from types of ground freezing, thus T.N. Kaplina proposed calling them *cryogenetic types* [*Kaplina, 1986*]. It is fundamentally important that the highlighted types of permafrost formation lead to it's different cryostructures. Thereby the solution of the inverse problem (the reconstruction of the conditions and types of deposit freezing) can be relatively unambiguous, unlike the ambiguity of determining the geological genesis of deposits based on its cryostructure.

It is sensible to consider syn- and epicryogenic deposits as cryolithogenic series of permafrost by analogy with the classification of genetic types of continental formations [*Shantser, 1966*]. Several cryogenic groups and types of deposits differing in formation conditions, the extent of diagenetic transformation of deposits before freezing and cryostructure can be highlighted in each of these series. From the standpoint of cryolithology, the development of a classification of cryogenetic groups and types for cryolithogenic deposits is particularly significant. Essentially, this approach is laid at the foundation of identifying groups and types of permafrost in N.N. Romanovskii's [*1993*] work, but it requires significant elaboration.

Based on the aforementioned principles of highlighting cryogenetic types of permafrost, syn- and epicryogenic permafrost with further smaller divisions are currently highlighted according to genesis. Parasyncryogenic and diacryogenic permafrost are considered as an independent cryogenetic series, but without further division. For cryolithogenic deposits, subgroups and types are herewith highlighted based on one principle, and for epicryogenic deposits – based on another principle. In both cases however, it is necessary to develop a more justified and detailed cryogenetic classification of deposits first, and secondly, the application of cryofacies analysis results in a clear and specific goal: determining the cryogenetic type of frozen deposits, and their group or series in case of insufficient data. Their spatial relationship allows us to i) reconstruct changes in geocryological conditions laterally and down the section over time, ii) to determine the order of freezing of the highlighted facies. Comprehensively solving the problems of facies and cryofacies analyses will allow us to reconstruct both the conditions of sediment deposition and the conditions of their freezing. As a result, we move to the next level of using results of cryolithological studies – cryolithostratigraphy.

CRYOLITHOSTRATIGRAPHY

As was shown above, the application of cryofacies analysis allows us to i) subdivide the permafrost section into cryofacies, ii) determine the cryogenetic type of each of them and the nature of cryogenic contacts. Further developing this approach, ***the complex of the cryofacies of one cryogenetic series which had formed during one freezing period represents a cryogenic formation***. Consequently, epicryogenic and syncryogenic formations can be considered, according to T.N. Kaplina [*1986*]. In this work, two other cryogenic formations (paleocryogenic and seasonally cryogenic) were also proposed, but according to absolutely different principle. Cryogenic formations have also been taken into consideration at a group level [*Alekseev, 2015*], which, perhaps, can further be actualized for cryolithogenic and synchronously-epicryogenic frozen deposits. The main goals of the "cryoformation" (geological formations in cryolithozone) and "cryostadial" (evolution of geological formations) analyses are the determination of geographical and geological formation conditions of permafrost at a cryogenic formation level and the study of the transformation peculiarities of fine-grained formations at all stages of their evolution, from eluvium to sedimentary rock, respectively [*Ershov, 1982*]. There is another field of study of Quaternary frozen fine-grained deposits – *cryolithostratigraphy*, i.e. the analysis of the permafrost cryostructure at meso- and macrolevels for stratigraphic subdivision of sections and reconstructing the history of Quaternary deposit formation in the cryolithozone.

Considering the ice content ranges, permafrost cryostructure has already been used for the subdivision of sections in the papers of M.M. Ermolaev [*1932*], B.I. Vtyurin [*Vtyurin et al., 1957*], A.I. Gusev [*1958*], N.N. Romanovskii [*1961*] and other researchers. The presence of ground ice was considered when subdividing the Upper Neopleistocene deposits as an independent stratigraphic horizon, which was later named the Yedoma Suite [*Vas'kovsky, 1963*]. A.I. Popov [*1965*] wrote that the properties of the structure and bedding of ground ice can be used for the development of stratigraphic charts. However, the data on ice wedges only were used in this work as well as in other analogous works. Later, the attention has been paid to changes in cryostructures in different horizons of permafrost. For example, T.N. Kaplina [*1981*], S.V. Tomirdiaro [*1982*] and others documented a change in cryostructures in Yedoma Ice Complex deposits from lens-type to microlense type and massive, which reflected their freezing under significantly harsher climatic conditions. Furthermore, a certain stratigraphic significance was also given to inclusions of various types of tabular ground ice [*Ivanov, Yashin, 1959; Badu et al., 1982*].

However, the direct assumption about the possibility and necessity of using the cryostructure of permafrost in solving stratigraphic problems was made for the first time during the Decision of interdepartmental stratigraphic meeting which took place in

Magadan in 1982, according to the author's knowledge. In a review of the stratigraphic studies of Quaternary deposits made by T.N. Kaplina it was stated that in the Yana-Kolyma lowland "...cyclic changes in the types of sedimentation and transformation of sediments by cryogenic processes were discovered, which made it possible to apply the cryolithological method for the stratigraphic subdivision of sediments ("cryolithostratigraphy"). Although this method was still at the beginning of its development, it was clear already that it has great prospects and is similarly valuable as the studies of moraine bedding in glacial regions [*Decision..., 1987*].

However, this method was not later mentioned in the Russian literature, although N.N. Romanovskii's work [*1993, p. 151*] mentions that "differences in the cryostructure of syncryogenic deposits of different ages offer additional possibilities for paleoclimatic and paleogeocryological reconstructions". Apparently, this is associated with a lack of developments in the i) conceptual apparatus of cryolithostratigraphy, ii) application methods of cryolithostratigraphy when conducting geological research in the cryolithozone, as well as iii) insufficient training of Quaternary geologists in the field of cryolithology. Furthermore, while in Russian literature "cryostratigraphy" has a different meaning [*Lisitsyna, Tumskoy, 2016*], the analogously used term in English scientific literature [*French, 2007; Lapalme et al., 2015*], which implies the study of cryostratigraphy itself (cryolithological research), which adds a degree of confusion. However, in "The principles of cryostratigraphy" [*French, Shur, 2010*], the authors define the main goal of cryostratigraphy as establishing the genesis of permafrost and to determining the history of its development, which can indirectly be used in solving stratigraphic problems and brings this approach closer to the understandings of Russian researchers.

Nowadays, appeared are works which discuss the fundamentals of cryolithostratigraphy as a branch of science. Thus, V.P. Melnikov and coauthors [*2015*] argue that cryolithostratigraphy is "a geocryological discipline which studies spatial and temporal relationships of cryogenic formations of permafrost". A basic subject of study is "a lithologically homogenous stratum which differs in material composition and cryostructure from under- and overlaying strata", which represents a permafrost facies. A cryogenic formation is simultaneously understood to be both a particular unity of permafrost facies and "a complex of paragenetically interconnected genetic types of deposits with cryogenic forms which are intrinsic to them and which have developed in a single freezing cycle".

Yu.K. Vasil'chuk [*2017*] has introduced another term – cyclocryolithostratigraphy. It implies "...the study of the vertical alternation of frozen ground units in Yedoma sections. The goal of cyclocryolithostratigraphy is the definition, description and interpretation of periodic and quasiperiodic variations in the permafrost cryolithostratigraphy (predominantly syncryogenic) and their application in developing and specifying the peculiarities of permafrost formation". In this meaning the cyclocryolithostratigraphy can be considered as a part of cryolithostratigraphy depending on the subject of study.

The main systemic descriptions of cryolithostratigraphy and cryolithostratigraphic studies of permafrost were formulated by T.N. Kaplina in her doctoral dissertation, but they were not fully published anywhere. In her opinion, cryolithostratigraphy is a branch or analogue of the climatic stratigraphy and "offers a basis for subdividing Quaternary deposits into geological bodies, for understanding their order in sections, for identifying the rhythmicity of geocryological events. The cryolithostratigraphy does not identify the position of geological bodies on a stratigraphic chart and should hence be applied with other stratigraphic methods" [*Kaplina, 1988, p. 269*].

How does the cryolithostratigraphic approach differ from other methods used within climatostratigraphic studies? Various paleoenvironmental research methods which are used in climatostratigraphy allow to reconstruct the past climatic, landscape and ecological conditions based on indirect data. Based on this, made are the conclusions regarding the climate harshness and the formation of the studied deposits is linked to corresponding thermo- and cryochrons.

The cryolithostratigraphic approach allows to reconstruct the order of freezing and thawing events that reflect patterns of both changes in regional climatic conditions and cryofacies ("micro landscape") conditions' susceptibility to change on a rather local level, which is not directly related to climatic changes. By applying similar methods (cryostructural method, petrographic studies of ground ice, its chemical and isotopic composition, etc.), we can obtain an additional information about freezing and thawing conditions which allows us to clarify and detail the paleoenvironmental reconstructions. While studying the interrelation between permafrost cryofacies we are able to reconstruct the accumulation order, freezing, washing and thawing of frozen deposits, which is particularly informative for cryolithogenic deposits. We can identify the cryogenetic type of each cryofacies, i.e. reconstruct their cryogenic history by determining the type of their cryostructure and the character of cryogenic contacts between them. We can unite deposits of same-aged cryogenetic types and cryofacies groups into cryogenic formations in case if the order of cryogenesis events on a certain territory do have some degree of a repeating patterns. On the level of cryoformations we can already solve problems related to cryolithostratigraphic subdivision of permafrost at a regional scale. Additional paleoenviron-

ment information obtained by applying other methods can allow us to juxtapose cryofacies and cryoformational structure of deposits with paleoclimatic characteristics during the deposition and move to paleoclimatic reconstructions and paleoclimatostratigraphic conclusions.

Paleocryolithological research has a special meaning and its own application specificity. They are associated with the characteristic layering deformations or specificities of deposit composition that are inherited from the development of cryogenic geological processes: frost heave of coarse grain-size material, frost heave within the active layer leading to cryoturbations, frost cracking, solifluction, local thermokarst, etc. Part of such deformations is geologically synchronous with freezing processes and is highlighted by their cryostucture within syncryogenic deposits. Other cryogenic disturbances could later be transformed during thawing and could after epigenetically freeze again (Fig. 4) or could be preserved in the structure of thawed deposits.

Traces of cryolithogenesis are often present in modern permafrost, reflecting traces of the history of its development and are preserved in many instances in thawed deposits. As a result, paleocryolithological studies can be conducted both within and outside the modern cryolithozone. In the first case traces of incomplete permafrost thaw are studied: in the majority of instances it is more or less unequivocally clear which processes and geocryological conditions were responsible for the formation of the primary cryostructure, what cryogenic processes took place and what they led to. Herewith, the history of cryolithogenesis, i.e. the order of cryofacies formation can be reconstructed based on both traces of the cryogenic processes development and their relationship to the modern cryostructure coupled with the cryostructure itself. In this case, results of paleocryolithological studies directly aid the solution of cryolithostratigraphic problems.

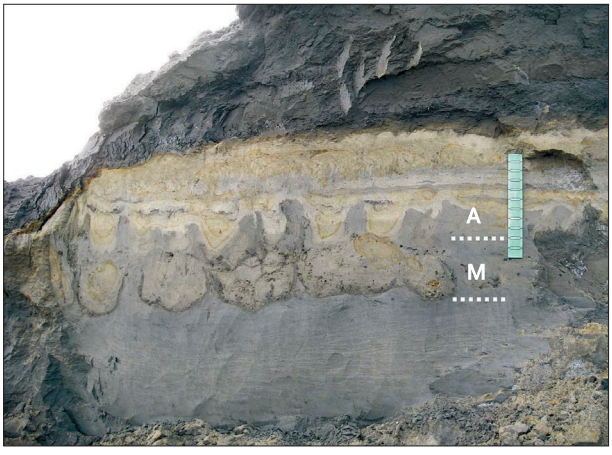

Fig. 4. Traces of cryoturbations in the relict seasonally thawed layer which reflect two stages of shrinking of its thickness: maximal (M) and average (A).

Presently the deposits are frozen.

In the second case, geological traces of cryolithogenesis are studied in areas of paleo-permafrost distribution. In this case the results of research obtained within the first branch often allow us to actualize results obtained within the second branch. However, it is essential to keep in mind that similar geological results can be related to the development of non-cryogenic processes and their diagnosis is not always certain since we are dealing with deposits which are already thawed, often for a long time. Outside the area of the modern cryolithozone we do not have, naturally, cryolithogenic deposits and almost never can certainly identify their derivatives. Therefore, cryofacies research and the cryolithostratigraphic analysis, which were developed for permafrost, would have a different meaning and basically are not applicable in the non-permafrost areas.

Nonetheless, subdividing deposits with traces of cryogenesis has a significant meaning for the reconstruction of past climatic and geocryological conditions, including the stratification of deposits and the periodization of the history of their development. The climatostratigraphic role of the cryolithostratigraphic approach increases towards the modern southern border of the cryolithozone. Furthermore, it is also significant in the area of discontinuous permafrost, in thawed deposits between isolated permafrost patches.

In the author's opinion, the main goal of cryolithostratigraphy in cryolithozone is the subdivision of horizons which had formed under similar geocryological conditions, and, as a result, can be used for relative periodization of Pleistocene and Holocene events. The history of development of cryolithogenic, primarily syncryogenic, deposits, can largely match the history of deposition and transformation (partial thawing and re-freezing) of sediments and buried tabular ground ice. The identification of the freezing stages and the transformation of frozen deposits during the emergence of taliks and theirs' secondary freezing, the formation of inter-ground massive ice, etc can be the results of cryolithostratigraphic research of epicryogenic deposits.

The main goal of cryolithostratigraphy outside of the cryolithozone (where it is sensible to consider it as paleocryolithostratigraphy) is the subdivision of horizons with traces of cryogenesis in specific geological epochs [*Kaplina, Romanovskii, 1960; Velichko, 1973, 2012; Sycheva, 2012*] and horizons without such traces. The author proposes to consider various horizons with traces of Pleistocene cryogenesis as various paleocryogenic formations characterized by i) their age and ii) boundaries between them (formations) that are differently aged thermochrons or interstadials. This is unlike the understandings of T.N. Kaplina [*1986*], who considered paleocryogenic

formations as all ground which had been subjected to cryogenesis in the late Cenozoic and are currently thawed.

Further developing the understandings of T.N. Kaplina, we define the *cryolithostratigraphy as one of the branches of climatostratigraphy that is the subdivision of geological bodies based on their cryostructure and/or postcryostructure, determination of their formation stages and subsequent transformation for the solution of stratigraphic problems.*

THE ORDER OF CONDUCTING CRYOLITHOSTRATIGRAPHIC RESEARCH

Initially, it was proposed to subdivide the frozen deposits in three stages while completing the cryofacies analysis [*Zhestkova, 1982; Kaplina, 1988*]. Subdividing of facies given their cryostructure and cryogenic formations is performed at the first stage; the reconstruction of conditions of deposit accumulation and freezing is performed at the second stage (determined are the genesis of deposits and paleoenvironmental freezing conditions); spatial-temporal changes in conditions of sediment deposition and freezing are established at the third stage. According to more recent understandings [*Melnikov et al., 2015*] subdivision of sections occurs differently: 1) highlighting of the layer (series of layers); 2) completion of a lithostratigraphic analysis of the layer or series of layers; 3) completion of a biostratigraphic analysis; 4) completion of a geochronological analysis; 5) completion of a textural-structural analysis of the cryostructure; 6) identification of the cryolithostratigraphical element (layer, series of layers); 7) identification of the cryostratotype.

In the author's opinion in both cases the subject at hand is not cryolithostratigraphic research, but rather complex cryolithogical and paleoenvironmental permafrost research. Furthermore, identifying cryostratotypes as elements of a permafrost section which have "typical cryostructures with individual characteristics for a homogenous facies" [*Melnikov et al., 2015, p. 12*] is fundamentally impossible, in the author's opinion. This is due to i) lateral variability of the cryostructure even within one cryofacies, and ii) almost annual dynamic of natural outcrops to which stratotypes must be connected [*Stratigraphic code..., 2019*]. Cryolithostratigraphic research proposed in this work is based on the i) completion of the cryofacies analysis and the identification of the cryogenetic type of permafrost, ii) determination of stages of cryofacies formation and iii) identification of cryogenic formations of cryo- and thermochrons. Specifically, the ratio between cryogenic formations allows us to subdivide permafrost into horizons which have cryolithostratigraphic significance. Coupling with additional paleoenvironmental data, the subdivided cryogenic formations receive a climatostratigraphic meaning and can be used in Quaternary stratigraphy.

The order of conducting research contains following steps:

1) identification of cryofacies based on their cryostructure;

2) determination of cryogenic contact types between them and the reconstruction of the order of their formation;

3) determination of the cryogenetic type of cryofacies deposits;

4) identification of cryoformations on the level of cryogenetic groups or series, the determination of spatial-temporal interrelations between them. Cryolithostratigraphic subdivision of frozen deposits is carried out at this stage;

5) supplementation by addition data for solving climatostratigraphic research questions and determination of the rank of cryoformations at regional or at local level.

The order of conducting research remains almost analogous while applying paleocryolithostratigraphy outside the area of the contemporary evolution of the cryolithozone. In this case, however, paleocryogenic properties are used for the identification of paleocryofacies and paleocryoformations. Usually, used are structural paleocryogenic properties preserved in thawed ground, rather than peculiarities of ground cryostructure.

CONCLUSION

The development of cryolithology and updates of Quaternary geological maps for vast territories of Siberia and the Russian Northeast have revived the needs in permafrost history research and its practical application – a cryolithostratigraphic approach for the subdivision of frozen deposits. For its actualization, proposed are i) the modern understanding of cryofacies and the principles of their identification, ii) some general types of cryostructure. Further, we introduced the concept of cryogenic contacts and justified their three types: sedimentary cryogenic, erosional cryogenic and thaw contacts. We proposed a new understanding of the cryogenic formation based on the developing science of cryogenetic types of frozen deposits. For the purpose of subdivision of frozen Quaternary deposits in the cryolithozone, we justified the cryolithostratigraphic approach based on existing research (first and foremost of T.N. Kaplina's). This approach is used most effectively beyond glacial areas and is a branch of climatostratigraphy. We have demonstrated that the paleocryolithostratigraphic approach can and must be used beyond the borders of the modern cryolithozone. We have justified the order of applying the cryolithostratigraphic studies and the order of using the cryofacies and cryoformational methods.

This work was completed with the financial support of RSF (grant 21-17-00054).

References

Alekseev, V.R., 2015. Geometry of the Cryolithozone. IMZ SO RAN, Yakutsk, 122 pp. (in Russian).

Astakhov, V.I., 2008. Foundation of Quaternary Geology. Izd-vo SPb University, St. Petersburg, 224 pp. (in Russian).

Badu, Yu.B., 2010. Cryolithology. Izd-vo KDU, Moscow, 528 pp. (in Russian).

Badu, Yu.B., Trofimov, V.T., Vasilchuk, Yu.K., 1982. General regularities of distribution and the kinds of massive ground ice in the northern part of Western Siberia plate. In: Massive Ground Ice of Cryolithozone. IMZ SO AN SSSR, Yakutsk, pp. 13–24 (in Russian).

Decision of interdepartmental stratigraphic meeting for Quaternary of East of USSR (Magadan, 1982), 1987. Explanatory letters for regional stratigraphic charts of Quaternary deposits of East of USSR. Magadan, 241 pp. (in Russian).

Demidyuk, L.M., Ryzhov, B.V., Sheko, A.I., 1963. On the genesis of enclosed depressions within Ingoda-Chita basin and it geotechnical investigation. In: Problems of Engineering Geology and Soil Science, iss. 1, 116–123 (in Russian).

Dostovalov, B.N., Kudryavtsev, V.A., 1967. General Geocryology. Izd-vo MGU, Moscow, 403 pp. (in Russian).

Ermolaev, M.M., 1932. Geological and geomorphological review of Bol'shoy Lyakhovsky Island. In: Trudy SOPS [Proceedings of SOPS], Yakutian series, iss. 7. Leningrad, pp. 147–223 (in Russian).

Ershov, E.D., 1982. Cryolithogenesis. Nedra, Moscow, 211 pp. (in Russian).

French, H.M., 2007. The Periglacial Environment. John Wiley & Sons Ltd., New York, 458 pp.

French, H., Shur, Yu., 2010. The principles of cryostratigraphy. Earth-Science Reviews, 101, 190–206.

Gusev, A.I., 1958. To the stratigraphy of Quaternary deposits on the western part of Coastal plain. In: Trudy NIIGA [Proceedings of the Institute of Geology of Arctic], 80 (5), 79–86 (in Russian).

Ivanov, O.A., Yashin, D.S., 1959. New data on geology of the Novaya Sibir` Island. In: Trudy NIIGA [Proceedings of NIIGA], 96 (8), 61–78 (in Russian).

Kaplina, T.N., 1981. Permafrost history of the Northern Yakutia in the Late Cenozoic. In: Evolution of Ice-rich Permafrost in Northern Eurasia. Nauka, Moscow, pp. 153–181 (in Russian).

Kaplina, T.N., 1986. About cryogenic formations. In: Ice-rich permafrost formation and forecast of cryogenic processes. Nauka, Moscow, pp. 3–14 (in Russian).

Kaplina, T.N., 1988. Cryolithogenesis during the Late Cenosoic on accumulative plains of North-East of USSR: Doctoral Thesis. Moscow, 317 pp. (in Russian).

Kaplina, T.N., Romanovskii, N.N., 1960. About ice-wedge casts. In: Periglacial forms on the USSR Territory. Nauka, Moscow, pp. 47–59 (in Russian).

Katasonov, E.M., 1965. Cryofacial investigations of ice-rich permafrost and some questions of Quaternary paleogeography in Siberia. In: Main problems of Quaternary investigations. To the VII Congress of INQUA, USA. Nauka, Moscow, pp. 286–294 (in Russian).

Katasonov, E.M., 1972. Regularities of development of cryogenic processes. In: Extended abstracts of XXII International Geographical Congress, Montreal. Nauka, Moscow, pp. 28–35 (in Russian).

Katasonov, E.M., 1973. Cryofacial analysis as the main method of cryolithology. In: II International Conference on Permafrost. Abstracts, vol. 3: Genesis, composition and structure of ice-rich permafrost and ground ice. Kn. Izd-vo, Yakutsk, pp. 29–37 (in Russian).

Katasonov, E.M., 2009. Lithology of Quaternary Frozen Grounds (Cryolithology) of the Yana Coastal Plain. PNIIIS, Moscow, 176 pp. (in Russian).

Krasheninnikov, G.F., 1971. Study of Facies. Vysshaya shkola, Moscow, 368 pp. (in Russian).

Lapalme, C.M., Lacelle, D., Davila, A.F., et al., 2015. Cryostratigraphy of near-surface permafrost in University Valley, McMurdo Dry Valleys of Antarctica In: Conference Paper: GeoQuebec. Quebec, Canada, Abs 352.

Lisitsyna, O.M., Tumskoy, V.E., 2016. Permafrost stratigraphy: modern knowledge and perspectives. In: Abstracts of 5th Conference of Russian geocryologists (Moscow, June 14–17, 2016). Moscow, vol. 2, pp. 195–201 (in Russian).

Mackay, J.R., 1966. Segregated epigenetic ice and slumps in permafrost, Mackenzie Delta area, N.W.T. Geographical Bulletin, iss. 8, 59–80.

Melnikov, V.P., Brouchkov, A.V., Khimenkov, A.N., 2015. Developing of the theoretical background of geocryology. Earth's Cryosphere XIX (2), 6–12.

Petrov, O.V. (Ed.), 2012. Dictionary of Geology. In three volumes. 3 ed. Vol. 3. P–Ya. VSEGEI, St. Petersburg, 440 pp. (in Russian).

Popov, A.I., 1953. Peculiarities of lithogenesis on alluvial plains under severe climate. In: Izvestiya AN SSSR [Bulletin of Academia of Science, USSR], Series Geography, No. 2, 29–43.

Popov, A.I., 1965. Underground ice. In: Ground Ice. Izd-vo MGU, Moscow, iss. 1, pp. 7–39 (in Russian).

Popov, A.I., Rozenbaum, G.E., Tumel, N.V., 1985. Cryolithology. Izd-vo MGU, Moscow, 239 pp. (in Russian).

Romanovskii, N.N., 1961. About structure of Yana-Indigirka onshore alluvial plain and conditions of it formation. In: Permafrost investigations, iss. II, 129–138.

Romanovskii, N.N., 1993. Foundations of Cryogenesis of Lithosphere. Izd-vo MGU, Moscow, 336 pp. (in Russian).

Saks, V.N., 1948. Quaternary in the Soviet Arctic. In: Trudy Vsesoyuznogo ANII [Proceedings of Soviet Arctic Institute]. Izd-vo Glavsevmorputi, Moscow, Leningrad, vol. 201, 131 pp. (in Russian).

Shantser, E.V., 1966. Principles of the studies of genetic types of continental sedimentary formations. In: Transactions GIN AN USSR. Nauka, Moscow, iss. 161, 239 pp. (in Russian).

Shvanov, V.N., 1982. Classification of sedimentary formations on composition characteristics. In: Newsletter of Leningrad State University, No. 24, 43–52 (in Russian).

Stratigraphic code of Russia. 2019. 3rd ed. VSEGEI, St. Petersburg, 96 pp. (in Russian).

Sycheva, S.A., 2012. Paleocryogenic events in periglacial area of the Central Russian Upland at the end of the Middle and Late Pleistocene. Kriosphera Zemli [Earth's Cryosphere], XVI (4), 45–56.

Tomirdiaro, S.V., 1982. Cryolithological criteria of stratigraphic division of eolian-cryogenic deposits of Yedoma complex on the North-East of USSR. In: Cryogenic Processes and Paleogeography of North-East Asia Lowlands. Izd-vo SVKNII DVNC AN SSSR, Magadan, pp. 54–58 (in Russian).

Tseisler, V.M., 2002. Analysis of formations. RUDN, Moscow, 186 pp. (in Russian).

Tumskoy, V.E., 2004. Geological structure and age of Ice Complex deposits around of Mus-Khaya outcrop (Yana River). In: Abstracts of International conference "Cryosphere of

oil-gas provinces" (Tyumen). Tisso, Moscow, p. 81 (in Russian).

Tumskoy, V.E., 2012. Peculiarities of cryolithogenesis in Northern Yakutia (Middle Neopleistocene to Holocene). Kriosphera Zemli [Earth`s Cryosphere], XVI (1), 12–21.

Usov, V.A., 2015. Cryolithogenic facies of the Arctic coastal zone. Gruntovedenie [Soil Science], No. 2, 19–25.

Vasil'chuk, Yu.K., 2017. Cycles in stratigraphy of Yedoma deposits. Part 1. Arktika i Antarktika [Arctic and Antarctic], No. 1, 62–83.

Vas'kovsky, A.P., 1963. Stratigraphy review of the Anthropohen (Quaternary) deposits of the far North-East of Asia. In: Geology of the Koryak Upland. Gos. nauch.-tekhn. izd-vo lit-ry po gornomu delu, Moscow, pp. 143–168 (in Russian).

Velichko, A.A., 1973. Main peculiarities of relic cryogenic relief and the principles of its mapping. In: Paleocryology in the Quaternary stratigraphy and paleogeography. Nauka, Moscow, pp. 121–134 (in Russian).

Velichko, A.A., 2012. Evolutionary Geography: Problems and Solutions. GEOS, Moscow, 563 pp. (in Russian).

Vtyurin, B.I., Gasanov, Sh.Sh., 1962. Cryofacial method and its importance. In: Reviews of the regional and historical cryology (Proceedings of Permafrost Institute, vol. XVIII). Izdvo AN SSSR, Moscow, pp. 103–107 (in Russian).

Vtyurin, B.I., Grigoriev, N.F., Katasonov, E.M., et al., 1957. Local stratigraphy

of Quaternary deposits onshore Laptev Sea. In: Proc. of Interdepartmental Meeting for Preparation of Uniform Stratigraphic Charts of Siberia, 1956. Geostoptekhizdat, Leningrad, pp. 564–572 (in Russian).

Vyltsan, I.A., 2002. Facies and Formations of Sedimentary Rocks. TGU, Tomsk, 484 pp. (in Russian).

Zhestkova, T.N., 1982. Formation of Criogenic Soil Structure. Nauka, Moscow, 216 pp. (in Russian).

Zubakov, V.A., 1986. Global Climatic Events in Pleistocene. Gidrometeoizdat, Leningrad, 288 pp. (in Russian).

Received February 25, 2021
Revised version received March 4, 2021
Accepted March 18, 2021

EARTH'S CRYOSPHERE
SCIENTIFIC JOURNAL

Kriosfera Zemli, 2021, vol. XXV, No. 4, pp. 14–21

GEOTHERMAL FIELDS AND THERMAL PROCESSES IN CRYOSPHERE

INFLUENCE OF METEOROLOGICAL CONDITIONS ON THE THERMAL INSULATION PROPERTIES OF MOSS COVER ACCORDING TO MEASUREMENTS ON SVALBARD

N.I. Osokin, A.V. Sosnovsky

Institute of Geography, RAS,
Staromonetniy lane 29, Moscow, 119017, Russia; osokinn@mail.ru, alexandr_sosnovskiy@mail.ru

On the basis of experimental studies, an assessment of the influence of air temperature and weather type on the heat-shielding properties of the moss cover has been given. It has been revealed that in sunny weather with light cloudiness, the highest temperature of the soil surface under 1 cm thick moss is almost by 13 °C higher than under 5 cm thick moss, while in cloudy weather that difference is 3 °C. The measurements has demonstrated that for the period of 06.07 to 08.08.2016, the average temperature of the 70 cm thick soil layer under the 5 cm thick moss cover was by 1.5 °C lower than that under the 1 cm thick one.

Key words: *meteorological conditions, moss cover, ground temperature, Svalbard.*

INTRODUCTION

To study the response of permafrost to modern climate changes and to develop methods to reduce the negative consequences of the permafrost degradation, it is necessary to study the effect of ground cover on the soil thermal regime. Ground covers have a significant effect on soil temperature [*Novikova, 2016; Kaverin et al., 2019*]. The most common ground cover in the permafrost zone is moss, which is a natural heat insulator. Thermal insulation properties of moss and their year-round dynamics are not studied enough. That is due to large species diversity of mosses and insufficient studies of their thermophysical parameters. The heat-insulating role of the ground covers of the Arctic tundra is considered in the monograph [*Pavlov, 2008*], which presents the results of studies of ground covers effect on the soil surface temperature. A review of studies of thermal conductivity of mosses is presented in [*Tishkov et al., 2013*].

Moss cover, as well as snow cover, reduces heat transfer between the surface air and the underlying substate. However, in contrast to the snow cover, which insulating role is revealed mainly in the period with negative air temperatures, the effect of the moss cover is year-round. The moss cover protects the surface soil layer from summer heating during the period with positive surface air temperatures and from winter cooling, especially under small snow thickness. The snow cover protects the ground from warming-up to positive temperatures only during winter thaws and snowmelt period. In the summer, the moss cover is the main factor which reduces ground heating and thawing, and in the cold season it serves only as an addition to the insulating effect of the snow cover.

To determine the effect of moss cover on the soil thermal regime in the warm season, the authors carried out field measurements for 30 days in July–August in the area of the hydrometeorological station (HMS) in Barentsburg (West Spitsbergen island). The purpose was to study the effect of moss cover on the soil temperature regime, depending on the air temperature and weather type. Previous studies have shown [*Tishkov et al., 2013*] that in mid-August near the Barentsburg settlement the soil surface temperature under 8 cm thick moss cover is by 4 °C lower than in its absence. The depth of loam thaw under 8 cm thick moss cover was 0.98 m with a 0 °C ground temperature at that depth. At the adjacent site without a moss cover, the loam temperature at a depth of 0.98 m was 4 °C with 1.9 m depth of thaw. According to the measurements, the depth of daily temperature changes was 0.1 m under the moss cover and 0.3 m without it. During the period of positive air temperatures, the presence of a moss cover lowers the soil temperature and significantly reduces the depth of thaw.

In the cold period of the year, the thermal conductivity of the frozen moss *Hylocomium splendens* var. *alascanum* is 3–4 times higher than in the summer [*Tishkov et al., 2013*]. This is because the thermal conductivity of ice is approximately four times more than that of water, and the moss water content increases before freezing due to autumn rainfalls. The frozen moss cover is a solid moss-ice monolith. Therefore, the frozen moss cover is not a significant obstacle to soil cooling in the cold season.

The begining time of residual thaw layer formation depends on climatic changes, the parameters of

snow and moss cover, and soil water content [*Kudryavtsev, 1978; Pavlov, 2008*]. Our calculations have revealed [*Sosnovsky, Osokin, 2018*] that for the conditions of the Svalbard Archipelago with 1-m thick snow cover and a sandy-loam with 18 % gravimetric water content, the presence of a 5 cm thick moss cover of *Hylocomium splendens* var. *alascanum* shifts the beginning of of residual thaw layer formation by 24 years, taking into account the data of the regional climate change model [*Forland et al., 2011*]. Thus, under conditions of low (4–5 °C) positive mean daily air temperatures on Svalbard, a decrease in the soil mean annual temperature under the moss cover by several degrees can compensate for a possible increase in air temperature during warming, which protects permafrost from degradation. In [*Cable et al., 2016*] it is noted that in some landscapes of Western Alaska, the absence of a moss layer indicates the absence of permafrost near the surface. Therefore, when calculating the effect of climatic changes on the state of permafrost, it is necessary to take into account the thermal insulation role of the moss cover.

The heat insulation properties of moss are characterized by its thermal resistance and depend both on its thermal conductivity and on features of exact species that determine its water content, density, and structure. The heat insulation role of moss determines the temperature difference between the surface and the moss layer base. It depends on thermal resistance of moss, meteorological conditions and underlying soil properties. In [*Alekseev, 2014*], it is noted that warming in the Arctic is associated with changes in incoming solar radiation regime. During sunny weather, the heat insulation role of moss increases compared to cloudy weather. That is due, in particular, to the different albedo values of the sediment surface and moss. The albedo of soil without vegetation is 17 %, those of black moss and green moss (solid cover) are correspondingly 18 % and 32 % (*http://www.ifaran.ru/...reports/Artamonov.pdf*), while in clear weather the total solar radiation is several times higher than in cloudy weather. As a result, the moss-covered sites will reflect significantly more solar radiation than the sites without moss cover. In cloudy weather, the difference in the temperature regime of these sites will be much smaller.

Water content of the moss and, as a consequence, its thermal conductivity [*Tishkov et al., 2013*] depend on meteorological conditions. Therefore, the variability of meteorological parameters under climate change will affect the heat-insulating role of moss and heat transfer in the 'atmosphere–soil' system.

Under the conditions of climate change, the number of hazardous meteorological phenomena increases [*A report..., 2020*], which include heavy precipitation. Over the past 20 years, its amount has been almost tripled. A decrease in the number of rainy days has been recorded on most of the land around the earth, except for high latitudes in the Northern Hemisphere. In the period of 2000–2099 an increase in the average intensity of precipitation is predicted throughout the land. Analysis of the mean annual precipitation for 1900–1999 has revealed positive trends over continental regions [*Semenov, Bengtsson, 2002*]. A disproportionate increase in heavy precipitation on land, including local maxima in Europe and the Eastern United States, has been identified. For Svalbard, the amount of the mean annual precipitation in most of the archipelago has increased by 10–20 % from 1915 to 2005 [*Forland et al., 2011*]. In rainy weather, part of the precipitation accumulates in the moss cover, increasing its water content and thermal conductivity.

The work [*Pokrovsky, 2019*] presents the results of the analysis of global and regional cloud cover for 1983–2009 obtained within the framework of the International Satellite Cloud Climatology Project (ISCCP). The results of the analysis have demonstrated a decrease in global and regional cloud cover by 2–6 %.

Thus, as a result of climate change and meteorological parameters, the heat-insulating role of the moss cover may change. Therefore, the study of the influence of air temperature dynamics, solar radiation, cloud cover and precipitation on the soil thermal regime under the moss cover will help to make more accurate predictions of permafrost degradation.

The aim of the research is to assess the influence of meteorological conditions on the thermal insulation properties of the moss cover and on the thermal regime the active layer of Arctic soils based on measurement data from Svalbard.

THERMAL PROPERTIES OF MOSS

There are dozens of moss species on Svalbard. They differ both in the thickness of the moss cover and in structural features. *Hylocomium splendens* var. *alascanum* is one of the most common moss species in the area of Barentsburg settlement (Spitsbergen). Its thickness is 5–8 cm and its density is 176 kg/m^3 with water content of 200 %. The moss cover affects near-surface permafrost thawing through the thermal state of the soil and its reaction to meteorological conditions changes, especially in summer. In that case, an important factor is the thermophysical properties of moss, which determine its heat insulation ability. A review of studies of the thermophysical properties of moss is given in [*Tishkov et al., 2013*]. The review presents the values of thermal conductivity of some types of moss obtained during field studies.

The thermal conductivity coefficients of *Hylocomium splendens* var. *alascanum* are calculated for the warm and cold periods of the year according to the formulas obtained in [*Tishkov et al., 2013*]:

$$\lambda_t = 0.0003w + 0.0645,\ \lambda_c = 0.0014w + 0.0645,$$

where w is water content of moss cover (%).

With a water content of 200 %, moss thermal conductivity coefficients in summer and winter are correspondingly 0.12 and 0.34 W/(m·K), and the thermal resistance of a 5-cm thick layer of moss is 0.40 and 0.15 (m^2·K)/W, correspondingly. In winter the thermal resistance of a 5-cm thick layer of moss with 200 % water content corresponds approximately to the thermal resistance of a 2.5-cm thick layer of snow with a density of 200 kg/m^3. Note that the consequence of these formulas is an increase in the coefficient of thermal conductivity of moss with an increase of its water content. Therefore, in sunny weather, when the water content of moss decreases, its thermal conductivity is lower. Thermal insulation properties of moss are enhanced compared to rainy weather.

The thermal conductivity of thawed moss varies within 0.1–0.2 W/(m·K) and depends on its species and water content [*Tishkov et al., 2013*]. The thermal conductivity of frozen moss increases 2–3 times with water content growth.

According to P.N. Skryabin [*Pavlov, 1980*], in the summer of 1978 at the Syrdakh station (Yakutia) for brie mosses, which are distinguished by a large species diversity, with a moisture content of 74–350 %, the values of thermal conductivity coefficient were 0.08–0.30 W/(m·K). At an average water content of 200 %, the thermal conductivity of moss was 0.14 W/(m·K).

RESEARCH AREA AND METEOROLOGICAL CONDITIONS DURING THE MEASUREMENT PERIOD

Soil temperature was measured in the Arctic tundra on the coast of Grönfjord Bay (Spitsbergen island) in the immediate vicinity of the Barentsburg hydrometeorological station (Barentsburg settlement) in the period from July 6 to August 8, 2016.

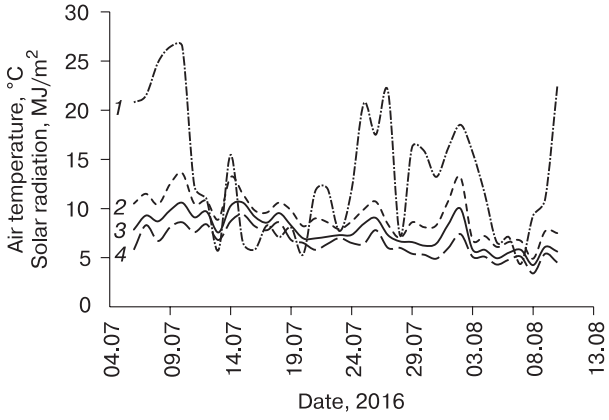

Fig. 1. Dynamics of total solar radiation (*1*) and air temperature.

Air temperature: *2* – maximum, *3* – average daily, *4* – minimum.

Spitsbergen is a mountainous area half of which is covered with glaciers. In the coastal zone, there are flat areas free of ice and occupied by Arctic tundra with poorly developed soil cover, low air temperatures, low soil organic matter content and frequent freeze-thaw cycles.

For the Spitsbergen island near Svalbard Airport, the mean-annual air temperature from 1961–1990 to 1981–2010 has increased from –6.7 to –4.6 °C. Over the calendar summer and winter months, the air temperature during these periods has increased from 4.2 to 5.2 °C and from –15.1 to –11.7 °C [*Forland et al., 2011*]. An increase in air temperature leads to an increase in the thickness of the seasonally thawed layer (STL). Monitoring of the STL thickness in a well drilled in Janssonhaugen 20 km from Longyear, the capital of Svalbard (*http://www.mosj.no/...*), has revealed that over 20 years (from 1998 to 2017), the STL thickness has increased 1.2 times, from 154 to 185 cm.

To measure the soil temperature, two sites with 1 cm thick (*Gymnomitrion* sp., liverwort with a dark surface) and 5 cm thick (*Hylocomium splendens* var. of green color) moss cover, with a diameter of at least 5 m each have been selected. Temperature sensors have been placed in sandy loam with a water content of 18 % to a depth of 0 to 90 cm with an interval of 10–20 cm and at a height of 10 cm above the moss surface. The STL thickness varied from 120 to 250 cm. The temperature recording interval was 30 minutes, which made it possible to track the influence of weather conditions variability on the temperature of STL. The air temperature (data from the website *http://rp5.ru/archive.php?wmo_id=20107*) during the observation period varied from 13.6 °C on July 10, 2016 to 3.4 °C on August 8, 2016 (Fig. 1). At the same time, the maximum daily temperature range was 5.8 °C and was recorded on August 2, 2016. During the measurement period, there were both days with low cloudiness and maximum total daily solar radiation and days with 100% cloudiness and showers with an intensity of up to 20 mm of precipitation have been recorded for several hours (Fig. 1).

Air temperature is largely determined by solar radiation. Thus, the daily maximum air temperature falls mainly on the maximums of the total daily solar radiation (Fig. 1). The maximum total daily solar radiation falls on July 9 and 10, 2016 and is equal to 26.5 MJ/m^2. The minimum total daily solar radiation was recorded on August 7, 2016 and is equal to 4.4 MJ/m^2. On this day, 26 mm of precipitation fell.

Small values of solar radiation fall on July 13, 16 and 20, 2016 (showers and drizzle) and amount to 5.3–5.8 MJ/m^2. The average value of the total solar radiation for the period from July 6 to August 8, 2016 is 13.3 MJ/m^2.

Influence of dayly dynamics of weather conditions on the thermal regime of the active layer under moss cover of different thickness

Let us consider the influence of meteorological conditions (air temperature, solar radiation, cloudiness and precipitation) on the thermal regime of active layer under moss cover of different thickness.

Figure 2, *a* shows the air temperature on July 9, 2016 according to the Barentsburg hydrometeorological station (73 m a.s.l.), air temperature at a height of 10 cm above the moss surface, temperature on soil surface and at depths of 10 and 20 cm under moss cover of 1 and 5 cm thick in clear weather, maximum daily radiation and an average wind speed of 3 m/s.

The measurements have demonstrated that in sunny weather with light cloud cover, the air temperature at a height of 10 cm above the surface of 1 cm thick moss (curve *2*) is higher than above 5 cm thick moss (curve *3*). After 9:00 this difference reaches 2 °C. At the same time, the highest air temperature at a height of 10 cm reaches 22 °C at 18:30. The highest air temperature at the Barentsburg HMS was 12.5 °C at 21:00.

Soil surface temperature under 1 cm thick moss (curve *4*) constantly increases due to solar radiation up to 23.4 °C at 16:00. At the same time, under 5 cm thick moss cover, the highest soil surface temperature reaches 10.6 °C at 17:00 (curve *5*), which is by 12.8 °C lower than under 1 cm thick moss. The measurements revealed that the maximum temperature difference of the soil surface under 1 cm thick moss and soil at 10 cm depth was 14 °C. The highest soil temperature at 10 and 20 cm depths under 1 cm thick moss was 9.6 and 7.2 °C, respectively. The soil temperature at 20 cm depth under 1 and 5 cm thick moss differed by approximately 1.5 °C (curves *6* and *7*).

Clear sunny weather was also observed on other days. On August 2, 2016, the maximum values of the soil surface temperature under 1 cm thick moss (at 16:30) and 5-cm thick moss (at 18:30) were 22 and 11 °C, respectively. The maximum soil surface temperature under 5 cm thick moss was recorded 2 hours later. The maximum air temperature at the Barentsburg hydrometeorological station on this day reached 13.2 °C at 15:00.

On a sunny day on July 26, 2016, with a total cloudiness of 10 %, the air temperature at 19:00 at a height of 10 cm above moss 1 cm thick and 5 cm thick was 18.5 and 16.9 °C, respectively. Note that on a cloudy and rainy day on August 07, 2016, with a heavy railfall (21 mm of precipitation) and total cloudiness of 100 %, the air temperature at 6:00 at a height of 10 cm above moss 1 cm thick and 5 cm thick was almost equal and amounted to 5.4 °C.

The difference between the soil surface temperature and the air temperature (on a sunny day on July 26, 2016) at a height of 10 cm above the moss cover 1 cm thick was 3.5 °C, while at a moss thickness of 5 cm it was 7.2 °C. The soil surface temperature under 1 cm thick moss was 5.2 °C higher than under 5 cm thick moss. The soil surface temperature under 5 cm thick moss basically does not differ from the air temperature at the hydrometeorological station.

The measurement results on a cloudy rainy day on July 13, 2016 (at an average wind speed of 2 m/s) of air temperature, soil surface temperature under moss 1 and 5 cm thick and the soil temperature at a depth of 10 and 20 cm are shown in Fig. 2, *b*.

On this day (July 13, 2016), 100% cloudiness and minimal daily solar radiation were noted. At the same time, 2 mm of precipitation fell at 6:00 and 9:00. After heavy rainfall occurred between 18:00 and 23:00 the soil surface temperature under 1 cm thick moss dropped by 2.5 °C (from 11.0 to 8.5 °C), and under a 5 cm thick moss it decreased by 0.7 °C (from 7.9 to 7.2 °C). At the same time, the soil surface temperature under the moss 1 cm thick was 3 °C higher than under the moss 5 cm thick, mainly in the daytime, while at night the difference was 2 times less. The soil

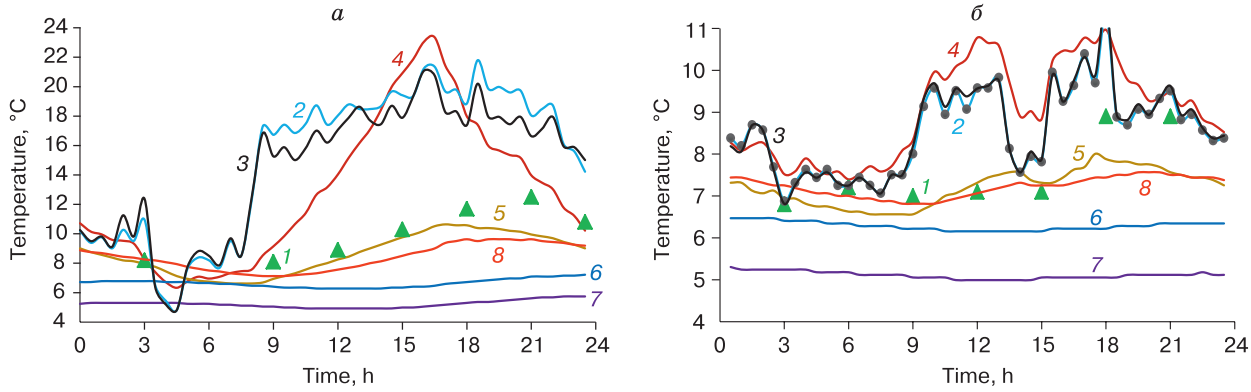

Fig. 2. Air and soil temperature on July 9, 2016 under clear weather and maximum daily radiation (*a*) and on July 13, 2016 under 100 % cloud cover and precipitation (*b*).

Air temperature: *1* – according to the data of the Barentsburg HMS; *2*, *3* – at a height of 10 cm above the moss surface. Soil temperature: *4*, *5* – on the surface; *6*, *7* – at a depth of 20 cm; 8 – at a depth of 10 cm. Moss thickness: 1 cm (*2*, *4*, *6*, *8*) and 5 cm (*3*, *5*, *7*).

temperature at a depth of 20 cm under moss 1 and 5 cm thick differed by approximately 1 °C. The soil surface temperature under the moss 5 cm thick (curve *5*) and the soil temperature at a depth of 10 cm under 1 cm thick moss (curve *8*) are quite close to the air temperature in the period up to 16:00.

A similar picture took place on August 7, 2016 under 100 % cloudiness and precipitation. At night, according to the data from the Barentsburg hydrometeorological station, the air temperature was 0.5 °C higher than above the moss surface, while in the daytime this difference changed sign and increased to 1 °C. At the same time, in the daytime, the soil surface temperature under a layer of moss 1 cm thick exceeded the air temperature above the moss (at a height of 10 cm) by almost 1.5 °C.

The amount of precipitation on August 07, 2016 was 10 and 11 mm at 6:00 and 9:00 and 3 and 2 mm at 18:00 and 21:00, respectively, with 100 % cloudiness. One hour after the shower began, at 18:00 the soil surface temperature under the moss 1 cm thick dropped from 8.6 to 5.8 °C, and under the moss 5 cm thick it lowered from 7.0 to 6.2 °C. Measurements have demonstrated that in cloudy weather the air temperature at a height of 10 cm above the moss cover 5 and 1 cm thick basically coincides (Fig. 2, *b*). The average daily difference between these temperatures was 0.2 °C. Under light cloudiness, as a result of the difference in moss albedo (due to its color), the temperature above moss 1 cm thick is 1 °C higher than that above moss 5 cm thick (Fig. 2, *a*). The air temperature at the Barentsburg hydrometeorological station (at a height of 2 m) is lower than the air temperature above the moss. The largest daily difference of those temperatures was about 4 °C (Fig. 2, *a*), with an average daily value of 2.7 °C.

Measurements of the soil temperature under the moss 1 and 5 cm thick on the coldest and warmest days along with the air temperature at a height of 10 cm above the moss have revealed the following. On a warm day of July 15, 2016 (mean daily air temperature T_a = 10.8 °C), the average soil temperature at a depth of 20–70 cm under a 1 cm thick layer of moss was 1.6 °C higher than under a 5 cm thick one. On a cold day of August 8, 2016 (T_a = 4.4 °C) this excess was 0.5 °C. The mean daily air temperature at a height of 10 cm above the moss 1 and 5 cm thick was 14.3 and 11.6 °C respectively on the warmest day, and 6.8 and 5.7 °C on the coldest day.

Let us consider the effect of the type of weather on the thermal insulation capacity of the moss cover. In clear weather at 16:00 the temperature on the soil surface and at a depth of 20 cm under a 5 cm thick moss cover is 10.5 and 5.1 °C, respectively (Fig. 2, *a*). In this case, the temperature difference will be 5.4 °C, while under the moss cover 1 cm thick this difference is 16.9 °C. The temperature gradient at a depth of 0–20 cm, which determines the heat fluxes into the soil, in these cases is equal to 27°C/m and 88°C/m, respectively. The heat-insulating effect of a moss cover 5 cm thick in sunny weather is 3.3 times greater than that of a moss cover 1 cm thick, which significantly reduces the heat flux into the soil.

In cloudy weather at the same time (Fig. 2, *b*) these gradients are equal to 13 and 22 °C/m, and the heat-insulating effecta moss cover 5 cm thick is 1.7 times greater than that of a moss cover 1 cm thick. Thus, in clear sunny weather, the heat-insulating effect of a moss cover 5 cm thick is almost twice higher that in cloudy weather. This is due to the greater role of the albedo of the moss cover in sunny weather (because of the greater value of the total solar radiation on a cloudless day, see Fig. 1) and a possible change in the moss water content. In sunny weather, there is a slight decrease in a moisture content of moss when it is heated under the sun, and a decrease in the coefficient of thermal conductivity.

The largest difference in soil surface temperature under a moss cover 1 cm thick on clear (Fig. 2, *a*) and cloudy (Fig. 2, *b*) days was 12.4 °C, while under a moss cover 5 cm thick that difference is almost 5 times less and equal to 2.6 °C.

Effect of moss cover on soil temperature during the observation period

The change in the mean daily temperature of air and soil under the moss 1 and 5 cm thick for the observation period from July 6 to August 8, 2016 is shown in Fig. 3. The average wind speed for this period was 2.7 m/s. The measurements have demonstrated that at local air temperature maxima, its values at a height of 10 cm above a 1 cm thick moss (curve *2*) are greater than those above 5 cm thick moss (curve *3*). Moreover, these values are higher than the air temperature according to the data from the Barentsburg hydrometeorological station (curve *1*). The largest temperature difference between the soil surface under the moss 1 and 5 cm thick (curves *4* and 5) fell on July 9, 2016 and amounted to 4.2 °C.

The average soil surface temperature over the period of measurements was 7.4 °C under moss 5 cm thick and 9.6 °C under moss 1 cm thick, with mean air temperature at the Barentsburg station equal to 7.9 °C. The mean soil temperature at a depth of 20 cm under moss 1 cm thick (curve *6*) was by 2.2 °C higher than that under moss 5 cm thick (curve *7*).

The largest difference in soil temperature at a depth of 20 cm under moss 1 and 5 cm thick, equal to 2.2 °C, fell on July 21, 2016. At an average air temperature of 7.9 °C, the average soil temperature at a depth of 20 cm was 5.4 °C (under 5 cm thick moss) and 6.6 °C (under 1 cm thick moss).

At the beginning of the measurement period on July 6, 2016, the soil temperature at a depth of 50 cm under moss cover 1 and 5 cm thick was 3.2 and 1.3 °C,

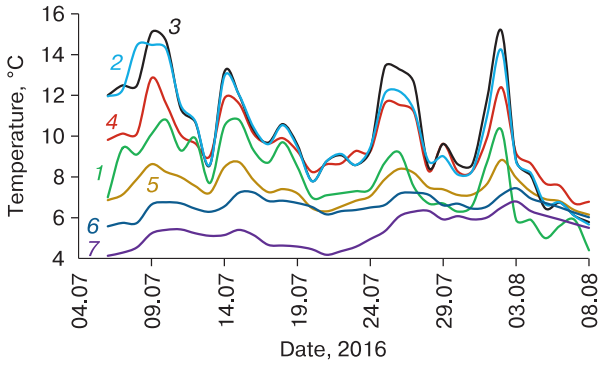

Fig. 3. Dynamics of air and soil temperature.

Air temperature: *1* – according to the data of the Barentsburg HMS; *2*, *3* – at a height of 10 cm above the moss surface. Soil temperature: *4*, *5* – on the surface; *6*, *7* – at a depth of 20 cm. Moss thickness: 1 cm (*2*, *4*, *6*) and 5 cm (*3*, *5*, *7*).

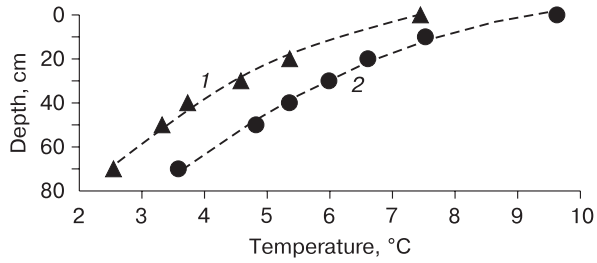

Fig. 4. Depth distribution of the average soil temperature for the period July 6 – August 8, 2016 under 5 cm (1) and 1 cm (2) moss cover.

respectively. The largest difference in soil temperature fell on July 16, 2016 and was 2.8 °C. The average soil temperature difference at a depth of 50 cm under the 1 and 5 cm thick moss was 1.5 °C.

The depth distribution of the soil temperature averaged over the period of July 6–August 8, 2016 at the depth of 0 to 70 cm under the moss 1 and 5 cm thick is shown in Fig. 4. The depth-averaged soil temperature under a 5 cm thick moss layer was 1.5 °C lower than under a 1 cm thick one. Thus, the removal of a moss cover 5 cm thick during the land development can lead to an increase in the active layer temperature by 1.5 °C. The mean soil temperature under the 1 and 5 cm thick moss cover over the measurement period at the depth of 70 cm, 40 cm and on the surface was respectively 3.6 and 2.5 °C, 5.4 and 3.7 °C, and 9.6 and 7.4 °C.

Air temperature influence on soil temperature under moss cover

Studies have demonstrated that at different air temperatures, the heat insulating role of the moss cover can be different. The soil surface temperature for moss 1 cm and 5 cm thick, depending on the mean daily air temperature at the Barentsburg hydrometeorological station, is shown in Fig. 5, *a*. The approximation of mean daily soil surface temperature (T_s) depending on the mean daily air temperature at the hydrometeorological station (T_a) for moss 1 cm thick is

$$T_s = 0.740\ T_a + 3.745,\ R^2 = 0.717,$$

and for the moss 5 cm thick is

$$T_s = 0.304\ T_a + 5.031,\ R^2 = 0.542,$$

where R^2 is the coefficient of determination.

These dependencies are statistically significant at a significance level of 5 %. With an increase in air temperature (at the Barentsburg HMS), the temperature difference of the soil surface under the moss of different thicknesses increases. At mean daily air temperature T_a = 4.4 °C, the mean daily temperature of the soil surface under the moss 1 and 5 cm thick is 6.8 and 6.1 °C, respectively, while at an air temperature of 10.8 °C these values were already 11.6 and 8.2 °C, respectively (Fig. 5, *a*). As a result, as the air temperature rises from 4.4 to 10.8 °C, the temperature difference between the soil surface under the moss cover 1 and 5 cm thick increases from 0.7 to 3.4 °C (Fig. 5, *a*).

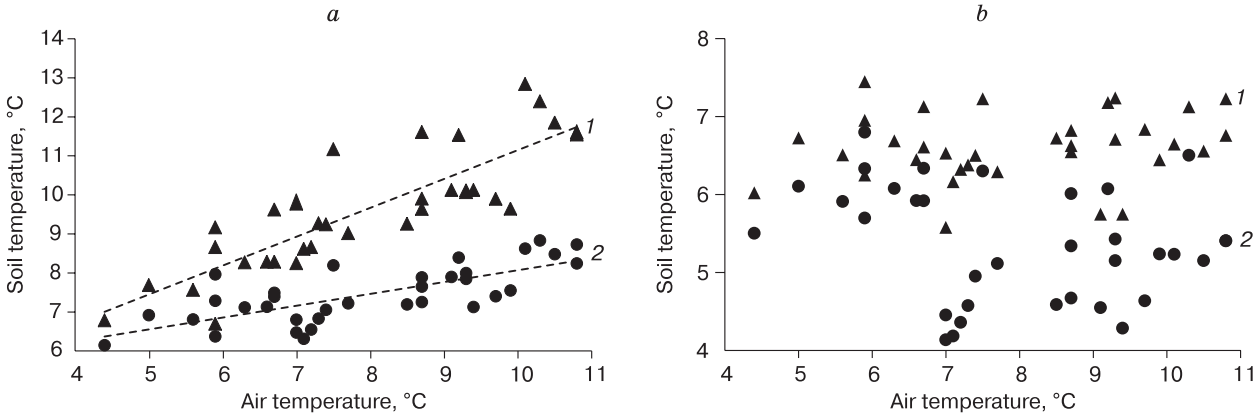

Fig. 5. Dependences of the soil surface temperature (*a*) and soil temperature at a depth of 20 cm (*b*) on the air temperature for moss with a thickness of 1 cm (*1*) and 5 cm (*2*).

The dependence of the soil temperature at a depth of 20 cm under the moss cover 1 and 5 cm thick on the air temperature is shown in Fig. 5, *b*. The figure demonstrates that at an air temperature of more than 7 °C, the average soil temperature at a depth of 20 cm under a moss cover 1 cm thick is 1.5 °C higher than that under a 5 cm thick moss cover. At an air temperature of less than 7 °C, the temperature difference between the soil under moss cover of 1 or 5 cm is almost two times smaller. Thus, with an increase in air temperature, the heat-insulating effect of the moss cover increases. In the presence of significant cloudiness and precipitation, the effect of moss cover on the soil surface temperature regime is much weaker.

This is due to the fact that the increase in air temperature by more than 7 °C occurs mainly due to solar radiation, which leads to the greatest temperature differentiation under the moss cover (Fig. 2, *a*). In cloudy weather, the air temperature and total solar radiation are lower (Fig. 1), and the temperature difference of the soil under the moss cover of different thickness and of different albedo values is smaller (Fig. 2, *b*). Another factor is the difference in the dynamics of soil temperature changes under the moss cover as the air temperature changes. So, with a decrease in air temperature, the initially warmer soil layer under the 1 cm thick moss (compared to moss 5 cm thick) will cool down faster than the soil layer protected by a 5 cm thick moss cover. As a result, the soil surface temperature under the 1 cm thick moss may temporarily become even lower than that under the 5 cm thick moss layer.

CONCLUSION

Under conditions of climate warming, both global and regional cloud cover changes, the number of rainy days decreases due to an increase in the intensity of showers and an increase in the number of days with extreme precipitation, and changes in the mode of incoming solar radiation occur.

The research results have revealed that depending on the type of weather and air temperature, the heat-insulating effect of moss cover changes.

In sunny weather with light cloudiness, the soil surface temperature under the moss *Gymnomitrion* sp. 1 cm thick with dark surface (the albedo of moss and soil are close) increases to 23.4 °C, while under the green moss cover of *Hylocomium splendens* var. 5 cm thick (the moss albedo is twice as high as soil albedo), the highest soil surface temperature is lower by 12.8 °C. In cloudy weather, the soil surface temperature under the 1 cm thick moss did not exceed 11 °C, which is almost by 12 °C lower than that in sunny weather, while the maximum air temperature according to the Barentsburg HMS is 12.5 °C (in sunny weather) and 8.9 °C (in cloudy weather), differed only by 3.6 °C.

The effect of moss cover on soil temperature is determined both by its thickness and by the albedo value. In addition, in rainy weather, part of the precipitation is accumulated in the moss cover, increasing its water content and thermal conductivity. Therefore, after rain, the rapid heating of soil under the moss cover can occur.

The measurements have revealed that with an increase in air temperature, the difference in the temperature of soil surface under the moss cover 1 and 5 cm thick increases, the soil surface temperature under a 5 cm thick moss cover increases grows much more slowly than that under a 1 cm thick moss cover.

In clear sunny weather, the heat insulating effect of the moss cover is almost twice stronger that in cloudy weather. That is mainly due to the greater role of the moss cover albedo in sunny weather as compared to cloudy weather.

It has been determined that for the period from July 6 to August 8, 2016, the temperature of the 70 cm thick soil layer under the 5 cm thick moss cover was, on average, by 1.5 °C lower than that under the 1 cm thick moss cover. As a result, under the 5 cm thick moss cover, the soil thawing depth will be much shallower and the permafrost will last longer.

Acknowledgments. *The research has been carried out within the framework of the State Assignment No. 0148-2019-0004 and with financial support from the RFBR project 17-55-80107 BRICS_a. Expeditionary research on Svalbard was carried out with the financial support of the state assignment 0127-2019-0009 and logistic assistance from the Russian Scientific Center on Spitsbergen (RSCSh).*

References

Alekseev, G.V., 2014. Arctic dimension of global warming. Led i Sneg [Ice and Snow], 54 (2), 53–68.

A report on climate features on the territory of the Russian Federation in 2019, 2020. Federal Service of Russia for Hydrometeorology and Environmental Monitoring (Roshydromet), Moscow, 97 pp. (in Russian).

Cable, W.L., Romanovsky, V.E., Jorgenson, M.T., 2016. Scaling-up permafrost thermal measurements in western Alaska using an ecotype approach. The Cryosphere, No. 10, 2517–2532.

Forland, E.J., Benestad, R., Hanssen-Bauer, I., Haugen, J.E., Skaugen, T.E., 2011. Temperature and precipitation development at Svalbard 1900–2100. Hindawi Publishing Corporation Advances in Meteorology, Article ID 89379.

Kaverin, D.A., Lapina, L.E., Pastukhov, A.V., Novakovsky, A.B., 2019. The impact of transformation in vegetation and soil cover on the soil temperature regime under winter road operation in Bolshezemelskaya tundra. Earth's Cryosphere XXIII (1), 16–25.

Kudryavtsev, V.A. (Ed.), 1978. General Geocryology]. Moscow University Press, Moscow, 464 pp. (in Russian).

Novikova, V.O., 2016. Soil temperature and vegetation cover in sandy steppe plot (Nature Reserve "Dnieper-Orelsky"). Biological Bulletin of Bogdan Chmelnitskiy Melitopol State Pedagogical University, vol. 6 (2), 5–13.

Pavlov, A.V., 1980. Calculation and regulation of permafrost regime of soil. Nauka, Novosibirsk, 240 pp. (in Russian).

Pavlov, A.V., 2008. Monitoring of cryolithozone. Publ. Houuse "Geo", Novosibirsk, 229 pp. (in Russian).

Pokrovsky, O.M., 2019. Cloud changes in the period of global warming: the results of the international satellite project. Issledovanie Zemli iz Kosmosa [Earth Research from Space], No. 1, 3–13.

Semenov, V.A., Bengtsson, L., 2002. Secular trends in daily precipitation characteristics: greenhouse gas simulation with a coupled AOGCM. Climate Dynamics, No. 19, 123–140.

Sosnovsky, A.V., Osokin, N.I., 2018. Impact of moss and snow cover on the sustainability of permafrost in West Spitsbergen due to climate change. Vestnik Kolskogo Nauchnogo Tsentra [Bulletin of the Kola Scientific Center of the RAS], No. 3, 179-185.

Tishkov, A.A., Osokin, N.I., Sosnovski, A.V., 2013. The impact of moss synusia on the active layer of Arctic soil and subsoil. Izvestiya Rossiiskoi Akademii Nauk. Seriya Geograficheskaya [Bulletin of the Russian Academy of Sciences. Geographic series], No. 3, 39-46.

URL: http://www.ifaran.ru/science/conferences/kislovodsk2014/reports/Artamonov.pdf (last visited: 02.03.2020).

URL: http://www.mosj.no/en/climate/land/permafrost.html (last visited: 02.08.2020).

URL: http://rp5.ru/archive.php?wmo_id=20107 (last visited: 02.08.2020).

Received September 13, 2020
Revised version received March 22, 2021
Accepted April 19, 2021

EARTH'S CRYOSPHERE
SCIENTIFIC JOURNAL

Kriosfera Zemli, 2021, vol. XXV, No. 4, pp. 22–29

SURFACE AND GROUND WATERS IN TERRESTRIAL PER,AFROST REGION

FORMATION AND EVOLUTION OF MORAINE-DAMMED PERIGLACIAL LAKE NURGAN, NORTHWESTERN MONGOLIA

G.V. Pryakhina[1], M.P. Kashkevich[1], S.V. Popov[1,2], V.A. Rasputina[1], A.S. Boronina[1,3], D.A. Ganyushkin[1], A.R. Agatova[4], R.K. Nepop[4]

[1] *St. Petersburg State University, 10th line V.O., 33, St. Petersburg, 199178, Russia; g65@mail.ru*
[2] *Polar Marine Geosurvey Expedition, Pobedy str. 24, Lomonosov, St. Petersburg, 198412, Russia*
[3] *State Hydrological Institute, 2nd line V.O., 23, St. Petersburg, 199004, Russia*
[4] *Institute of Geology and Mineralogy, SB RAS, Akademika Koptyuga ave. 3, Novosibirsk, 630090, Russia*

The shrinking of mountain glaciers under the impact of climate warming is a global process. It leads to the formation of periglacial lakes in the areas of degrading glaciation. The lifetime of moraine-dammed lakes is ephemeral on the geological time scale. They are characterized by dynamic instability and are prone to catastrophic outbursts in the case of destruction of moraine dams. Often, catastrophic floods are accompanied by mudflows. Glacial outburst floods and mudflows cause significant damage to the infrastructure and populated localities in the mountain foothills. In this study, we present the stages of formation and evolution of a periglacial water body on the example of Lake Nurgan (Tsambagarav, northwestern Mongolia). Based on the results of the comprehensive field research, we have described the transgressive, regressive, and post-regressive phases of the periglacial reservoir evolution.

Key words: *moraine-dammed lakes, periglacial lakes, formation of periglacial lakes, moraine-dammed lakes outbursts.*

INTRODUCTION

Degradation of modern glaciation in many mountainous areas leads to the formation of moraine-dammed lakes. Such water bodies are interpreted as short-lived lakes on the geological time scale. Catastrophic failure of dams in periglacial lakes often results in glacial lake outburst floods (GLOFs) with high discharge rates and flow velocities sufficient to trigger mudflows [*Vinogradova et al., 2017; Chernomorets et al., 2018*].

Much interest has recently been attracted to hazardous exogenous processes in the Altai Mountains in the aftermath of the catastrophic outburst flood of moraine-dammed Maashey Lake. This event occurred on July 15, 2012 due to the erosional activity of torrents caused by heavy rains; they destroyed the rock glacier damming the lake. The ensuing lake outburst flood thus triggered a high-magnitude mudflow event [*Dokukin, 2015*].

Most scientific papers related to the study of moraine-dammed lake outbursts are aimed at studying the process of formation of GLOFs and at recognition of their mechanisms and controlling factors [*Emmer, Cochachin, 2013; Kidyaeva et al., 2018; Neupane et al., 2019*]. Much fewer publications address the problems of the formation and evolution of periglacial water bodies. The area of the Altai Mountains is relatively little studied in this respect, although, according to [*Ganyushkin et al., 2016*], the area of alpine glaciation tends to reduce there, which suggests an increase in the number of moraine-dammed lakes.

The authors hope that this research will contribute to the understanding of the origin and evolution of moraine-dammed periglacial lakes. We consider these problems by the example of Nurgan Lake (Altai mountain system, Tsambagarav, Northwestern Mongolia), a typical representative of moraine-dammed lakes in the mountains.

OBJECT OF STUDY

Nurgan Lake is located in the area of the Tsambagarav Range of the Altai Mountains (Fig. 1) and belongs to the type of moraine-dammed alpine lakes. After the retreat of the Eregtiyn Glacier originated on the northeastern and northern slopes of the dome-shaped Tsast-Ula peak (4208 m a.s.l.) with an area estimated at 4.94 km^2 [*Ganyushkin et al., 2016*], the lake has lost its direct contact with this glacier. At present, their connection is maintained through two relatively large streams fed by the glacier and discharged into the lake. The major discharge of the glacier is through an outlet tunnel in the ice-cored moraine dating back to the Little Ice Age (LIA) with the inlet and outlet zones located at 3255 and 3185 m a.s.l., respectively. The northwestern part of the lake basin bears evidence of the earlier failure of the lake-damming moraine in the form of a V-shaped channel (Fig. 2, *a*). This is where an outlet stream from the lake is formed.

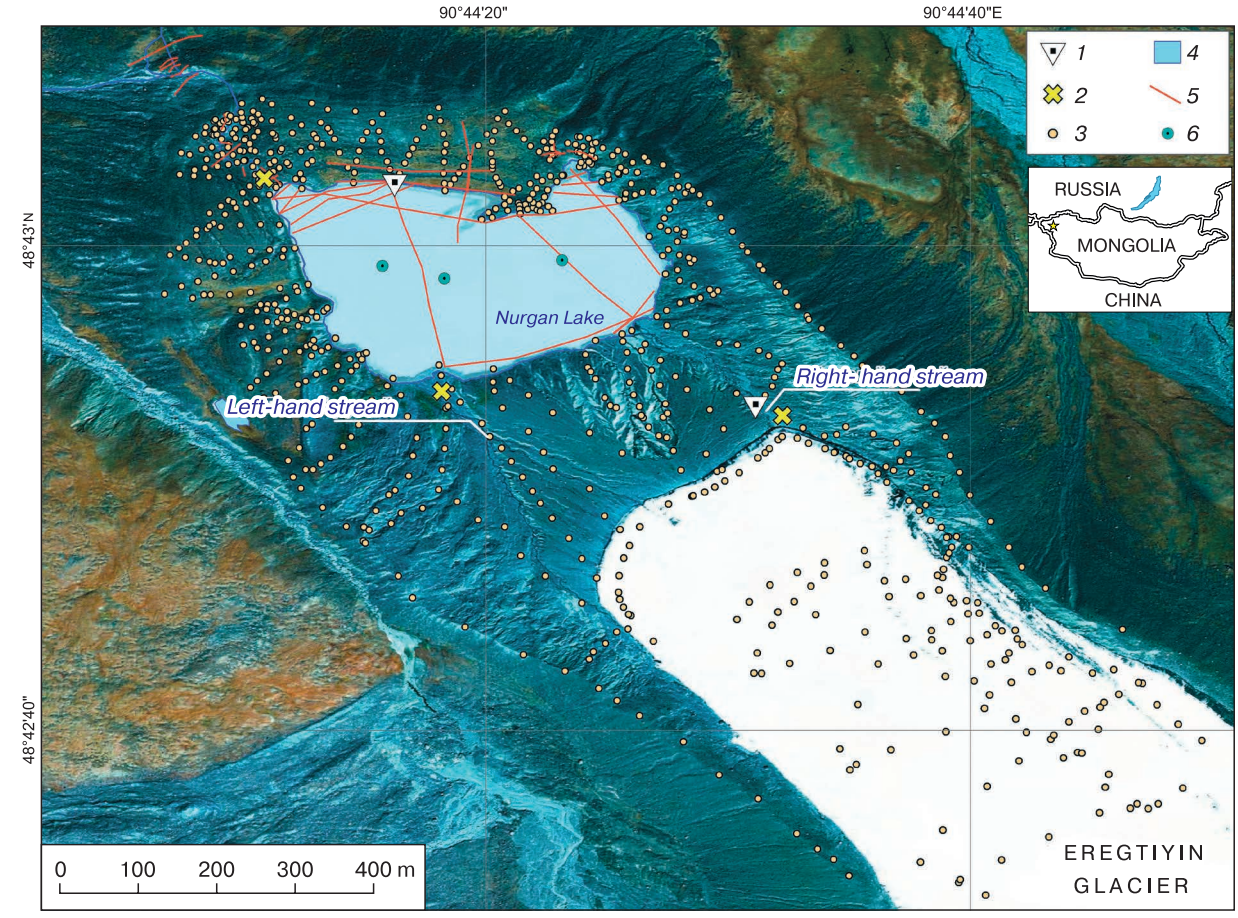

Fig. 1. Schematic map of the study area.

1 – gauging stations; *2* – stream velocity measuring points; *3* – tacheometric measurement points; *4* – bathymetric survey region; *5* – GPR survey profiles; *6* – water sampling points. Blue line shows the only outlet stream from the lake.

Fig. 2. View over Nurgan Lake and moraine dam from the glacier (*a*), northern slope of the moraine (*b*).

Photos by A.S. Boronina and S.V. Popov, August 2019. The dashed lines indicate moraine fragments that document possible past high water levels with the elevation relative to the WGS 84 ellipsoid.

MATERIALS AND METHODS

In July–August 2019, comprehensive field studies of the Nurgan Lake area were performed within the framework of the expedition of the St. Petersburg State University. Figure 1 illustrates the scope of the fieldwork.

Bathymetric surveys were conducted from a manned inflatable boat. The lake depths were measured using a electronic sonar Garmin ECHOMAP 42cv chartplotter (Garmin Ltd., Taiwan). The lake boundary was mapped using a Garmin GPSmap 64st with GPS and GLONASS receiver, and the bathymetric scheme was compiled using the Surfer 16 specialized mapping software (Golden Software Inc., USA).

A tachometric survey of the lakeshore areas and the glacier surface topography was completed using a Trimble M3 DR 5″ total station (Trimble Navigation Ltd, USA). The data processing was largely based on previously developed algorithms [*Popov, Boronina, 2019*]. The lake water level monitoring was conducted in the period from July 29 to August 5 with measurements taken twice a day at a temporary gauging station. The gates for measuring stream flow velocity and water sampling for turbidity were located in streams fed from the Eregtiyn Glacier near their confluence with the body of water and at the outlet stream from the lake.

The stream velocity was measured by a flow velocity meter FVM-1 (Russian abbreviation: ИСП-1). The volume of water collected in the lake over a 24-hour period was inferred from water level observations using the water volume curve. The ratio between the volumes of water entering the lake and discharged from it was judged from the water flow monitoring data on a daily basis for the two inlet streams and the outflowing watercourse. Turbidity of the water samples was determined in the Laboratory for Geoecology and Environmental Monitoring of the Institute of Earth Sciences of St. Petersburg State University in compliance with the methodology provided in [*Potapova et al., 2006*]. For $\delta^{18}O$ isotope analysis, the water was sampled in the central offshore area of the lake from different depths with a 5 m sampling interval, starting from the surface. The obtained data were processed at the Climate and Environmental Research Laboratory of the Arctic and Antarctic Research Institute (AARI, St. Petersburg) using a Picarro L2120-i gas analyzer. Distilled tap water with a $\delta^{18}O$ value of –9.79 ‰ relative to the IAEA VSMOW (Vienna Standard Mean Ocean Water) standard was used as a reference sample.

The retreat rate of the slope brow with developing thermokarst were studied in 10 points at different sites of the lakeshore on July 29, August 3, and August 6, 2019 (Fig. 3).

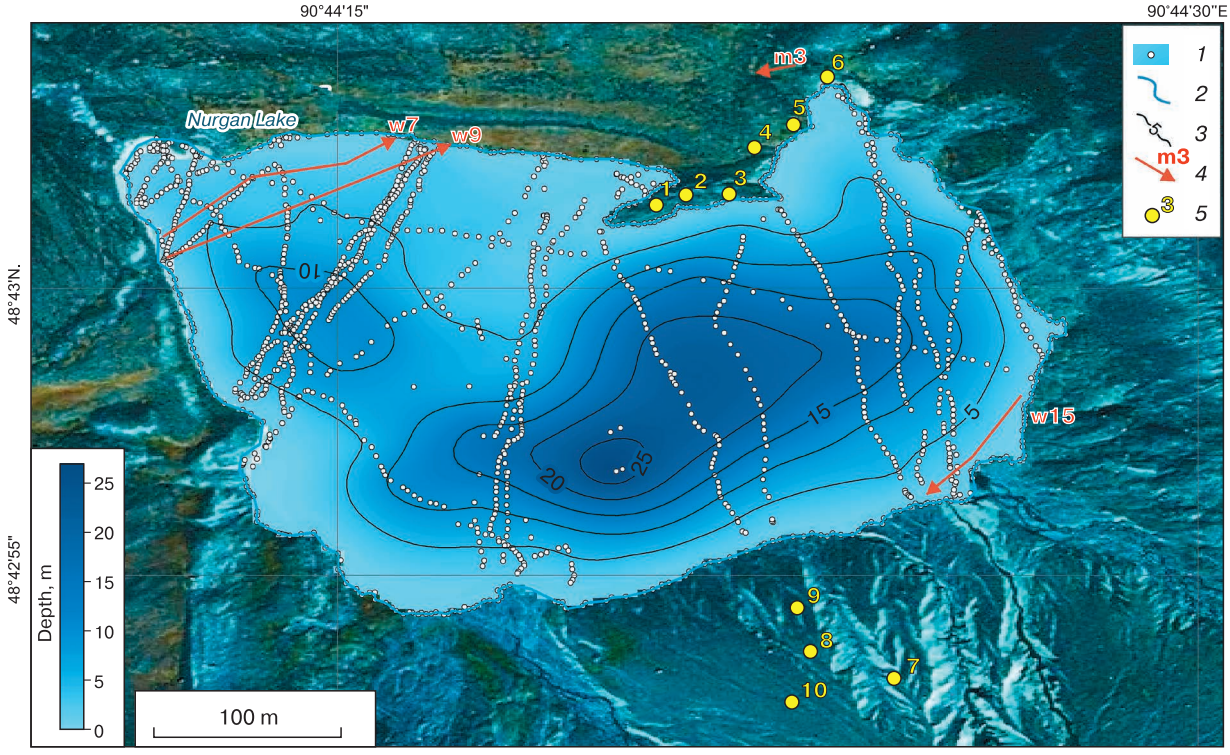

Fig. 3. Bathymetric map of Nurgan Lake.

1 – depth measuring points; *2* – shoreline; *3* – water depth lines (5 m section); *4* – GPR survey lines and their numbering; *5* – thermokarst monitoring points.

The geophysical studies of the Nurgan Lake area and its surrounding moraine deposits involved GPR (Ground Penetrating Radar) surveys using a domestic GPR OKO-2 tool (Logistics Systems LLC, Russia) coupled with a shielded 400 MHz frequency antenna (AB-400). The GPR data were processed and depicted with the Geoscan32 software (Logistics Systems LLC, Russia).

RESULTS AND DISCUSSIONS

Origin of the lake basin and transgressive phase of its evolution

The lake basin structure and its morphometric characteristics affect the hydrological regime of the lake (in particular, the water-level and the water temperature) and also indirectly indicate the origin of the lake bowl.

Analysis of the Nurgan Lake bottom relief revealed its complex pattern that includes depressions alternating with levelled areas. The area with greatest depths (up to 25 m) identified in the southern part of the lake immediately contacts the area with armored dead ice. In view of a greater steepness of the slopes on the eastern side of the lake, considerable water depths tend to be found immediately at the water's edge. Another depression is located in the western part of the lake, where it is up to 10 m deep (Fig. 3). The bottom relief is more gentle in the northern and northeastern parts of the lake. According to [*Zimnitskiy, 2005*], alternation of depressions and uplifts within the offshore areas is inherent in the relief of periglacial lakes which are completely or partially carved in the ice.

The instrumental role played by ice in the formation of the lake basin is also evidenced by the geophysical studies conducted over the lake water area (Fig. 4). The wave pattern of the obtained GPR sections has revealed a layer of ice with inclusions of boulders of various sizes beneath the surface layers of bottom sediments made up by finely dispersed material (fluvioglacial deposits) and coarse-grained material (terrestrial material deposited as a result of debris transport from glacier moraine).

Results of the modeling also indicate the presence of bottom ice. The GPR time sections (Fig. 4, *c*) represent numerous diffracted waves produced by heterogeneous media. The travel time curve of one of them was modeled within the dipping layer medium model [*Popov, 2017*] and is shown in the time section. The layer-by-layer modeling has demonstrated that the best match between the real and modeled travel time curves is achieved when the medium's relative permittivity is ~3.17 which is typical of ice [*Macheret, 2006*].

It is thus highly possible that the lake began to form on the surface of ice which was already stagnant (in quiescent phase) and located below the glacier after the Little Ice Age (LIA) that culminated ca. AD 1810–1820 [*Ganyushkin et al., 2016*]. This was succeeded by the transgressive phase of the evolution of Nurgan Lake. This phase featured the lake basin filling by melt water with a gradual rise in the water level and an enlargement of the basin's extent and depth. Simultaneously, the layer of bottom sediments accumulated. The thickness of the upper layer of fluvioglacial deposits inferred from the GPR data in different parts of the lake bottom varies from 0 cm (steep sites) to 20 ± 2 cm (flat sites). These are underlain by the layer of terrigenic sediments from 0.5 to 1 m (±2 cm) thick. With sedimentation rate assumingly equal to 0.5 mm/year for ice-dammed glacial lakes [*Anan'eva et al., 1996*], a layer of finely dispersed material was likely to have formed over the past 200 years on the lake floor.

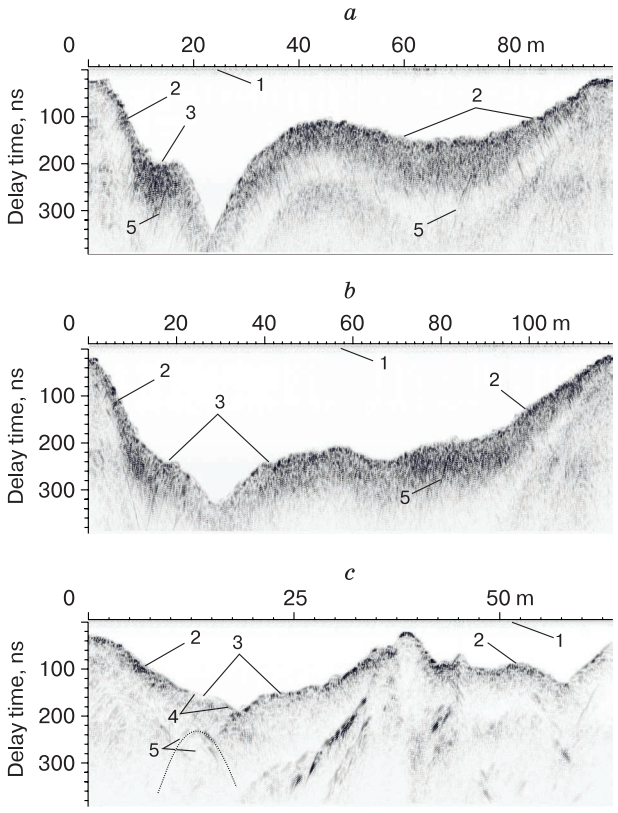

Fig. 4. GPR time section along the GPR survey lines w7 (*a*), w9 (*b*) and w15 (*c*).

1 – direct wave; reflections: *2* – from the lake sub-bottom, *3* – from the terrace, *4* – from fluvioglacial deposits; *5* – diffracted wave. The calculated travel-time curve is shown by dashed line (*c*). For positions of the GPR survey lines see Fig. 3.

Regressive phase of the lake evolution

By the time of the field work, Nurgan Lake had shrunk (following the main phase of the regressive stage) both in area and water volume, which is evidenced by the preserved imprints in the relief mark-

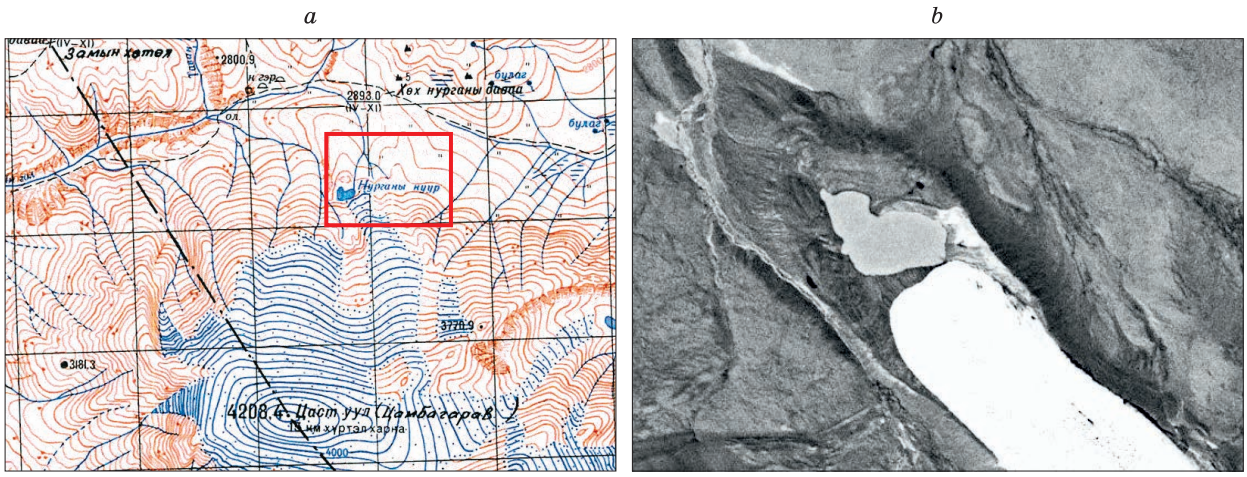

Fig. 5. Topographic map of the Tsambagarav Range (*a*) and a fragment of the Corona image (*b*).

ing out changes in the volume of water and in the direction of water discharge from the moraine-dammed lake. The geomorphological observations have revealed two lake terraces remaining on the northern slope of the lake basin. Their elevations are 2988 and 2991.5 m a.s.l., both being considerably higher than the present-day water level and marking the former levels (Fig. 2, *b*). Technically, this is a short V-shaped valley beginning from the level of the upper terrace and cutting through the lateral moraine ridge in the northeastern part of the lake basin. The incision mark reaches an elevation of 2994 m, which is about 11 m higher than the present-day water level in the lake. Presently, this valley is free from water flow. On the 1:100,000 topographic map (M 46-110) of the study area (1969), based on the 1948–1949 aerial photography data (Fig. 5, *a*), the Nurgan Lake outlet stream is located in the northeastern part of the moraine. The analysis of the Corona satellite image taken on August 11, 1968 (Fig. 5, *b*) revealed that at that time there had already been a stream in the northwestern part of the moraine, and the lake area was 54,450 m^2 (i.e., it was smaller than its present extent). This implies that the hydrological network represented on this fragment of the map most likely reflects the situation in 1948–1949.

It can therefore be assumed that lake water levels tended to be high within the interval between the end of the LIA and the mid-20th century. The moraine dam failure in the northwestern part in the period between 1948 and 1968 was accompanied by the formation of a new outflow from the lake and a drawdown of the lake water level. Dimensions of the formed water passage were inferred from the tacheometric survey; they were as follows: the maximum width was 165 m along the crest of the moraine dam 30 m across the bottom; the depth was ~17 m; the area and the average width were 1640 m^2 and 96 m, respectively.

Since the outburst flood occurred against the background of the functioning outlet stream in the northwestern part of the moraine, the major controlling factors could be either an excess amount of water (compared to the streambed capacity) flowing into the lake or the accompanying destabilizing processes that weakened the moraine dam.

Post-regressive evolution of the lake

The formation of the channel in the moraine did not result in the complete emptying of the lake basin; the surface runoff was maintained through the lake outlet stream in the northwest. We will reproduce the further development of the body of water and consider the main factors affecting the state of moraine-dammed lakes. Among them, the major role belongs to the *lake filling pattern in the periods of maximum ablation*.

As the considered region is characterized by low precipitation (mean annual precipitation is 200–300 mm) [*Otgonbayar, 2012*], the runoff of meltwater from the glacier is the main source of the lake recharge. This was confirmed by the stable-isotope analysis, which demonstrated that the $\delta^{18}O$ content in the water of Nurgan Lake is relatively stable at different depths and equals 16.2 ‰. This is a compelling evidence in favor of the assumption that the lake is mainly being fed from the glacier. The total volume of water collected in the lake during the 24-hour period was inferred from a relationship between the amounts of water entering the lake and discharged from it with due account for the change in the lake level. It averaged 4,388 m^3. At this, the total inflow was estimated at 10,436 m^3, of which 8,208 m^3 (79 %) accounted for the river channel inflow, and 2,160 m^3 (21 %) for catchment-wide water inflow. The volume of discharged water totaled 6,048 m^3.

A comparative estimate of the extent of the body of water for the period between 1968 and 2019 (based

on the satellite image taken in 1968 and the results of the bathymetric survey in 2019) indicated a 12 % increase in the lake water area over 51 year, while the water level has decreased by 3 m. This attests to the fact that during the period of the greatest contribution of water from the glacier (both on daily and seasonal scale), the lake inlet flow was greater than the outlet flow, i.e., the filling of the lake with water proceeded faster than the discharge of water from the lake.

Note that the outlet water flow from the lake proceeds through a shallow channel, whose configuration vanishes at a distance of about 70 m from the stream head, prompting the water to filter into the moraine and thus decreasing the flow velocity. The stream carrying capacity explicably decreases with the increasing glacier melt runoff, so the water mass starts collecting in the relief depressions giving rise to small lakes and creating additional backwater (Fig. 6). Silting of these areas with fluvioglacial material carried by the lake outlet water flow may reduce their filtration capacity and eventually result in the flooding.

The second factor capable of triggering the process of lake degradation that may end up in its disappearance is *intensive accumulation of solid material, which suggests the basin's increasingly filling with alluvial, fluvioglacial, proluvial sediments* [*Zimnitskiy, 2005*]. Analysis of the samples indicated that the level of water turbidity in the outlet stream is almost 15 times lower than in the glacier-melt runoff streams: 5.7 vs 90.2 mg/L (in the left-hand stream), respectively. For the entire period of ablation, the amount of solid material deposited in the lake is estimated at 107 tons per year, which is 95 % of the overall solid material coming with the glacial runoff.

The third factor is the *dam stability, which is largely controlled by the processes of filtration and thermal erosion in the body of the moraine dam*.

The field studies revealed no filtration through the moraine, while it is known that the cores of dead ice or frozen ground may be contained inside the LIA moraines whose melting leads to fast disintegration of rocks [*Korup, Tweed, 2007*]. According to [*Chistyakov, Ganyushkin, 2015*], thermal erosion driven be the recent climate warming has intensified significantly in the Altai Mountains. Thus, the area affected by intense thawing accompanied by ground failure was detected by the surveys in the northeastern part of the slope of the studied lake basin, which implies a substantial increase in thermal erosion during the period of enhanced ablation. Within a week of the field work, the maximum edge displacement relative to the survey marks (stakes) reached 2.18 and 1.54 m for stakes 4 and 5, respectively (Fig. 3) with the average displacement of 0.65 m.

The geophysical investigation of the moraine dam (a 400 MHz GPR profiling) indicates that the boundary between the upper dry and the underlying water-saturated sediments (number 1 in Fig. 7, *a*) is traced throughout almost the entire studied section at a depth of ~2 m. Another boundary (number 2 in Fig. 7, *a*) is identified lower and is characterized by less contrasting reflections. This boundary is probably associated with a transition between wet and frozen rocks with inclusions of ice lenses. The region of contrasting reflections (Fig. 7, *b*) is assumingly attributed to the contact between patches of buried glacial ice and the surrounding rocks interpreted as water-saturated due to their seasonal thawing. The maximum GPR study depth (with AB-400 antenna) of moraine sediment was about 5 m, which is associated with the high content of a conductive clay component in the sediment and, as a result, a high attenuation of the electromagnetic wave with depth.

The presence of the dry/wet rock boundary is confirmed by the observations. Figure 8, *a*, *b* portrays the outcrop wall directly at the GPR survey site. The GPR profile ran parallel (~2 m apart) to the bluff edge (Fig. 8, *c*). The measuring tape position corresponded to the profile center.

Fig. 6. Outlet stream from Nurgan Lake.

The photos were taken by A.S. Boronina from one place on August 6, 2019 at 12:55 (*a*) and 14:55 (*b*).

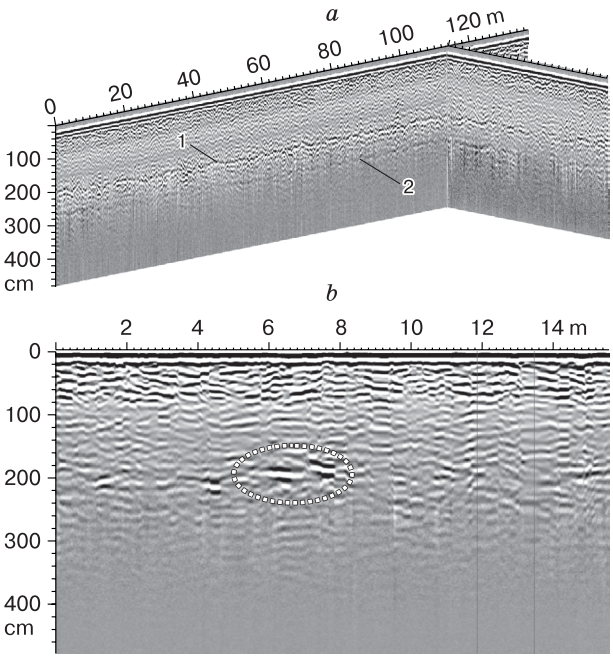

Fig. 7. Results of the GPR surveys in the area of sediments deposited by moraine.

a – northern lakeshore: 1 – boundary between dry and wet deposits, 2 – boundary between wet and the underlying frozen deposits; *b* – northeastern lakeshore: bright reflections (highlighted with a dashed line) on the GPR images correspond to the position of ice lenses.

Thus, during the field work, no large ice lenses were detected in the moraine body (to a depth of 5 m from the surface), whose thawing could involve the formation of internal drainage channels. At a depth of 2.5–2.8 m from the surface, the ground was permanently frozen and possibly included separate ice lenses. While thawing, the latter produced the overlying water-saturated active layer. The portion of the moraine dam located below the water level was very likely in a stable state, given that the survey did not reveal the signs of submoraine ice ablation and erosion.

CONCLUSION

Analysis of the obtained results allows identifying the stages of a periglacial lake evolution and major factors controlling this process. As is the case with many lakes of this type, after its appearance, Lake Nurgan passed into a transgressive stage of evolution that lasted for about 150 years. During this period, the lake basin formation and its filling with glacial meltwater took place. Thus, after the inception of the lake on the surface of stagnant ("dead") ice, it gradually transformed into a moraine-dammed lake. At this stage, the amount of the inflowing glacier-melt runoff was the major control. The authors believe that during this period, all of the glacier-melt runoff was captured by the lake, which resulted in its filling to the maximum possible level. The moraine dam failure led to a partial discharge of the lake and its transition

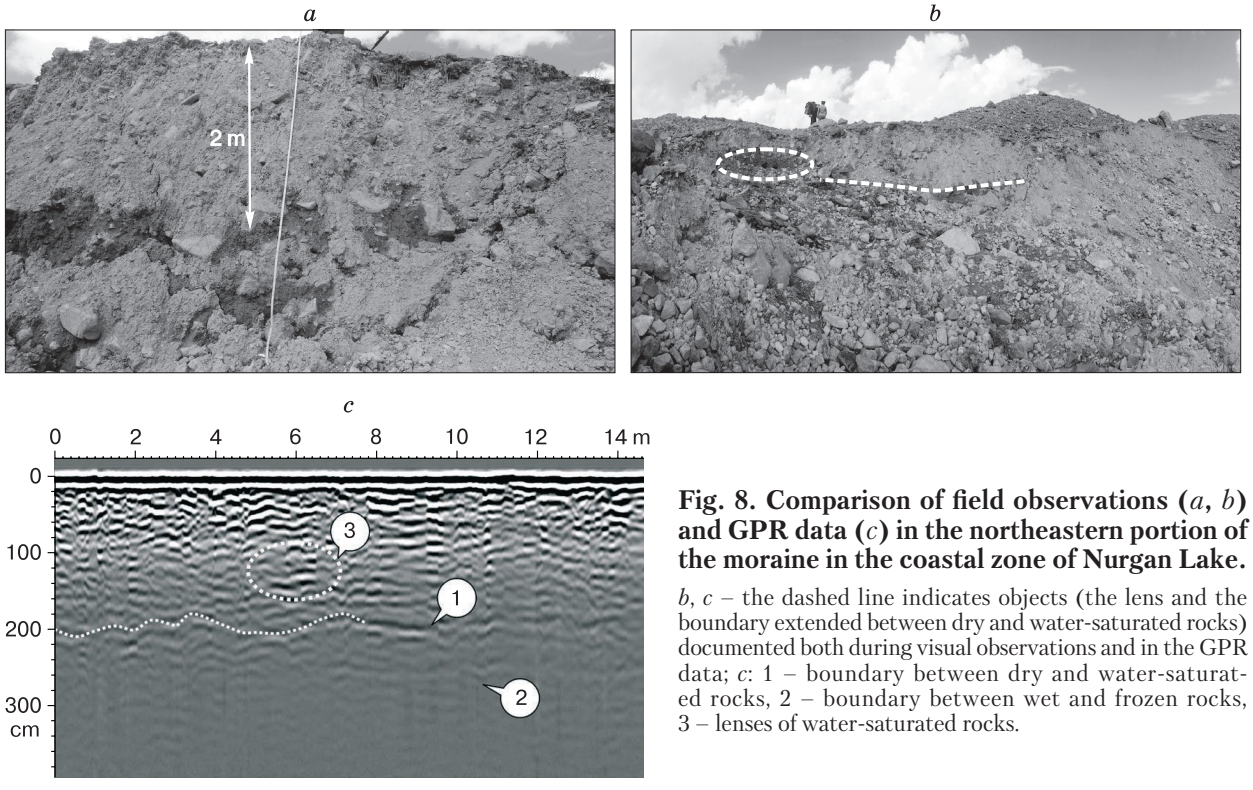

Fig. 8. Comparison of field observations (*a*, *b*) and GPR data (*c*) in the northeastern portion of the moraine in the coastal zone of Nurgan Lake.

b, *c* – the dashed line indicates objects (the lens and the boundary extended between dry and water-saturated rocks) documented both during visual observations and in the GPR data; *c*: 1 – boundary between dry and water-saturated rocks, 2 – boundary between wet and frozen rocks, 3 – lenses of water-saturated rocks.

into the regressive stage, which is also characteristic of many lakes of this type. As one can infer from the shape and size of the carved channel, the moraine dam failure occurred rapidly as a consequence of the lake water outflowing over the moraine ridge and eroding its body. The major controls of this process were: (i) the water pressure exerted on the dam body and (ii) stability of the dam which could be affected by both the external forces (seismic activity) and the internal moraine processes. The latter included water filtration and thawing of frozen soil. The absence of large glacial "ice cores" (inferred from the geophysical data) in the upper 5-meter layer of the undisturbed portion of the moraine and evidences of buried ice on the side slopes of the channel allowed dismissing this factor of the dam destabilization. The significant deepening of the lake basin was primarily liable for the partial rather than complete draining of the lake.

After partial destruction of the moraine dam, Nurgan Lake entered the stage of slow filling. Since then, the lake area has shown only a 12 % increase (~0.2 % per year). The lake filling rate has been affected by the existing lake discharge pattern and the fact that the glacier-melt runoff mostly escapes the lake being discharged from the basin through an ice grotto at 3185 m a.s.l. and giving rise to the Eregtiyn-Gol River. At the present stage of its evolution, the lake can be generally interpreted as a quasi-stable object.

Unfortunately, a short period of the water body regime monitoring precluded more reliable prediction of its further evolution. We should however pay attention to some trends which, given a certain combination, may affect the evolution of the body of water to the extent that it returns to the active transgressive phase. These include:

– presently poorly developed outflow channel from the lake and the associated water-level fluctuations;

– the presence of areas with developed thermokarst processes in the moraine dam;

– possible moraine failure with subsequent blocking the flow channel by moraine material, thereby adding to the water level in the lake.

The intensive melting of the Eregtiyn Glacier under the impact of modern climate warming can result in the Eregtiyn-Gol River flow redirecting straight into the lake, which will significantly contribute to its water level rise.

Acknowledgments. *The authors would like to express their sincere gratitude to D.V. Bantsev for his help in conducting the field work and for providing data on the isotope analysis of the water samples.*

This study was supported by the Russian Foundation for Basic Research, project no. 19-05-00535-a "Natural catastrophes and transformation of the landscapes of SE Altai and NW Mongolia during the Last Glacial Maximum)".

References

Anan'eva, E.G., Efremov, Yu.V., Parunin, O.B., 1996. Some features of sedimentation in the Great Caucasus mountain lakes. Litologija i poleznye iskopaemye [Lithology and Mineral Resources], No. 4, 359–365.

Chernomorets, S.S., Petrakov, D.A., Aleynikov, A.A., et al., 2018. The outburst of Bashkara Glacier lake (Central Caucasus, Russia) on September 1, 2017. Earth's Cryosphere XXII (2), 61–70.

Chistyakov, K.V., Ganyushkin, D.A., 2015. Glaciation and thermokarst phenomena and natural disasters in the mountains of North-West Inner Asia. In: Environmental Security of the European Cross-Border Energy Supply Infrastructure, NATO Science for Peace and Security Series C: Environmental Security. M.G. Culshaw et al. (Eds.), pp. 207–218, DOI: 10.1007/978-94-017-9538-8_13.

Dokukin, M.D., 2015. Extraordinary glacial lake outburst floods in 2012–2013 (based on remote sensing data). In: Proc. of the North Caucasus Institute for the design of water management and land reclamation construction, Pyatigorsk, pp. 82–97 (in Russian).

Emmer, A., Cochachin, A., 2013. The causes and mechanisms of moraine-dammed lake failures in the Cordillera Blanca, North America Cordillera, and Himalayas. AUC Geographica, 48 (2), 5–15.

Ganyushkin, D.A., Otgonbayar, D., Chistyakov, K.V., Kunaeva, E.P., Volkov, I.V., 2016. Recent glacierization of the Tsambagarav ridge (North-Western Mongolia) and its changes since the Little Ice Age maximum. Led i Sneg [Ice and Snow], 56 (4), 437–452.

Kidyaeva, V.M., Petrakov, D.A., Krylenko, I.N., et al., 2018. An experience in modeling the Bashkara lakes outbursts. Georisk [Georisk], XII (2), 38–46.

Korup, O., Tweed, F., 2007. Ice, moraine, and landslide dams in mountainous terrain. Quatern. Sci. Rev. 26, 3406–3422.

Macheret, Yu.Ya., 2006. Radio-echo Sounding of Glaciers. Nauchnyi mir, Moscow, 392 pp. (in Russian).

Neupane, R., Chen, H., Cao, C., 2019. Review of moraine dam failure mechanism. Geomatics, Natural Hazards and Risk, 10 (1), 1948–1966.

Otgonbayar, D., 2011. Glacier-water resources of closed-drainage areas of Western Mongolia: current assessment and trends of change. PhD Dissertation Abstract. Tomsk, 170 pp. (in Russian).

Popov, S.V., 2017. Determination of dielectric permittivity from diffraction traveltime curves within a dipping-layer model. Earth's Cryosphere XXI (3), 75–79.

Popov, S.V., Boronina, A.S., 2019. Software for processing data of tachometric survey. In: Geodesy, Cartography, Geoinformatics and Cadastre: Abstracts of the III Russian Conference in Applied Science, pp. 258–263 (in Russian).

Potapova, T.M., Fedorova, I.V., Parshina, T.V., 2006. Methods for determining the granulometric and geochemical composition of bottom sediments and suspended sediments: a teaching aid. Izd-vo SPbGU, St. Petersburg, 94 p. (in Russian).

Vinogradova, T.A., Kazakov, N.A., Vinogradov, A.Yu., et al., 2017. Hazardous hydrological phenomena (concise lectures): Teaching aid. Tipografija "Znak", St. Petersburg, 128 pp. (in Russian).

Zimnitskiy, A.V., 2005. Formation, distribution and dynamics of periglacial lakes in the Western and Central Caucasus (within the borders of Russia). PhD Dissertation Abstract. Krasnodar, 22 pp. (in Russian).

Received October 3, 2020
Revised version received January 17, 2021
Accepted February 18, 2021

EARTH'S CRYOSPHERE
SCIENTIFIC JOURNAL

Kriosfera Zemli, 2021, vol. XXV, No. 4, pp. 30–39

PERMAFROST ENGINEERING

EFFICIENCY OF SURFACE COOLING OF FROZEN FOUNDATION SOILS USING A FORCED REFRIGERANT CIRCULATION UNIT

J.B. Gorelik[1], A.K. Khabitov[2], I.V. Zemerov[1]

[1]*Earth Cryosphere Institute, SB RAS, Malygina str. 86, Tyumen, 625026, Russia; gorelik@ikz.ru, zemerov.utmn@gmail.com*
[2]*Giprotyumenneftegaz, Respubliki str. 62, Tyumen, 625000, Russia; prof.power@yandex.ru*

A method for surface cooling of frozen foundations has been proposed. It includes heat insulation through the soil surface and a unit for forced circulation of a refrigerant. The latter is used only in summer during the entire period of operation of the structure. The method has important advantages in comparison with the known methods of surface cooling: a) a seasonally thawed layer can't be formed at any time of the annual cycle and the cooling impulse enters the ground base throughout the entire calendar year; b) in urban conditions, the use of a machine cooling method (instead of seasonally operating cooling systems) is quite reasonable since it does not require significant space for its implementation. Analysis of the results of temperature fields calculating demonstrates quick cooling of the ground base: for all calculation options, the temperature at the depth of zero annual amplitude in the second year of operation reaches a value corresponding to hard frozen state of most of the soils. The decrease becomes even more significant in the third year of operation. The calculation results are rather weakly dependent on the distance between the cooling elements of the applied cooling system within the considered range of variation of that value (from 0.7 to 1.0 m).

Key words: *frozen soils, seasonal thawing layer, ground temperature regime, heat-insulation layer, forced cooling, time to reach the required temperature.*

INTRODUCTION

Surface methods of cooling and thermal stabilization of frozen soils of the structure foundations eliminate the need to perform laborious work on drilling the soil, its moving and deepening it into the base of the elements of cooling devices and require significantly lower implementation costs in comparison with other methods. The gain in reducing labor intensity is most obvious when such work must be carried out manually on a previously prepared pile field, or in the presence of overlapping of the ventilated underfloor space of buildings [*Dolgikh, 2014; Abrosimov et al., 2018*]. At the same time, all the cooling experience available until recently indicates that surface methods are significantly inferior in cooling efficiency both in terms of the duration of reaching the design temperature regime and in the amount of temperature decrease at the base [*Makarov, 1985; Konovalov, 1989; Bubelo, 2003*]. However, relatively recently, based on the analysis of the formation mechanism of a temperature shift in the presence of covers of arbitrary nature on the soil surface [*Gorelik, Zemerov, 2020*], it was possible to select a surface coating design that can provide the required temperature in the base at a sufficiently high cooling rate. Such the coating includes a layer of high-quality heat insulation and a cooling element of a horizontal, naturally operating tubular system laid under it on the ground surface (GET) [*Dolgikh et al., 2014*]. Since the depth of seasonal thawing is significantly being reduced with high-quality heat insulation, then with the onset of the cold period, the thawed layer quickly freezes. After that, the 'zero curtain' disappears [*Kudryavtsev, 1978*], the cold from the surface (cooling impulse) begins to spread into the depth of the soil, and that process continues until the end of the winter period. As a result, the duration of cooling impulse increases significantly in comparison with the usual freezing conditions.

Since in winter time a sufficiently low temperature is maintained on the soil surface, under the layer of snow and heat insulation (due to the action of cooling element of the GET system), and the bottom of the active layer is located close to that surface, then the temperature at its bottom will be much lower for a long time than under normal conditions. As a result of the enhanced action of those two factors, – a decrease in the average annual temperature at the base of the seasonal freezing layer and an increase in the duration of the cooling impulse – the above-noted increase in the cooling rate is possible when the required temperature at the base is reached. The corresponding calculation results and their analysis are given in [*Gorelik, Khabitov, 2021*], where the main emphasis is placed on the use of the GET cooling system, which is capable of operating only in the winter season. However, as shown in that work, the cooling

intensity significantly increases if for a short time (during one summer season) a forced circulation of refrigerant unit is connected to the evaporator of the GET system. In the presence of high-quality heat insulation, the summer source of cold prevents the formation of a layer of seasonal thawing, thereby eliminating the power-intensive process of its freezing in winter. In that case, the duration of the cooling impulse reaches its maximum value, which leads to the reaching of a positive effect. At the same time, it is not difficult to understand that if, in the considered scheme of surface cooling, the use of the condensing unit of the GET system is completely excluded, reserving the forced cooling unit, which will be switched on only during the summer period of the entire service life of the structure, then the formation of a layer of seasonal thawing on the soil surface under the heat insulation will be impossible. In that case, the formation of temperature at a depth of zero annual amplitude occurs under the influence of the average annual temperature on the soil surface (the concept of the average annual temperature at the bottom of the active layer loses its meaning here).

Approximate estimates of the average annual surface temperature, performed according to the formulas given in [*Gorelik, Khabitov, 2021*] demonstrate a quite comparable result of cooling by the method proposed here in comparison with the options for using the GET system. In fact, the proposed method replaces the use of cooling devices in the winter season (using the GET system) for summer time by machine way. That replacement has significant advantages in urban areas, where the placement of very large capacitor units in residential areas will inevitably lead to known problems. The use of a machine cooling method is a completely industrial method that does not require significant space for its implementation. We also note that at present, domestic manufacturers have developed and mastered the production of units with the necessary parameters [*Okunev, Dolgikh, 2017*].

In addition to the aforesaid, the proposed method can be used in a number of areas of the globe with a hot climate with a global rise in temperature to create zones of climatic comfort. They can be created in the near-surface layers of the soil by surface cooling. However, we will not dwell on that issue in this article.

The purpose of this work is to calculate the cooling of frozen foundations using sufficiently accurate methods, to analyze them and to draw conclusions about the effectiveness of the proposed cooling method.

Calculation procedure for cooling using a forced circulation refrigerant unit

Calculations of the temperature dynamics in the basement soils with the machine cooling method have been performed for a building with an underfloor space having lateral dimensions of 12 × 24 m and, in general repeat the same procedure used in [*Gorelik, Khabitov, 2021*] for the GET cooling system. The design and location of the cooling system elements within the pile field are shown in Fig. 1. The evaporator pipes of the cooling system are laid in a coil along the major axis of the building and covered with a leveling layer of sand. Standard heat-insulating panels are laid end-to-end along the leveling layer (with the necessary trimming at the points of pile bypass) within the entire surface of the ventilated underfloor space.

The horizontal distance between the axes of adjacent evaporator tubes (L) is taken in two versions: 1.0 m and 0.7 m, the diameter of the tubes (D) is 37 mm. The thickness of the heat insulation of the standard panel (h) is 100 mm, the thermal conductivity coefficient of the material (λ_i) is 0.03 W/(m·°C). The main trends in the behavior of temperature fields can be determined for a soil homogeneous in terms of thermal properties. The heterogeneity of those properties can only be associated with local quantitative deviations from the general trend in the behavior of temperature, which do not fundamentally affect the general nature of its change. That is justified by the fact that, in the problem under consideration, the frozen soil lying below the bottom of the active layer does not change its state in the course of temperature changes.

To describe the dynamics of temperature in it, in a first approximation, we can neglect the change in the amount of unfrozen water with temperature (which is a good approximation for sandy and sandy-loam soils, and for water-saturated fine-dispersed soils, the calculation error is not critical). In that approximation, the process of heat transfer is purely conductive and is described by the classical equation

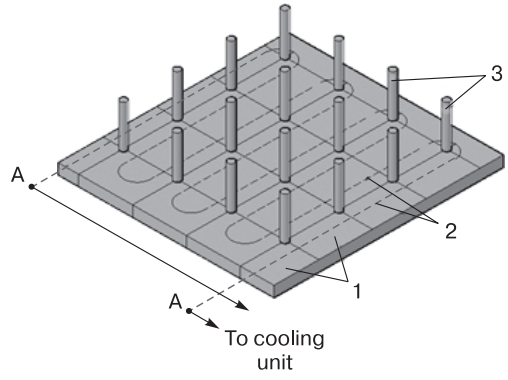

Fig. 1. Layout of elements of the cooling system in the underfloor space of the building (above-foundation structures are not shown).

1 – heat insulation plates; 2 – evaporator pipe (cooling element); 3 – foundation piles; A – points of connection of the cooling unit to the cooling element.

of thermal conductivity [*Kudryavtsev, 1978*] with variable coefficients (thermal conductivity and volumetric heat capacity) varying along the vertical coordinate in accordance with the change in soil properties through the section. In standard calculation schemes, the change in these coefficients along the vertical is approximated by step functions, which makes it possible to reduce the heat conduction equation to a form containing only one parameter – the thermal diffusivity of frozen soil (μ_f), which also depends on the vertical coordinate. The change in that parameter in different type of soils within the entire range of their density and water content, determined, for example, from the table of thermal properties [*SNiP 2.02.04-88, 1990*], can be represented as: $\mu_f = k \cdot 10^{-6}$ m^2/s, where the k value is within a rather narrow range: $0.5 \leqslant k \leqslant 1$. This means that general conclusions about the behavior of temperature in frozen soils can be obtained for a constant value of the μ_f coefficient from the specified range, while they remain valid (with small quantitative variations) for a wide range of practically important cases.

For ease of comparison with the results of calculations in [*Gorelik, Khabitov, 2021*], in all calculation options, the same soil characteristics are adopted as in the cited work (indexes for thawed soil and frozen soil are taken correspondingly as *u* and *f*). Thermal conductivity coefficient: $\lambda_u = 1.75$, $\lambda_f = 1.80$ W/(m·°C); volumetric heat capacity: $C_u = 2.68 \cdot 10^6$, $C_f = 2.20 \cdot 10^6$ J/(m^3·°C); density of dry soil: $\gamma_s = 1500$ kg/m^3; soil water content: $w = 0.2$. The transition of a unit volume of frozen soil to the thawed state is characterized by the value of the latent volumetric heat: $\kappa_v = \kappa \gamma_s w$, where $\kappa = 3.34 \cdot 10^5$ J/kg ($\kappa_v = 10^8$ J/m^3) – that value in the considered cooling method is important only for the surface soil layers beyond the building plan projection. The soil water content due to unfrozen water: $w_u = 0$. The freezing point of soil: $t_b = 0$ °C. The initial temperature of the soil at the base (t_0) is taken as –0.7 °C.

The problem setting includes the heat conduction equation for a half-space (excluding the inner regions of the circles corresponding to the location of the evaporator tubes), which is written in enthalpy form for the purpose of applying numerical solution methods [*Samarsky, Vabishchevich, 2003*]:

$$\frac{\partial H}{\partial \tau} = \frac{\partial}{\partial y}\left(\lambda \frac{\partial t}{\partial y}\right) + \frac{\partial}{\partial z}\left(\lambda \frac{\partial t}{\partial z}\right), \qquad (1)$$

where: y, z are horizontal and vertical coordinates; enthalpy $H(t)$ is a function of temperature t at an arbitrary point of the soil body and is determined taking into account the heat of the phase transition localized near the interphase boundary:

$$H(t) = \begin{cases} k_v + C_u, & \text{if } t \geq 0\ ^\circ C, \\ C_f t, & \text{if } t < 0\ ^\circ C. \end{cases}$$

After differentiation with respect to temperature and time, on the left side of the (1), before the derivative of temperature with respect to time, a factor is formed which has the meaning of the effective heat capacity of soil and contains a δ function of temperature for which the smoothing procedure can be carried out [*Samarsky, Vabishchevich, 2003*]. For the numerical solution of the equation (1), the setting of boundary conditions on the moving boundary (which is formed during seasonal processes outside the contour of the structure) is not required.

The boundary condition on the upper surface of the soil is set by the 3rd kind condition:

$$\alpha\left(t_a(\tau) - t_s\right) = -\lambda\left(\frac{\partial t}{\partial z}\right)_s .$$

Here t_s is the temperature of the soil surface (determined during the counting process); λ is the thermal conductivity coefficient of the soil, which, depending on its state, takes the values of λ_u or λ_f; α is the coefficient of heat exchange between the soil surface and air, which takes on the values of α_s (summer) or α_w (winter) in the corresponding seasonal intervals. Their determination has been carried out according to the method of work [*Gorelik, Pazderin, 2017*]. The calculated values of those coefficients turn out to be equal: $\alpha_s = 23.2$, $\alpha_w = 1.12$ W/(m^2·°C).

According to the data of [*Okunev, Dolgikh, 2017*], on the evaporator wall, the cooling unit can maintain the temperature within the range of –15 to –32 °C. For calculations, the maximum temperature value out of that range is taken. Accordingly, the boundary condition on the side of the evaporator tube during the active period of the unit operation is written in the form of a constant temperature $t_t(\tau) = -15$ °C. The start of operation of the unit and its interruption are associated with the dates of the spring and autumn transition of the average daily air temperature through 0 °C. In the calculation examples those dates are taken as May 01 and October 01.

The progress of air temperature ($t_a(\tau)$) throughout the year is taken as a piecewise constant function of mean-month temperatures. As in the work [*Gorelik, Khabitov, 2021*], data on air temperature have been taken from the Urengoy Meteorological Station (Table 1). Within the underfloor space, the soil body is considered as a two-layer vertically, where the upper layer corresponds to heat insulation and is characterized by thickness (h), thermal conductivity coefficient (λ_i), and zero contribution of the phase transition heat to the effective heat capacity.

The coordinate system is located in a horizontal plane which coincides with the soil body surface, its center coincides with the geometric center of the building in the plan. The *Oz* axis is directed vertically downward, the *Ox* and *Oy* axes lie in the horizontal

Table 1. **Annual variation of air temperature at the Urengoy Meteorological Station**

Month	Mean air temperature,°C	Month	Mean air temperature,°C
January	–26.4	July	15.4
February	–26.4	August	11.3
March	–19.2	September	5.2
April	–10.3	October	–6.3
May	–2.6	November	–18.2
June	8.4	December	–24.0

plane and are directed, respectively, along the long and short axes of the building. The dimensions of the computational domain along each of the axes are determined by the radius of thermal influence [*Gorelik, Pazderin, 2017*] and when calculating for no more than a 5-year period, that radius does not exceed 35 m. Thus, the boundaries of the computational domain should be removed by 35 meters from the boundaries of the underfloor-space contour in plan and at the same distance into the depth of the soil vertically. At those boundaries, the heat flux is set to zero.

The problem is solved numerically. A finite-difference scheme is used, in which the domain of the required function is covered by the computational grid [*Aziz, Settary, 2004*]. To obtain discrete analogs of the equations, the model uses the control volume method [*Patankar, 2003*]. In [*Gorelik et al., 2008*], a finite-difference analogue of the equation (1) is presented.

The calculation procedure used here has been repeatedly tested on various problems and described earlier [*Gorelik et al., 2014, 2019; Gorelik, Khabitov, 2019a,b*].

CALCULATION RESULTS AND THEIR DISCUSSION

As demonstrated in [*Gorelik, Khabitov, 2021*], when using surface methods, there is an optimal sequence of installation and switching-on of the cooling system elements. In the case under consideration, such a sequence includes the following stages: a) *the initial stage* starts from the beginning of the first winter period and finishes with its end, no elements of the cooling system are installed, the seasonally thawed layer completely freezes due to the atmospheric natural cold; b) *the stage of installation of the cooling system elements* begins at the end of the first winter season: the evaporator of the system is laid, a leveling layer of sand is added, and the entire surface is covered with heat insulation, the cooling unit is connected, the work is completed by the beginning of the summer season; c) *the stage of forced cooling* is counted from the beginning of the summer season: the cooling unit is turned on, which operates continuously until the start of the new winter season, after which it is turned off. Further, the process is periodically repeated with a fully connected cooling system for the entire service life of the structure, while in the summer there is cooling by means of a forced cooling unit, and in winter, a certain amount of cooling is added from the atmospheric air due to the imperfection of the applied heat insulation (although the characteristics of its material taken in the calculations are quite high). An important feature of the described method is the absence of a layer of seasonal thawing at any time of the annual cycle, which eliminates the need for a very power-intensive process of its freezing, and the effect of the cooling impulse continues throughout the year.

Figure 2 presents the results of calculating the temperature fields at the basement of the building at $L = 1$ m in the central section ($x = 0$) for the 1st and 2nd year of the building's operation; the calculation results for the edge of the building ($x = 12$ m) are presented in Fig. 3. Similar results for $L = 0.7$ m are presented in Fig. 4, 5. The lines in the field of Figures 2–5 demonstrate the position of the isotherms in the considered section of the basement, the numbers along the line indicate the corresponding temperature of the isotherms. The color scale at the bottom demonstrates the correspondence of a certain color in the picture field to the calculated temperature value.

Figure 6 presents the three-year dynamics of temperature change in the central section and along the edge of the building at a depth of 0.2 m and at a depth of zero annual amplitude ($z_0 = 10$ m).

Comparison of the temperature fields shown in those figures demonstrates a high rate of decrease in soil temperature at the base both in its central section and along the edge of the building: in all options of the calculation, the temperature at a depth of zero annual amplitude in the second year of operation reaches a value corresponding to the solid-frozen state of most soils. An even more significant decrease is reached in the third year of operation (Fig. 6, *b*, *d*). Such rates of temperature decrease correspond to similar results for the most effective options of surface cooling with the combined use of the GET system and a forced cooling unit, which are considered in [*Gorelik, Khabitov, 2021*]. The rate of temperature decrease is several times higher than the typical values of 3–5 years for the known methods [*Vyalov et al., 1979; Khrustalev, Nikiforov, 1990*]. The calculation results are rather weakly dependent on the distance between the evaporator tubes (L) within the considered range of its value (from 0.7 to 1.0 m).

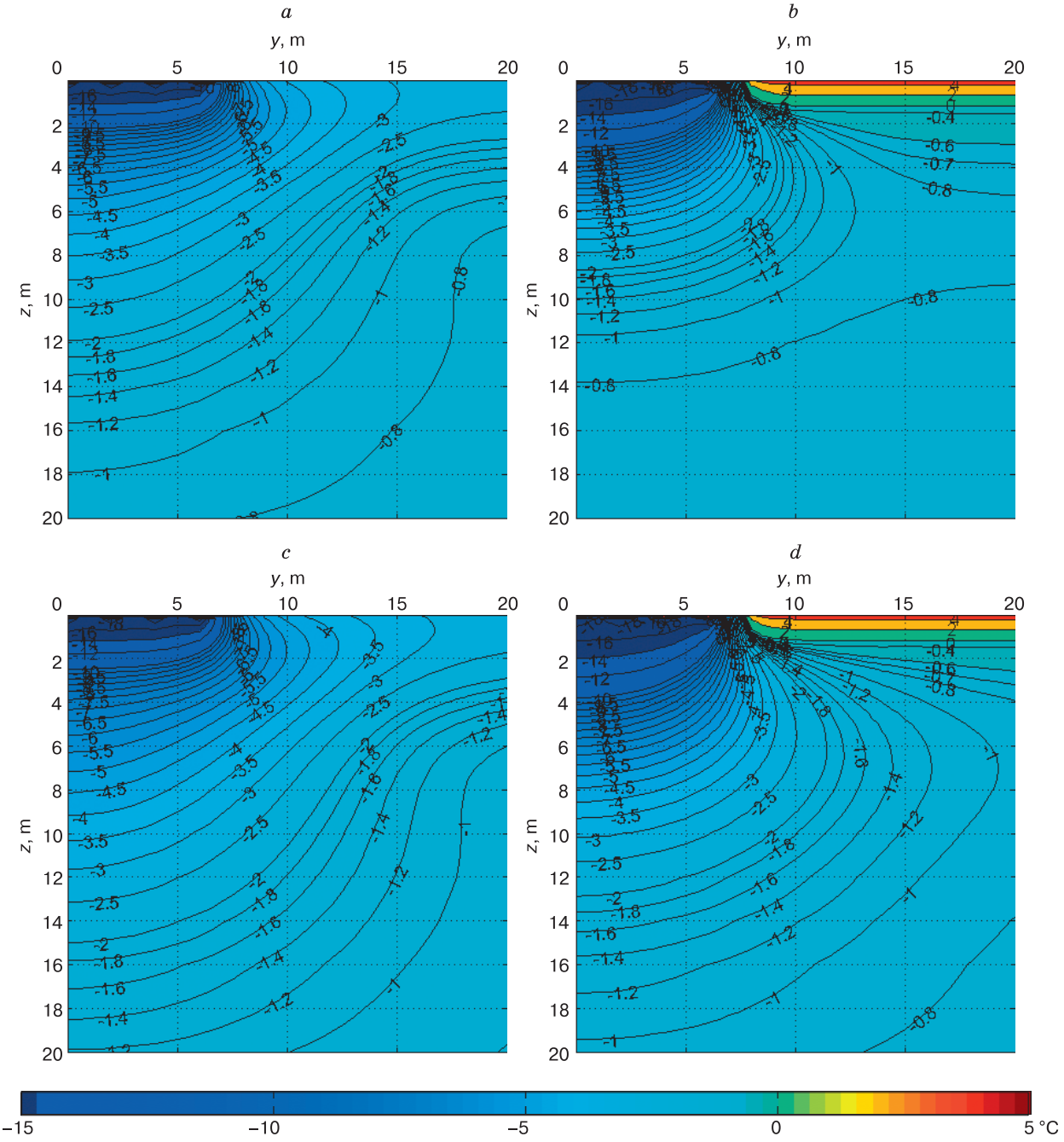

Fig. 2. Temperature fields at the base of the building in the central section (x = 0) with the distance between the evaporator pipes (L) equal to 1 m.

a, b – the 1st year of operation; c, d – the 2nd year of operation; a, c – end of winter; b, d – end of summer.

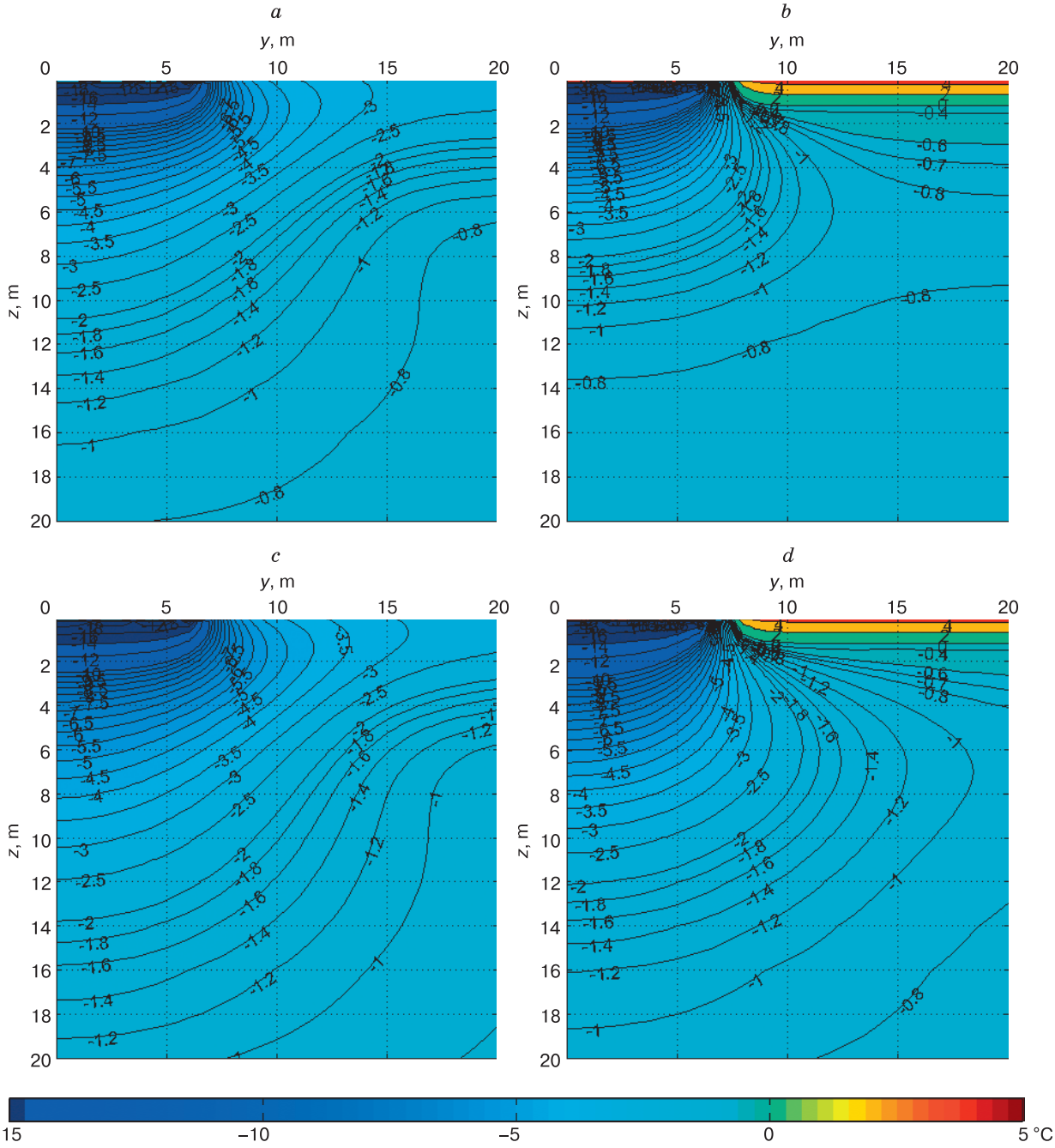

Fig. 3. Temperature fields at the base for the edge of the building (x = 12 m) with the distance between the evaporator pipes (L) equal to1 m.

a, b – the 1st year of operation; c, d – the 2nd year of operation; a, c – end of winter; b, d – end of summer.

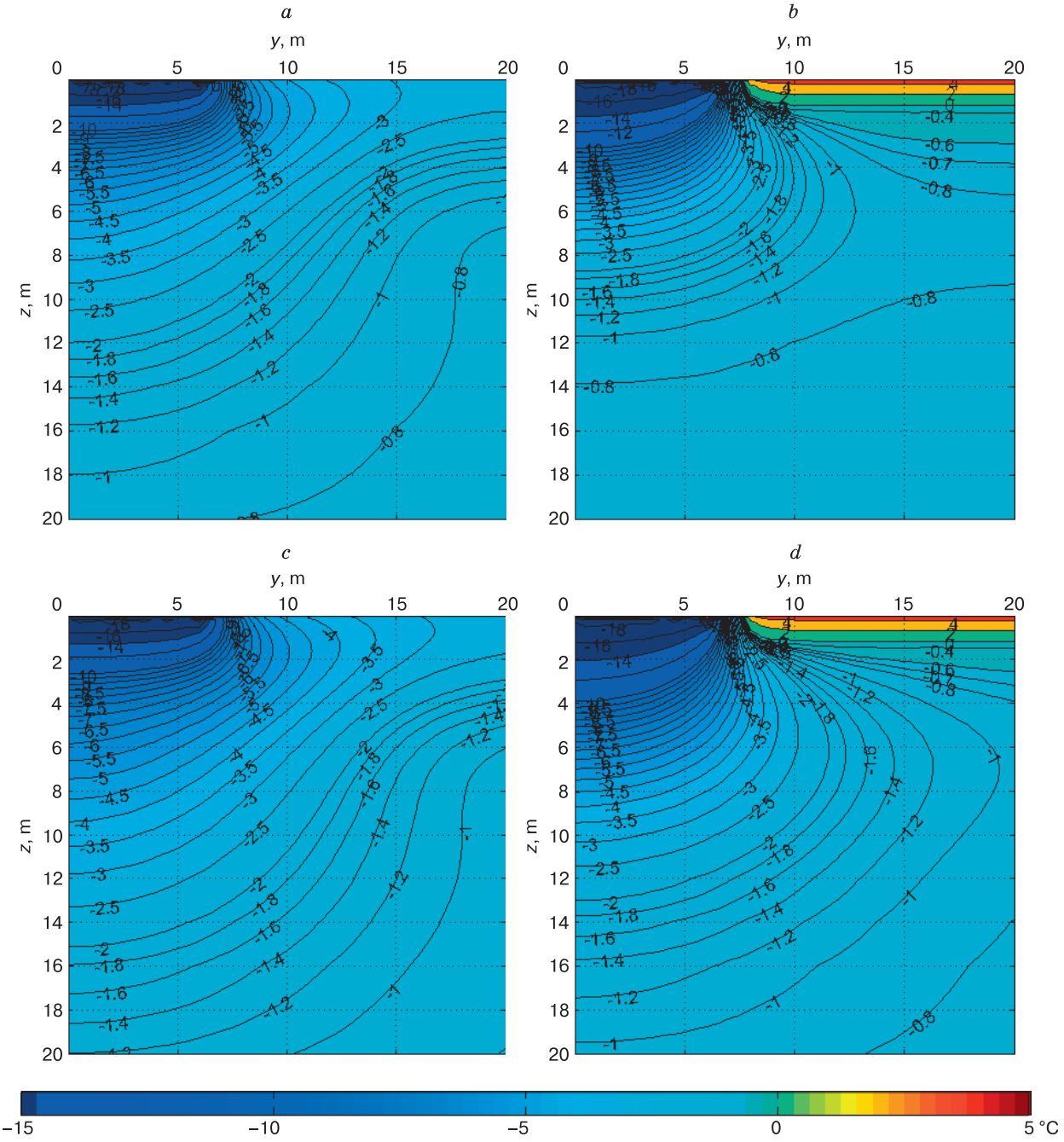

Fig. 4. Temperature fields at the base of the building in the central section (x = 0) with the distance between the evaporator pipes (L) equal to 0.7 m.

a, b – the 1st year of operation; c, d – the 2nd year of operation; a, c – end of winter; b, d – end of summer.

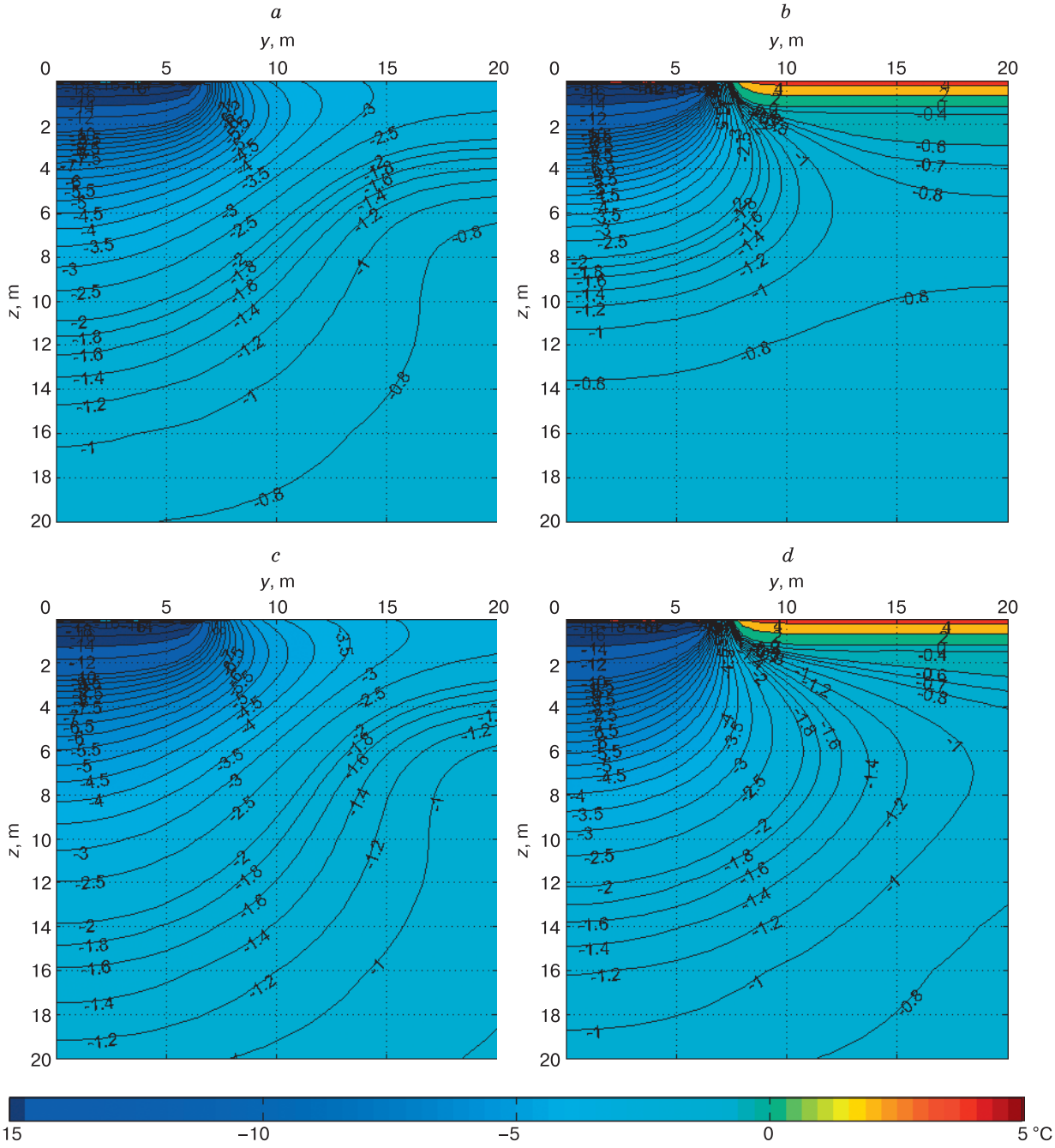

Fig. 5. Temperature fields at the base for the edge of the building (x = 12 m) with the distance between the evaporator pipes (L) equal to 0.7 m.

a, b – the 1st year of operation; c, d – the 2nd year of operation; a, c – end of winter; b, d – end of summer.

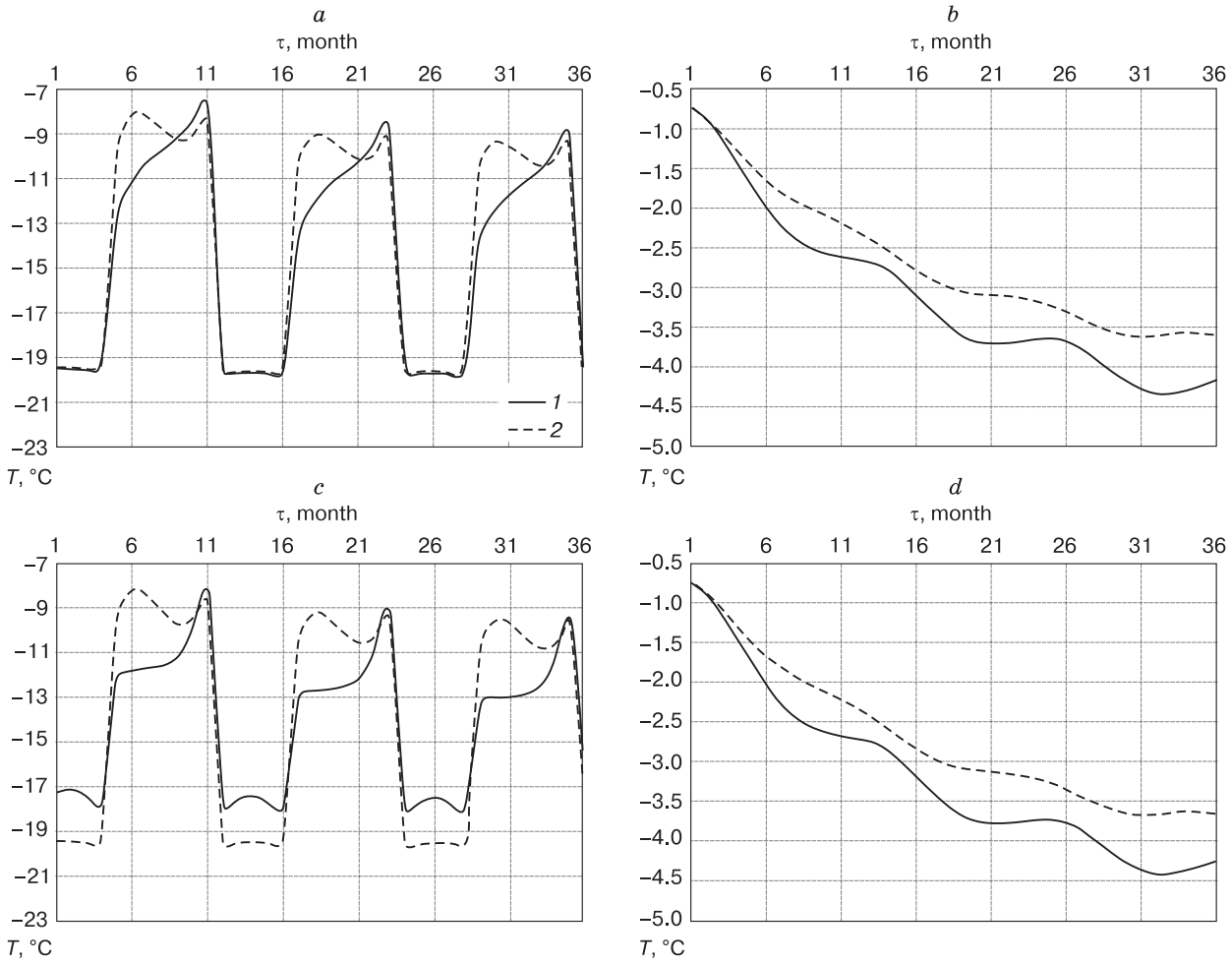

Fig. 6. Temperature dynamics at the base of the building at a depth of z = 0.2 m (a, c) and at a depth of zero amplitudes z_0 = 10 m (b, d) for the central section (1) and for the edge of the building (2) within 3 years of operation.

a, b – L = 1 m; c, d – L = 0.7 m; 1 – x = 0; 2 – x = 12 m.

CONCLUSION

A method of surface cooling is proposed. It includes the placement of heat insulation on the soil surface and cooling pipes laid under it, connected to a forced circulation unit of the refrigerant with the latter turned on only in the summer period of the year during the entire service life of the structure. The method has important advantages: a) at any time there is no possibility of the formation of a seasonal thawing layer, which eliminates the need to freeze it, as a result of which the cooling impulse enters the basement of the structure throughout the entire calendar year; b) in the conditions of urban development, where the placement of very large condensing units of the natural convective system GET will inevitably entail the emergence of certain problems, the use of a machine cooling method is quite industrial, which does not require significant space for its implementation.

The results of mathematical modeling of the process of temperature field formation in a frozen soil with a surface cooling method using the considered technical means, presented in the article, allow us to draw the following conclusions:

1. Comparison of the temperature fields presented in Figures 2–5 demonstrates a high rate of decrease in soil temperature at the basement both in its central section and along the edge of the building. In all calculation options, the temperature at a depth of zero annual amplitude in the second year of operation reaches a value corresponding to the solid-frozen state of most soils. An even more significant decrease is reched in the third year of operation (Fig. 6, *b*, *d*).

2. High rates of temperature decrease correspond to similar results for the most effective options for

surface cooling with the combined use of the GET system and a forced cooling unit, which are considered in [*Gorelik, Khabitov, 2021*]. The calculation results are rather weakly dependent on the distance between the evaporator tubes L within the considered range of variation of its value (from 0.7 to 1.0 m).

3. The rate of temperature decrease is multiple times higher than the values of 3–5 years, typical of the known methods [*Vyalov et al., 1979; Khrustalev, Nikiforov, 1990*].

The results obtained in this work may turn out to be very important for the development of technologies for the restoration of buildings and structures which have undergone deformations during operation due to a violation of the temperature regime of frozen soils of their foundations.

Acknowledgements. *The work has been carried out within the framework of the theme of the state assignment Reg. R&D No. AAAA-A17-117051850061-9.*

References

Abrosimov, A.I., Teplyakov, A.V., Zaletaev, S.V., et. al., 2018. The increezing of pile stability by employment of cooling systems in the aired underfloor space. In: Proceeding of Council of Earth's Cryology (Moscow, May 15–16, 2018). MGU, Moscow, vol. 2, pp. 9–15 (in Russian).

Aziz, H., Settary, E., 2004. Mathematical modeling of stratum systems. Institute of Computer Investigations, Moscow; Izhevsk, 416 pp. (in Russian).

Bubelo, R.V., 2003. Stabilization of Negative Temperature in the Base's Frozen Soils by Surface Cold Accumulators: Author's abstract of PhD thesis. Moscow, 23 pp. (in Russian).

Dolgikh, G.M., Okunev, S.N., Podenko, L.S., et al., 2014. Safety, efficiency and wieldyness of the thermostabilized systems for permafrost states. In: Systems for Thermal Stabilization of Permafrost. Collection of Papers by Specialists from NPO "Fundamentstroiarkos" Company for 2010–2014. Acad. Publ. House "Geo", Novosibirsk, 218 pp. (in Russian).

Gorelik, J.B., Khabitov, A.K., 2019a. The influence of the boreholes'heat insulation on the determination of the minimal distance between its outfalls at permafrost. In: Bulletin of Tyumen State University. Physical and Mathematical Modeling. Oil, Gas, Energy, 5 (2), 10–26.

Gorelik, J.B., Khabitov, A.K., 2019b. About efficiency of adaptation of the thermostabilizers for building activity in Permafrost. In: Bulletin of Tyumen State University. Physical and Mathematical Modeling. Oil, Gas, Energy, 5 (3), 25–46, DOI: 10.21684/2411-7978-2019-5-3-25-46.

Gorelik, J.B., Khabitov, A.K., 2021. Affectivity of surface cooling of frozen ground in connection with mechanism of temperature shift formation. Earth's Cryosphere XXV (2), 24–37.

Gorelik, J.B., Pazderin, D.S., 2017. Correctness of formulation and solution of thermotechnical problems of forecasting temperature field dynamics in the ground base of structures on permafrost. Earth's Cryosphere XXI (3), 45–54.

Gorelik, J.B., Romanyuk, S.N., Seleznev, A.A., 2014. Some characteristics of the calculation methods of the frozen soil's thermal state in the flare facility foundation. Kriosfera Zemli [Earth's Cryosphere], XVIII (1), 57–64.

Gorelik, J.B., Romanyuk, S.N., Habitov, A.K., 2019. Constraining thaw

boundary around multiple wells with regard to their joint thermal effect. Earth's Cryosphere XXIII (2), 67–73.

Gorelik, J.B., Shabarov, A.B., Sysoyev, Yu.S., 2008. The dynamics of frozen ground melting in the influence zone of two wells. Kriosfera Zemli [Earth's Cryosphere] XII (1), 59–65.

Gorelik, J.B., Zemerov, I.V., 2020. Influence of the surface water reservoir to the thermal regime of frozen ground. In: Tyumen State University Bulletin. Physical and Mathematical Modeling. Oil, Gas, Energy 6 (1), 10–40, DOI: 10.21684/2411-7978-2020-6-1-10-40.

Khrustalev, L.N., Nikiforov, V.V., 1990. A stabilization of the building's bases in permafrost. Nauka, Novosibirsk, 209 pp. (in Russian).

Konovalov, A.A., 1989. Cooling of frozen bases for addition of their solidity. Krasnoyarsk State University Publishing House, Krasnoyarsk, 202 pp. (in Russian).

Kudryavtsev, V.A. (Ed.), 1978. General Geocryology. MSU Publishing House, Moscow, 464 pp. (in Russian).

Makarov, V.I., 1985. Thermosyphons in High-Latitude Construction Engineering. Nauka, Novosibirsk, 169 pp. (in Russian).

Okunev, S.N., Dolgikh, G.M., 2017. Adaptation of the mobile compressor – condenser aggregate without oiling for freezing of the oil and gas building's bases at the North regions. Sphere. Oil and Gas No. 1, 40–42.

Patankar, S.V., 2003. Calculation solution of heat and convection changes at flow in the channeles. MEI Publishing House, Moscow, 312 pp. (in Russian).

Samarsky, A.A., Vabishchevich, P.N., 2003. Computational heat transfer. Editorial URSS, Moscow, 784 p. (in Russian).

SNiP 2.02.04-88, 1990. Basements and foundations in permafrost grounds. Gosstroy SSSR, Moscow, 56 pp. (in Russian).

Dolgikh, G.M., 2014. Systems for Thermal Stabilization of Permafrost. Collection of Papers by Specialists from Fundamentstroiarkos R&D Company for 2010–2014. Acad. Publ. House "Geo", Novosibirsk, 218 pp. (in Russian).

Vyalov, S.S., Alexandrov, Yu.A., Mirenburg, Yu.S., Fedoseev, Yu.G., 1979. Artificial cooling of the ground with employment of the thermal piles. In: Engineering Geocryology. Nauka, Moscow, pp. 72–90 (in Russian).

Received October 20, 2020
Revised version received February 28, 2021
Accepted March 14, 2021

EARTH'S CRYOSPHERE
SCIENTIFIC JOURNAL

Kriosfera Zemli, 2021, vol. XXV, No. 4, pp. 40–48

SNOW COVER AND GLACIERS

RECENT GLACIER SURGES IN THE WESTERN PARTS OF PETER THE FIRST RIDGE (PAMIR)

S.L. Desinov

Institute of Geography, RAS, Staromonetny per. 29, Moscow, 119017, Russia; sdesinov@gmail.com

Analysis of the glacier surges during 2015–2020 in the western parts of Peter the First Ridge, Pamir, is carried out based on the interpretation of images taken from the International Space Station, as well from Landsat, RapidEye and Sentinel satellites. It is established that massive ice blocks' breaking off from glaciers and their rapid descent down the valley is not unique for that region. The damage caused to human economic activity as a result of the investigated glacier surges is described. Periods of pulsation of some glaciers are determined.

Key words: *glacier surge, pulsating glacier, Didal Glacier, Surkhob, Vayzirek, Peter the First Ridge, satellite image*.

INTRODUCTION

Surging glaciers, also known as pulsating or surge-type glaciers, are a fairly formidable natural phenomenon and occupy a special place in glaciology, but remain largely understudied. Among mid-latitude mountain regions, surging glaciers are most common in the Pamirs, where they were investigated by the IG RAS researchers (Institute of Geography of the Russian Academy of Sciences). Results of their study were successfully applied as *Directions for compilation of Inventory of surging glaciers of the USSR* [*1982*]; the map of surging glaciers of the Pamirs (1983) which was made part of the *Atlas of Snow and Ice Resources on the Earth* [*1997*]; *Inventory of surging glaciers of the Pamir* [*1998*]. In recent years, this topic has received much interest from foreign scientists as well [*Mölg et al., 2018; Goerlich et al., 2020*].

One of the first and most intriguing glacier surges studied in the Pamirs by the Russian glaciologists occurred in 1974. The implications of the actively advancing Didal glacier during the summer of 1974 were that a ~600 m long fragment broke off from its tongue which travelled a distance of 3 km down the valley. The surging was accompanied by a discharge of large amounts of water which destroyed the bridge in the lower part of the valleys [*Rototaev, 1974; Suslov, 1974*].

Such natural phenomena involving detachment of huge portions of mountain glaciers and their fast moving downhill occur fairly regularly in different parts of the globe, which can be exemplified by the events documented for Kolka (1902 and 2002) [*Kotlyakov et al., 2014*], Allalin (1965) [*Dolgushin, Osipova, 1982*], Ravak (1967) [*Dolguschin, Osipova, 1982*], and Aru (2016) glaciers [*Gilbert et al., 2018*]. Published literature also contains a few mentions of the evidence of ice masses likewise shearing away in the past in Pamir valleys [*Rototaev, 1978*]. The question as to whether they are inherent in the Pamir surging glaciers and how frequently they occur is therefore of great interest. This requires observations on the patterns of after-surge motion for the glaciers with confirmed surges, as well as on the dynamics of glaciers that were so far not marked by surges.

Despite the established fact that glaciers surge with some periodicity, this phenomenon is interpreted as long-term, with its cycle commonly spanning several decades. Although surging glaciers have been monitored in Russia since the 1960s, sufficient data have not yet been accumulated. However, several intriguing natural events reported from the Pamir Mountains in recent years, have largely contributed to the existing knowledge of surge-type glaciers for deeper study of the issues posed.

With this paper, we begin a series of publications to provide an overview of glacier surges in the Pamir Mountains since 2001.

BRIEF CHARACTERIZATION OF STUDY REGION

The investigated glaciers are located on the northern slope of the Peter the First Ridge in the western Pamirs, a generally east-west trending mountain range. Although the highest peak rises to 6785 m (Moskva Peak) in its eastern part, the heights of this mountain range are generally lower and measure from 3800 to 5400 m (Fig. 1) within the study area.

Peter the First Ridge branches into two subordinate ranges in the area occupied by the eponymous glacier. All glaciers investigated by the author are located on the northern slope, while they belong to the basins of two different rivers: Surkhob (glaciers numbered 504, 505, 506, Didal) and Obikhingou (glaciers 85 and 88). These rivers subsequently merge, to

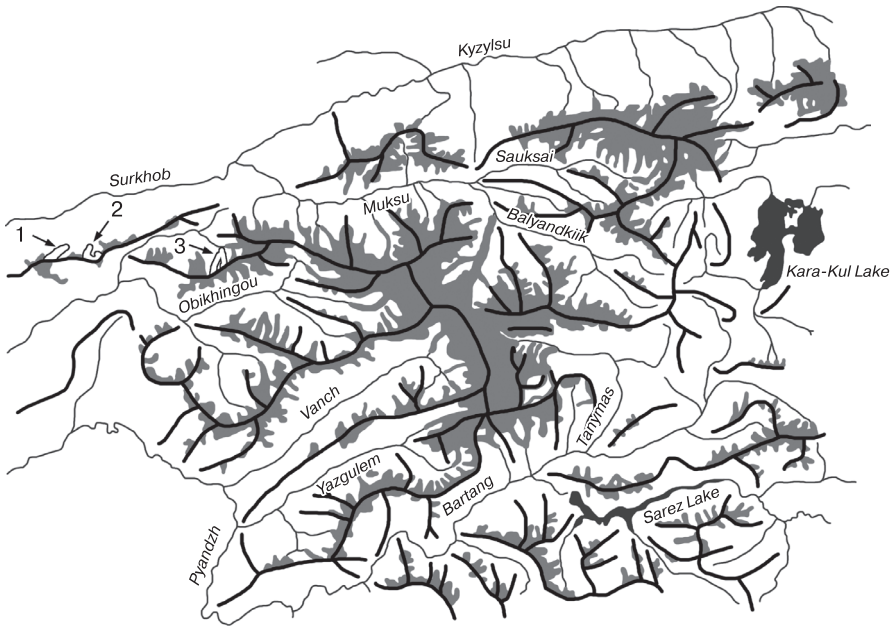

Fig. 1. Schematic view of Pamir glaciation and locations of the studied glaciers.

1 – Didal Glacier; 2 – group of glaciers 504–507; 3 – glaciers 85, 88.

form the Vakhsh River (one of the elements of the Amu-Darya River).

The slopes of the mountain range dipping towards the Surkkhob River that runs parallel to it from the north, are very steep (ca. 3 km) at a distance of 12–15 km. The outflowing streams' valleys commonly form narrow gorges (V-shaped valleys), while those extending from the southern chain of the mountain range towards the Obikhingou River are generally with broader and flatter floor (U-shaped valleys); the elevation difference and relief dissection are also remarkable there.

There are no weather stations in the area embracing the investigated glaciers. The two stations in the Surkhob and Obikhingou valleys are located at a considerable distance from the glacier entities under study and at lower hypsometric levels, so that one can count them out.

DATA PROCESSING METHODS

Since 2001, the Institute of Geography RAS, have been partnering with the Rocket and Space Public Corporation (RSC) Energia in carrying out the Uragan space experiment consisting in observations and photographing the Earth's surface from the Russian Orbital Segment (ROS) of the International Space Station (ISS). The experiment results largely underlie this work. We also used images obtained from several remote sensing satellites, topographic maps of scales 1:100 000 and 1:50 000, and data from the *Inventories of the USSR glaciers* [*1971, 1978*] and of *Inventory of surging glaciers of Pamir* [*1998*].

The ISS-produced images taken in the visible part of the spectrum have a spatial resolution of up to 5 m and encompass a time period of the past 20 years. This makes them appropriate for dynamics analysis of natural objects (glacier entities). The Global Mapper software enabled geographically aligned image rectification, as well as delineation of glaciers contours and allowed measuring distances between key points on the surface. The measurement error is not more than 10 m.

Images from a number of international Earth remote sensing satellites have recently become available free in the public domain. This paper uses a time series analysis of Landsat, Sentinel-2, and RapidEye imagery with a spatial resolution of 15, 10, and 7 m, respectively. Given that declassified high-resolution data contain images only after 2016, they were used as a minor resource (i.e. do not provide a sufficient variable image coverage). These images were processed with the ArcGIS, a GIS software suite.

Not all of the images available for the analysis, had the required brightness and contrast characteristics. For more distinct delineation of the glacier fronts and surface morphology, many images were processed using IrfanView software capable of viewing and editing most graphics formats.

Satellite images remarkably document changes in glacier extent, however with some discreteness. It is therefore not always possible to determine the exact date and timing of simultaneous events. In such cases, one needs to specify a time period at the beginning of which the event has not yet taken place,

whereas at the end, it is interpreted as post-event with its impacts already manifested.

We have also analyzed open-source meteorological and earthquake data for the area. The former show no significant time-specific variations as compared to the mean annual values, while the weather stations available in the study area are located at a considerable distance from the investigated glaciers, at completely different hypsometric levels. Since the latter (earthquake data) suggest the absence of remarkable events within a radius of several hundred kilometers during the investigation period, they were therefore rejected from this analysis.

Didal Glacier surges in 2015–2016

Didal Glacier is located on the northern slope of the Peter the First Ridge, and is related to the group of glaciers on the left side of the Surkhob River valley. This is a complex valley glacier exposed to the northeast, and is numbered 513 in *Inventory of USSR Glaciers* [*1971*]. The glacier meltwater forms the headstream of the Dara River.

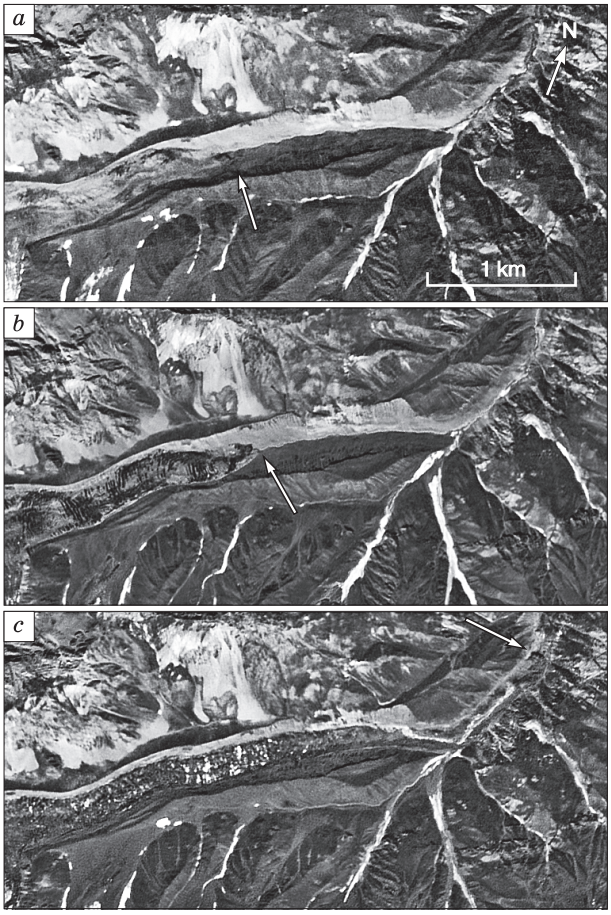

Fig. 2. Surge stages of Didal Glacier. Photo taken onboard the ISS.

a – August 2014; *b* – August 2015; *c* – July 2016. The arrows show the position of the lower end of the tongue.

V.I. Lipsky [*1902*] in his observations of the glacier during the 1897 expedition, marked visible signs of a recent surge (e.g., highly crevassed glacier surface and "terrible snowslide"), which can be interpreted as analog of the 1974 surges. Different sources suggest that yet another glacier surge occurred in 1929 or 1939 [*Inventory..., 1998*]. The 1974 glacier surge accompanied by detachment of a portion of the glacier terminus and its moving rapidly down the valley was discussed in [*Rototaev, 1974; Suslov, 1974*]. The surge left the glacier terminus largely shrunk (in 2014, the glacier had a length of 3350 m, its terminus elevation was 3060 m asl). Considering the surge pattern and the hazard that may ensue (in the case of repeated events) for the infrastructure located in the valley downstream, the author conducted systematic satellite imagery-based monitoring of the glacier changes.

While the glacier gradually recovered from the surge of 1974, there were no remarkable signs of its changes until 2015. The surface of the moraine material covered the glacier tongue was generally levelled with lateral moraines; its ice had locally developed sinks.

Changes became explicitly discernible early in the summer of 2015. The volume of ice dramatically increased in the middle portion of the tongue, with a salient boundary suddenly appeared between the activating region (surge wave) of the glacier and the region remaining quiescent, i.e. dead (material from a previous surge) stagnant basal part with a length of about 500 m. While rare large transverse crevasses became visible in the activating region, most of the surface was still relatively smooth and continued to be buried under a layer of dark surface moraine.

By August, the front of the glacier activating part had been distinctly outlined, while its surface became chopped into blocks and was lighter in color. By September, the front of the activating region had reached the lower line of the tongue position; the glacier had thus began advancing forward. It moved intensely during the autumn and winter, while in February–March 2016 some slowdown was observed. In April the movement accelerated again, and by June the surge front had reached its ultimate position. Didal Glacier advanced down the valley to a distance totaling 1950 m, at an average rate 7.2 m/day (Fig. 2). The glacier terminus came to a standstill at an elevation of 2550 m asl.

As such, the glacier advancement is referred to as classical. There was nothing which would remind of the glacier's front portion detachment reported in 1974.

The data on the surges of 1897, 1929 (or 1939), 1974 and 2016 allow determining the intervals between them, as follows: 32 (42), 45 (35) and 42 years.

One can only wonder how often Didal Glacier surges follow the 2015–2016 classical scenario or the 1974 scenario. According to the global statistics of

the study of surging glaciers, the phenomenon of a head part separation and its rapid descent down happen extremely rarely. However, the events which occurred almost synchronously with the above discussed Didal Glacier surges, have shown a great similarity with those reported from the Dara River valley in 1974 in its immediate vicinity.

Surges of glaciers No. 504, 505 and 506 during 2016–2019

The Vostochny Shurak (aka Shuraki Kapali) River valley located 8–10 km to the east of the Dara River valley and Didal Glacier is also attributed to the Surkhob River basin and is seated on the left slope. The three small-sized unnamed glaciers in the upper part of the valley are numbered 504, 505 and 506 in the glacier inventory. These are exposed to northwest, north and northeast and have areas of 0.3, 0.3 and 0.2 km^2, respectively [*Inventory..., 1971*]. Slightly further down the valley, glacier 507, the largest among them, comes out of the valley on the left. The literature sources contain a mention of its internal surge in 1949 [*Inventory..., 1998*]. However, no surging activity of glaciers 504, 505 and 506 has hitherto been mentioned in published literature.

Above glacier 507, the valley structure is described as trough-like. At the point of the glacier debouch into the valley, the latter slightly expands, and almost immediately passes into a narrow canyon. As the valley approaches its mouth, it widens again. The confluence of the Vostochny Shurak and the Surkhob rivers occurs in the western part of the Tajikobod district center.

Glaciers 504 and 506 are valley glaciers, while glacier 505 is corrie-hanging glacier. The dimensions specified in [*Inventory..., 1971*] (from aerial photography 1956) for the glaciers (No.) are: 1.0 km (504), 0.6 km (505) and 0.8 km (506). Analysis of satellite images showed that the glaciers length gained by the by 2015 was 450 m and 120 m for No. 504, 505, respectively, while the length of glacier No. 506 remained unchanged.

At the beginning of June 2016, one could observe the left part of the tongue of glacier 505 (250 m long) breaking off and slowly sliding down the slope. In a month and a half, its front part advanced by 160 m and lost 50 m in height. A time period spanning the latter half of July, specifically, between the 15th and 24th (it was impossible to determine the more precise timing), is referred to as the onset of rapid advance of the detached mass of ice down the valley. After running out 2.5 km, the masses approached the valley widening, opposite the glacier 507 outlet on the left, where a major portion of the discharged mass spread out taking the shape of a "snout". However, a small portion sheared away from the masses and slid down the river canyon as a narrow body (1220 m long and 80–90 m wide). The distance between the upper boundary of this body and the descended, already motionless, masses is about 450 m.

The lower edge of the bulk masses ("snout") has advanced by 3650 m from the former lower elevation point of the glacier. Thus, the cumulative advance down the valley totaled 5320 m (Fig. 3).

Ice that came downhill was highly fractured and heavily laden with rock debris. During the first month after the surge, the surface-exposed ice soon became compacted, and the surface smoothed out and totally moraine-covered.

A year later, in early July 2017, glacier 504 likewise started moving. However, given that it was larger than glacier 505, the magnitude of surges was greater. Almost the entire 1280 m long tongue broke away and slid downhill. At the end of May, the tongue surface elevation remarkably rose which was followed by enhanced crevassing. The upper boundary of the

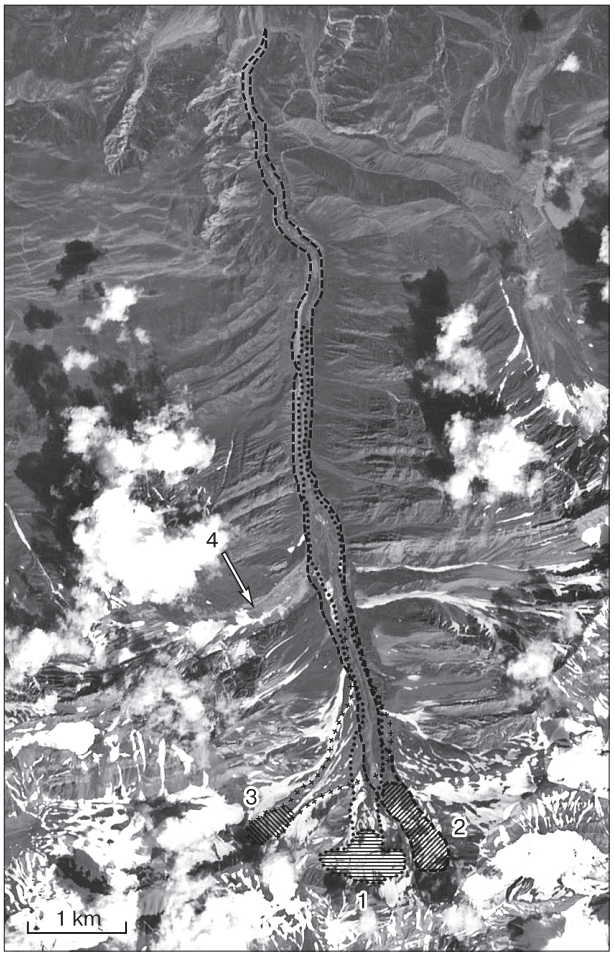

Fig. 3. Boundaries of the area affected by surges of glaciers 504–506. Photo taken from Sentinel-2 satellite, 2017.

1 – glacier 505 in 2016; 2 – glacier 504 in 2017; 3 – glacier 506 in 2019; 4 – glaciers 507. The striated areas were occupied by glaciers before the described events.

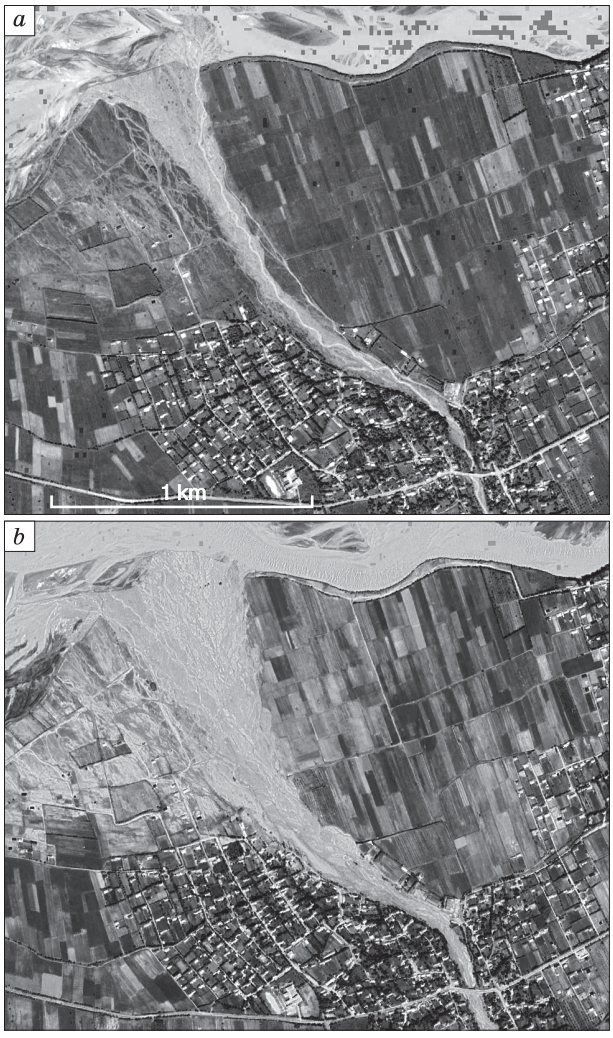

Fig. 4. Near-mouth zone of the Vostochy Shurak River. Sentinel-2 imagery.

a – June 2017; *b* – August 2017.

surge zone transpired as rare large crevasses developing from one side to the other, across the entire glacier's width. Over a month time, significant mass transfer occurred from the back of the tongue to its front, and the front of the glacier has moved forward to a distance of 180 m along its length, losing 40 m in height. On July 11, the active surge was succeeded by another phase: the ice came down in dramatic fashion. The traces of the previous descent of glacier 505 described above were therefore blocked, and formed an identical snout at the same place of the valley widening. A significant portion of the ice which, similarly to the previous year, passed through the narrowing down the valley, however, this time, it has advanced further without detaching from the snout residing on higher elevation and extending as a single tongue.

The Vostochny Shurak River canyon was filled with ice almost to the brim. The ice moved downstream to a distance totaling 7840 m. A small ice-dammed lake (~11,000 m^2) formed in the contact zone between the descended ice and the tongue of glacier 507. A month later, the water found its way and discharged through a natural conduit leaving the lake completely drained and, ultimately, nonexistent.

During first post-surge days, the material making up the snout abounded with rock debris was already dark in color. However, the surface of the tongue that descended beneath it was very light in color at first, which suggests that it was largely composed of loose ice. In a month's time, it darkened, the surface subsided considerably because of the ice rapidly melting, and soon became rock debris-covered.

While the previous year's surge-related hazards practically did not affect the infrastructure located in the lower part of the Vostochny Shurak River valley, the 2017 events' impact was measurable. In last 2 km upstream of the Vostochny Shurak River confluence with the Surkhob River, it flows in the cultivated margin between the fields of Tajikobod district. The ice-rockslide-avalanche event in the upper reaches of the valley released considerable amount of water, which strongly affected the river banks. Comparison of images taken in June and August 2017, i.e. before and after the event, has shown that the width of the Vostochny Shurak River bed has more than doubled in its mouth area. As many as 20.5 hectares of fertile land (Fig. 4) and several buildings have been destroyed or partially washed away.

The third stage of the aforementioned events occurred late in June 2019. This time round, the process affected glacier 506, at a much more moderate scale, though. In the period from June 24 to 26, its ice descended down the valley only by 1300 m, thus failing to approach glacier 507. A mudslide flowed down a lower slope, without severe impacts. Unfortunately, cloud screening of the satellite image precluded a detailed reconstruction of this event.

At the end of the summer of 2020, masses of glacier 504 which came down three years earlier, became compacted. The tongue that descended through the river canyon to rest below glacier 507, in a severely degraded state, its lower edge has receded 1300 m from the July 2017 outlines. Waters of the Vostochny Shurak River carved their way through the ice. Its channel's arches locally collapsed, forcing the river to come onto the surface. In 2 or 3 years' time, one should expect a breakup of what is presently interpreted as a single body into separate parts and their rapid disappearance.

The question as to whether the above mentioned events represent a random and unique combination of natural controls for this valley or whether they occur with some periodicity remains open. Given that the systematic monitoring of glaciers in the Pamirs cov-

ers mainly the central and eastern (more expressly glaciated) areas, published literature provides no mention (descriptions) of earlier comparable surges. Besides, obtaining regular images with high level of definition was problematic until recent times, therefore the researcher would simply miss out on the signs of such processes.

At this, a number of indirect indications confirm this event to be not one-off. These include: the satellite image taken in 2008 clearly showing traces of mudflow mass transfer from the upper reaches of the valley towards glacier 507 and passing it by on the right side. However, the absence of evidence of any significant mass transport may suggest that a mass wave that came down either was small in size and short-lived (i.e. ice could have already melted), or that initially it was rock-debris laden mudflow, rather than ice.

Also worth nothing is that the image taken in July 1976 from a helicopter (Fig. 5) shows the upper reaches of the valley from glacier 507 (debouching from the gorge to the right of the observer) and above; large dark mass exactly at the place where the snout formed in 2016 and 2017. The extents of glaciers 504 and 505 are found to be lesser, as compared to what they were in 2015, before the initiation of the latest surges. Glacier 506 is poorly visible due to the slope bend. The volume of material that mantle the valley bottom can be interpreted as slope or mudflow deposits, however we find the inference about this to be ice that had previously descended more appropriate. Given that several glacier reservoirs overlap these deposits, the material removal occurred earlier than 1976.

In the upper reaches of the valley, geomorphological traces of the past hypothetical events, if they existed, were destroyed in 2016–2017. Although the Vostochny Shurak River mouth zone, specifically, on its left bank, exhibits discernible traces of ancient watercourses (Fig. 4), one can hardly claim these to be remnants of a mudslide similar to the one occurred in 2017. In equal measure, they can be associated either with floods caused by heavy rains, or with a gradual displacement of the main stream bed to the right.

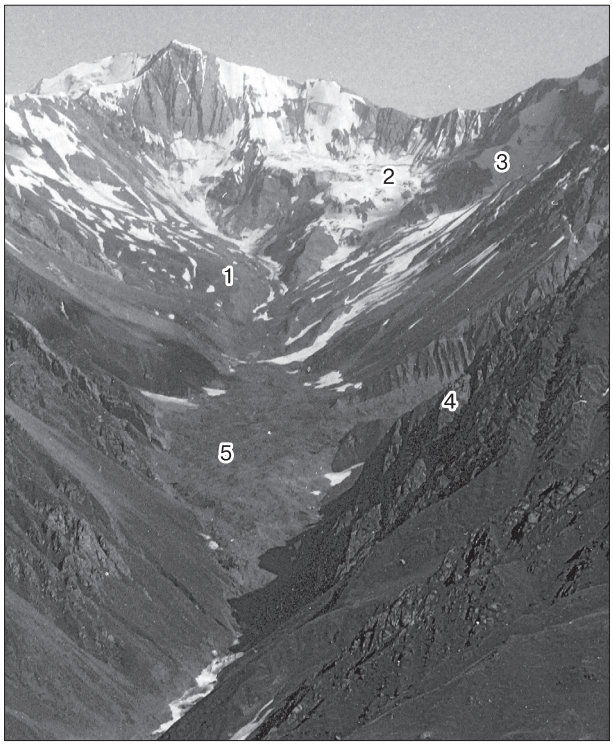

Fig. 5. Upper reaches the Vostochy Shurak River valley in 1976.

1 – glacier 504; 2 – glacier 505; 3 – glacier 506; 4 – debouch of glacier 507 into the valley; 5 – ice avalanche descended from higher elevations. Photo by V. Rudakov.

Surges of glaciers 85 and 88 in 2013–2017

The space between the two branches (northern and southern) of the Peter the First Ridge is occupied by the Vaizirek River valley, a tributary of the Shaklysu River. These rivers belong to the Obihingou River basin, with the Aizirek River feeding from Peter the First Glacier. Almost immediately (1 km down the headstream), a leftward side valley merges with it perpendicularly and is divided into two branches 2 km upstream. They accommodate two unnamed glaciers referred to in [*Inventory..., 1978*] as glacier 85 (eastern) and glacier 88 (western). Until relatively recently (late in the 19th century), they were an integrate part of Peter the First Glacier, however later separated from it contemporaneously with retreat of the majority of Pamir glaciers.

These are valley glaciers generally exposed to the north. Their lengths are 8.1 km (glacier 85) and 6.6 km (glacier 88), and their areas are 4.6 and 3.7 km^2, respectively [*Inventory..., 1978*].

Both of the glaciers are interpreted as surging. Glacier 88 advanced in 1975–1978, leaving a 480 m space to the Vaizirek River [*Desinov, 1984*]. Surging activity of glacier No. 85 was reported for 1990–1992 [*Inventory..., 1998*], catching up with the Vaizirek River and the opposite side of its valley, thus blocking the river with an ice-dam. At this, however, no ice-dammed lake was formed, most likely because the glacier approached the river at the waning stage of the surge (i.e. the energy of motion has largely declined and its speed lowered), thus allowing the waters of the blocked river to escape.

From that time on and until 2013, the glaciers had been degrading. The Vaizirek River was freed from the "glacial ice roof" only in 1999. By 2013, the lowest glacier points had been distanced from the Vaizirek River by 2050 m (glacier 85) and 2820 m (glacier 88).

In 2012, a surge wave was reported from glacier 88. At that time, it was documented 4360 m from the Vaizirek River and 1540 m from the lowest glacier point. In 2013, it approached the glacier terminus, and the glacier began to advance in December, preceded with its steep and remarkably expressed front.

Glacier 88 was advancing forward in the year of 2014. By August, it had reached the zone of confluence of with the glacier 85 valley and began to encroach onto its highly down-wasted thin tongue which still remained in this place after the previous surge. In October, glacier 88 reached the opposite (right-hand) coastal moraine. By that time, the advance amounted to 1310 m at an average rate of 12 m/day. However, after October, the movement decelerated to a few first meters per day, and the glacier

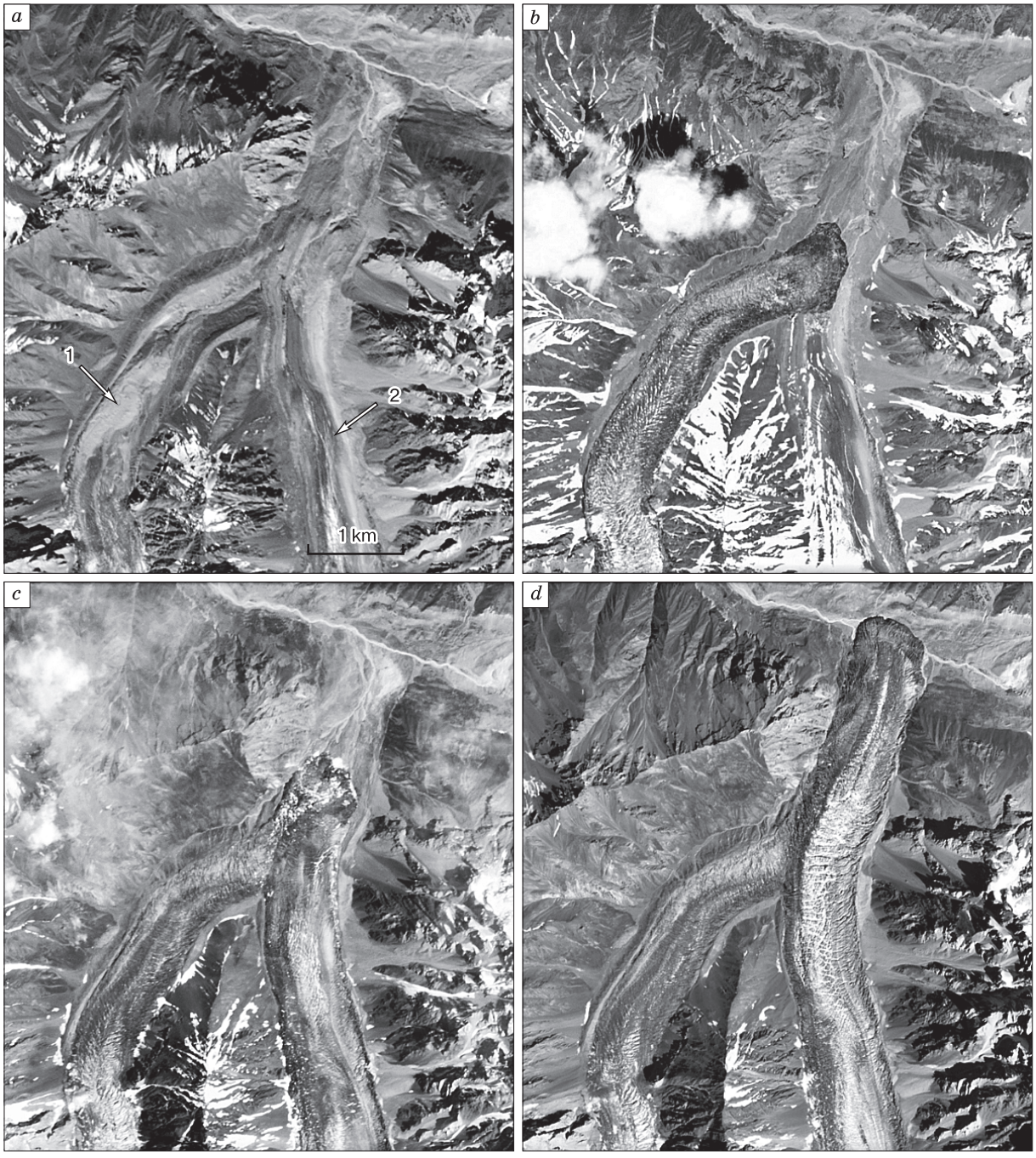

Fig. 6. Surge stages of glaciers 85, 88.

a – September 2013; *b* – July 2015; *c* – August 2016; *d* – August 2017. *a*, *d* – RapidEye imagery; *b*, *c* – images from the ISS. 1 – glacier 88; 2 – glacier 85.

flowed down the valley for another 370 m, with its front spreading out as a snout. By April 2015, the glacier advance had been arrested.

Thus, independent advance of glacier 88 was 1680 m, the surge front stopped at 1140 m from the Vaizirek Rv.

Shortly before that, signs of activation of glacier 85 became noticeable. In late autumn 2014, the activation front was remarkably identifiable and at that time located 850 m above the contact between the degrading tongue of glacier 85 and the advancing glacier 88. By September 2015, the activating part had reached the contact zone, while ice, having encountered a dam made up by glacier 88 that arrived six months earlier, began aggrading in its front to form a swell extending across the valley. In December, glacier 85 broke the dam's resistance by finally succeeding in setting it in motion and began to descend down the valley, pushing the ice of glacier 88 in its front.

Importantly, during the surge of glacier 88, its tongue had a classical appearance for this phase (i.e. ubiquitously crevassed, chopped into blocks), while at the post-surge phase (the spring of 2015) its tongue surface gradually became smooth out and covered with moraine material, thereby suggesting the glacier to have passed into the recovery stage. Therefore, further lowering of the glacier's basal part (its former snout) was driven by the energy gained from the surge of glacier 85, rather than by its own energy. This means that glacier 85 being in its active phase, moved the lower terminus of the neighbor already in its quiescent phase (Fig. 6).

During 2016 and the first half of 2017, glacier 85 continued its advancement. Like a bulldozer, it moved the ice of glacier 88 in its front, gradually shifting it leftwards. By January 2017, the masses reached the Vaizirek River, and the opposite side of the valley at the end of February. The Vaizirek River became again blocked, however without formation of ice-dammed lake, similarly to the previous surge. While the glacier terminus has practically stopped there, however, until August 2017, ice masses continued to aggrade and bulge in the frontal part, thereby gradually increasing its elevation. The glacier position of 1992 were restored, with the previous surge coming to an end. Although it should be noted that this time the valley was filled not only by its ice: a strip about 100 m wide on the left side of their common valley and an arc up to 150 m wide in the frontal part were composed of the material transferred by glacier 88.

Counting its ice alone, glacier 85 has advanced by 1900 m, and by 2050 m with adding up the ice of glacier 88. The maximum speed of movement documented in the autumn of 2016 amounted to 9 m/day.

The onset of glaciers degradation is evidenced primarily by first sinks appeared in the "ice roof" over the Vaizirek River in the summer of 2019, although its integrity remained generally preserved during the summer of 2020. It is obvious that the river will be completely freed only in a few years' time, and the glaciers will be gradually retreating until they become separated at their valleys confluence.

Thus, glaciers 85 and 88 have been jointly surging for more than 5 years. Individually, the surge periods lasted 25 and 37 years for glacier 85 and 88, respectively.

CONCLUSION

The satellite monitoring data have shown that glacier surge-driven detachment of a glacier portion and its rapid descent down the valley is not unique for the northern slope of the Peter the First Ridge. Based on numerous literature mentions of the indications of similar phenomenon in other regions of the Pamirs, one can make a preliminary inference about such scenario being widespread in this mountain system. Given the paucity of observations, a final conclusion can hardly be expected about the combination of surge-driving factors. Note that all the glaciers described in this paper surged during the summer when the content of free water in the ice column is explicably enhanced. However, the question whether this is the only appropriate factor is debatable. The slope steepness of the Peter the First Ridge and geology of the underlying surface may also make difference.

Evidences of surging activity were noted for three glaciers (numbered 504, 505 and 506) of the Surkhob River basin. Repeated surges were documented for glacier 513 (Didal), which also belongs to the Surkhob River basin; the latest surge allows estimating the surge period as 35–42 years. For the two glaciers (85 and 88) of the Obikhingou River basin, surges were reported repeatedly, thereby enabling estimation of their surge periods, as follows: 25 years for glacier 85 and 37 years for glacier 88.

Since the studied surges of ice masses can lead to catastrophic consequences and significant damage to economic activity, additional research is needed to identify a complex of factors that can cause such developments. Besides, this requires regular monitoring of the upper reaches of mountain valleys for the sake of early warning of the population. This issue appears the more so salient despite the fact that no connection with the weather factors has thus far been revealed, since it is highly likely to exist and to be recognized with longer series of observations. In the context of global climate warming, the latter may affect the area of a glaciated region to the extent that saturation of the glacier body with water during the summer will enhance, thus making probability of a surge higher.

The study was conducted within the state order AAAA-A19-119022190168-8.

References

Atlas of Snow and Ice Resources on the Earth, 1997. Institute of Geography RAS, Moscow, 392 pp. (in Russian).

Desinov, L.V., 1984. Over the Pamir glaciers: the route of V.I. Lipsky's expedition. Priroda [Nature], No. 2, 53–65.

Dolgushin, L.D., Osipova, G.B., 1982. Surging Glaciers. Goscomgidromet, Leningrad, 192 pp. (in Russian).

Directions for compiling the inventory of surging glaciers of USSR, 1982. Materials of Glaciological Investigations, issue 44, pp. 208–234 (in Russian).

Gilbert, A., Leinss, S., Kargel, J., et al., 2018. Mechanisms leading to the 2016 giant twin glacier collapses, Aru Range, Tibet. The Cryosphere, vol. 12, 2883–2900.

Goerlich, F., Bolch, T., Paul, F., 2020. More dynamic than expected: an updated survey of surging glaciers in the Pamir. Earth Syst. Sci. Data, vol. 12, 3161–3176.

Inventory of USSR Glaciers, 1971, Vol. 14, issue 3, part 6. The Surkhob River basin between the Obikhingou and Muksu river outlets. Gidrometeoizdat, Leningrad, 92 pp. (in Russian).

Inventory of USSR Glaciers, 1978, Vol. 14, issue 3, part 9. Obikhingou River basin. Gidrometeoizdat, Leningrad, 110 pp. (in Russian).

Inventory of surging glaciers of Pamir, 1998. Materials of Glaciological Investigations, issue 85, pp. 3–136 (in Russian).

Kotlyakov, V.M., Rototaeva, O.V., Nosenko, G.A., et al., 2014. Karmadon catastrophe: what happened and what we should expect in the future. "Kodeks" Publishing House, Moscow, 184 pp. (in Russian).

Lipsky, V.I., 1902. Upper Bukhara. Results of three years' travels in Central Asia in 1896, 1897 and 1899. Part 2. Izd-vo RGO, St. Petersburg, 120 pp. (in Russian).

Mölg, N., Bolch, T., Rastner, P., et al., 2018. A consistent glacier inventory for Karakoram and Pamir derived from Landsat data: distribution of debris cover and mapping challenges. Earth Syst. Sci. Data, vol. 10, 1807–1827.

Rototaev, K.P., 1974. Surging Didal glacier, Pamir. Materials of Glaciological Investigations, issue 27, pp. 188–189 (in Russian).

Rototaev, K.P., 1978. Dynamically unstable glaciers in the central Pamirs. Materials of Glaciological Investigations, issue 33, pp. 201–207 (in Russian).

Suslov, V.F., 1974. Surges and collapses of Didal glacier in 1974. Materials of Glaciological Investigations, issue 27, pp. 189–191 (in Russian).

Received August 22, 2020
Revised version received March 4, 2021
Accepted March 24, 2021

EARTH'S CRYOSPHERE
SCIENTIFIC JOURNAL

Kriosfera Zemli, 2021, vol. XXV, No. 4, pp. 49–51

CHRONICLE

ANDREY GEORGIEVITCH SKVORTSOV
(*on the 75th anniversary***)**

G.V. Malkova

Earth Cryosphere Institute, Tyumen Scientific Centre SB RAS,
Malygina str. 86, Tyumen, 625026, Russia; galina_malk@mail.ru

The article reflects the main milestones of the scientific activity of A.G. Skvortsov, Candidate of Technical Sciences, a renowned specialist of the ECI TyumSC of SB RAS. Andrey Georgievich is a specialist in the field of seismoacoustic researches of shallow sections. He is the author of original methods of seismic exploration, successfully used both in the cryolithozone and beyond it.

Key words: *seismic survey, inverse-velocity section, geophysical monitoring.*

Skvortsov Andrey Georgievich, Candidate of Technical Sciences, Leading Researcher of the Laboratory for Cartographic Modeling and Forecasting the State of Permafrost Geosystems at the Earth's Cryosphere Institute of the Tyumen Scientific Center of the Siberian Branch of the Russian Academy of Sciences, was born on July 24, 1946 in the city of Noginsk, Moscow Oblast, into a family of teachers. After graduating from high school, he entered the Sergo Ordzhonikidze Moscow Geological Prospecting Institute and graduated in 1970 with a degree in geophysical methods of prospecting and exploration of mineral deposits.

Immediately after graduation, A.G. Skvortsov was assigned to the All-Union Scientific Research Institute of Hydrogeology and Engineering Geology (VSEGINGEO) in the laboratory of geophysical methods. In 1970–1980, the circle of scientific interests of Andrei Georgievich had been formed: the application of seismoacoustic methods in engineering geology, hydrogeology, geocryology and ecogeology. He was directly involved in theoretical and expeditionary research, participated in scientific conferences, writing articles and monographs.

During those years, with the participation of A.G. Skvortsov, the works have been published which

are still in demand as scientific and methodological manuals for specialists in the field of seismic acoustics:

– Study of frozen sandy-clayey soils using a complex of borehole geophysical methods. Skvortsov A.G. In: Proceedings of VSEGINGEO, 1977, issue 116: Geophysical methods for solving hydrogeological problems, pp. 76–86.

– Seismoacoustic methods for engineering geocryological research. Goryainov N.N., Skvortsov A.G. In: Engineering permafrost: Proceedings of the III International Conference on Permafrost. Novosibirsk, 1979, pp. 267–272.

– Study of landslides by geophysical methods. Goryainov N.N., Bogolyubov A.N., Varlamov N.M., Nikitin V.N., Matveev V.S., Skvortsov A.G. Nedra, Moscow, 1987, 157 pp.

– Artificial Activation of Landslides. Postoev G.P. et al. Nedra, Moscow, 1989, 134 pp.

– Application of Seismoacoustic Methods in Hydrogeology and Engineering Geology. N.N. Goryainov (Ed.). Nedra, Moscow, 1992, 264 pp.

In 1985, A.G. Skvortsov was awarded the VDNKh bronze medal for the development of a methodology for seismic studies on landslides, and in 1987, he has successfully defended his Ph.D. thesis on "Seismic methods of studying landslides" and was given the degree of Candidate of Technical Sciences.

Since 1996 to the present, A.G. Skvortsov has been working at the Federal State Budgetary Institution, the Earth's Cryosphere Institute, SB RAS, as a leading researcher. His scientific interests are connected with the study of the propagation patterns of seismic waves in the upper part of the geological environment, both in the permafrost zone and beyond it. In the course of research, based on the analysis of a representative series of experimental data, A.G. Skvortsov has established the basic fundamental regularities of the propagation of shear SH-waves in inverse seismic-geocryological and seismic-geological sections. As a result, for non-lithified permafrost deposits, the typification scheme for seismic-geocryological sections according to their inversion-degree has been proposed. It has been found that similar types of inverted seismic-geological sections are quite common outside the permafrost zone.

By means of theoretical calculations and their comparison with actual experimental data, significant differences in the kinematics of reflected SH-waves in the conditions of inverse velocity sections in comparison with normal velocity sections have been revealed. Those differences turned out to be so significant that, by analogy with the term "low-velocity zone" for normal velocity sections, the concept of "high-velocity zone" for inverse velocity sections has been introduced. As a result of his studies, he has created and successfully introduced into the practice of geophysical work a unique technique of high-resolution seismic exploration on shear waves (HSSW), intended for a detailed study of the structure of the upper part of the geological section in conditions of inverse velocity sections. Especially noteworthy is the high efficiency of that technique within urbanized areas, as evidenced by the numerous positive examples of its use in the cities of Moscow, Norilsk, Novorossiysk, Mirny, etc. The performed studies correspond to the world level, and in a number of fundamental positions they have no analogues in our country and abroad.

For the study, monitoring and spatial-temporal forecasting of slope processes, under his leadership at the ECI of Tyumen Scientific Center of the SB RAS, the method of multi-wave various-azimuth seismic prospecting (MWVASP) has been developed and successfully introduced.

When carrying out his experimental studies, A.G. Skvortsov pays much attention to the used technical base. He has developed a number of three-component borehole seismic probes. The probes are used to perform vertical seismic profiling (VSP) surveys in wells. Studies by the VSP method are an important part of the developed HSSW technique. In addition, in recent years, he has been in constant contact with the developers of modern high-frequency seismic equipment. The purpose of that work is to optimize and improve the technical requirements for equipment, to participate in field-testing of modernized versions of seismic stations in various natural and seismic geological conditions, as well as to participate in the development of technical specifications for the creation of new generations of seismic equipment.

The results of many-years research by A.G. Skvortsov are reflected in more than 160 scientific publications, including several monographs. We can distinguish only a small fraction of the main publications of recent decades:

– Features of the structure of the field of elastic vibrations in non-lithified permafrost. Skvortsov A.G. Kriosfera Zemli [Earth's Cryosphere], 1997, I (3), 66–72.

– Monitoring of the stress-strain state of the coastal slope at the Bolvansky geocryological station using seismic exploration. Skvortsov A.G., Drozdov D.S., Malkova G.V., Smetanin N.N., Ukraintseva N.G. Kriosfera Zemli [Earth's Cryosphere], 2006, X (2), 46–55.

– Informative value of geophysical research in engineering surveys in permafrost zone. Zykov Yu.D., Skvortsov A.G., Koshurnikov A.V., Pogorelov A.A. Engineering Surveys, 2009, No. 12, 57–63.

– Results of studying the geocryological conditions of the Arctic territories using geophysical methods. Melnikov V.P., Skvortsov A.G., Malkova G.V., Drozdov D.S., Ponomareva O.E., Sadurtdinov M.R., Tsarev A.M., Dubrovin V.A. Geology and Geophysics, 2010, 51 (1), 169–177.

– Seismic microzoning of the territory of Kaliningrad. Aleshin A.S., Anosov G.I., Bessarab F.S., Drobiz M.V., Dementyev Yu.V., Pogrebchenko V.V.,

Rogal L.A., Skvortsov A.G., Tsarev A.M., Chugaevich V.Ya. Engineering Surveys, 2014, No. 9–10, 68–79.

– The use of seismic and ground-penetrating radar methods in geocryological research. Sadurtdinov M.R., Skvortsov A.G., Sudakova M.S., Tsarev A.M., Malkova G.V. Bulletin of the NESC of FEB RAS, 2017, No. 4, 75–86.

The most important advantage of A.G. Skvortsov's research is the organic combination of solving theoretical problems with experimental observations and testing various methods and technologies in the field. A.G. Skvortsov actively participates in the organization of full-scale modeling, implementation and popularization of research results. The developed methods are in demand in production, as evidenced by numerous contractual and scientific-methodical works carried out by the Earth's Cryosphere Institute of the Tyumen SC SB RAS throughout Russia from Kaliningrad to Blagoveshchensk.

A.G. Skvortsov successfully conducts pedagogical and educational work. He lectures regularly at international scientific and practical conferences and seminars on the topic of "High-resolution shear wave seismic (HRSW) – physical foundations, technology and application experience".

He is a guest-lecturer for geophysics students at the M.V. Lomonosov Moscow State University. Andrey Georgievich takes an active part in the organization, management and implementation of field geophysical research, transfers his knowledge and vast experience to the undergraduate and graduate students.

Andrey Georgievich enjoys the well-deserved respect of the institute's staff. He is distinguished by high professionalism, great diligence, integrity, dedication, scientific intuition and practical skills, inexhaustible optimism and love of life.

We wish the Hero of the Day health, long happy years of life and further creative success!

Received April 2, 2021

Kriosfera Zemli, 2021, vol. XXV, No. 4, pp. 52–53

STANISLAV ALEKSEEVICH LAUKHIN (*23.11.1936–04.06.2021*)

M.R. Sadurtdinov, D.S. Drozdov, O.E. Ponomareva

Earth Cryosphere Institute, Tyumen Scientific Centre SB RAS, Malygina str. 86, Tyumen, 625026, Russia; mr_sadurtdinov@mail.ru

On June 4, 2021, Stanislav Alekseevich Laukhin, a recognized specialist in Quaternary geology of the North of Russia, professor of the Department of Engineering Geology of the GGF MGRI, Doctor of Engineering Sciences, an unusually purposeful and tireless person, passed away.

Key words: *geocryology, Quaternary geology, Stanislav Alekseevich Laukhin.*

Stanislav A. Laukhin was born on October 23, 1936 in the city of Pushkino, Moscow region. After graduating from high school in 1954, he began studying for his master's in geoscience at the Faculty of Geology, Lomonosov Moscow State University. His own commitment to excellence, good teachers, and fieldwork in the Western Sayan helped Stanislav, then a student, to identify his core research interests. What really attracted him was Quaternary geology and biostratigraphy of Siberia. However, prompted by contemporaneous science developments and industry demands, his research focus had slightly changed and in 1967 he defended his PhD thesis on the Late Cenozoic stratigraphy and paleogeography of the North Angara region.

Later, while still holding on the cherished ambition of his attempt to draw nearer to Quaternary research, S.A. Laukhin had had to change jobs several times incidentally solving different tasks. Among other things he conducted various-scale geological survey of Cenozoic deposits in Siberia and the Far Eastern North; examined cascade of the Lower Angara hydropower stations and provided geological and geomorphological justification of the related projects; was engaged in forecasting and searching for placer deposits, from study of gold-bearing provinces in Cenozoic depressions in Northeast Russia). His involvement in these fields of research often provided an opportunity to explore new geographical areas and allowed Stanislav to be exposed to a huge amount of new factual material on Quaternary geology, which he collected and studied, and eventually developed a passion for a new frontier in geology – geoarchaeology.

In the 1980–1990s, S.A. Laukhin studied the history of Paleolithic humans, their movements driven by climate changes, and the emergence of the Bering Land Bridge. Stanislav A. Laukhin discovered Kymyneikey site in Chukotka, the latest explored at that time (1987), and participated in the commencement of systematic geoarchaeological investigations of the Kurtak Archaeological Region (upper Yenisei River in the south of the Krasnoyarsk Region) for which he build the first ever paleotemperature curve spanning most of the Cenozoic of the Northeast Asia (1993)*.

The wide geography of S.A. Laukhin's fields of research encompasses regions from the Urals to the Bering Strait and from Tiksi to Tuva.

In total, he authored more than 500 publications, including 11 monographs (with coauthors) and 40 articles published in the Transactions (Doklady) of the USSR/Russian Academy of Sciences. As many as 97 of his articles have been published or translated and reissued abroad in 23 countries (USA, England, France, Spain, Germany, China, etc.).

Stanislav A. Laukhin was a full member of the Russian Academy of Natural Sciences, a member of the Commission on Paleoecology and Human Evolution within the Russian Academy of Sciences, President of the INQUA Subcommittee on Paleolithic Geoarchaeology. As a committed scholar, he considered his lifelong love of science and research work to be a major asset to him and tried to dismiss everything that distracted him from his passion.

In 1996, S.A. Laukhin successfully defended his doctoral dissertation entitled "The Plio–Pleistocene geological history of North Asia and stages of its populating by Paleolithic humans".

S.A. Laukin's achievements in the field of archeology, paleoecology were highly commended by the scientific community, the Academy of Sciences, the Ministry of Geology of the USSR. A novel mollusk Gibbulnopsis (Primipupilla) lauchini Popova was named after him. As a member of Organizing Committees, S.A. Laukhin was awarded a Golden badge and a Diploma of the USSR Mingeo (Ministry of Geology) for organizing and conducting the 11th INQUA Congress and the 27th International Geological Congress (Moscow, 1984). In 2000, he was awarded a State scientific scholarship, and Honorary Diploma of the Presidium of Siberian Branch of the Russian Academy of Sciences in 2006.

Stanislav A. Laukhin's teaching career, which began in 1963, was interrupted for only brief periods and lasted until the end of his life.

The academic courses taught by S.A. Laukhin include: "Practical course of the USSR geology" and "Quaternary geology with introduction to paleontology" at Moscow State University; "Geology of placer deposits" at the Institution of Additional Professional Training affiliated with Mingeo, USSR; "Engineering geology" at Moscow Institute of Municipal Economy and Construction; "The Earth's cryosphere" as academic subject, and his own original course "Paleogeocryology" at Russian State University for Geological Prospecting (MGRI). Already seriously ill during the past few years, Stanislav A. Laukhin delved into teaching, however, always found time for science and with all his extraordinary perseverance continued to keep up his favorite research.

Received July 28, 2021

* Pushkar, V.S., 2016, Stanislav Alekseevich Laukhin: From the Mediterranean to Chukotka and from Tiksi to Macau. Tikhookeanskaya geologia [Russian Journal of Pacific geology], 35 (5), 117–118.